THE EFFECTS OF CLIMATE CHANGE ON SEA WATER INTAKE AND OUTFALL SYSTEMS IN THE CASPIAN SEA

by

Pelin Uzun

B.S., Civil Engineering, Boğaziçi University, 2016

Submitted to the Institute for Graduate Studies in
Science and Engineering in partial fulfillment of
the requirements for the degree of
Master of Science

Graduate Program in Civil Engineering

Boğaziçi University

2019

ACKNOWLEDGEMENTS

I would like to express my endless gratitude to my thesis supervisor, Assoc. Prof. Emre Otay for introducing me to the field of coastal engineering and changing my career path in a way that makes me incredibly grateful and strong. I would also like to thank him for his valuable guidance, encouragement and support throughout this study and the project we have studied together.

I would like to thank GAP Construction Co. for sharing their project with me and allowing me to use it in my thesis.

I would specially thank Murat Cenk Gerdanlı - MCG Mühendislik for his precious comments and help.

I would like to express my appreciations to Uludağ University Department of Hydraulics for their endless friendship, supports and help. I would specially thank Assoc. Prof. Adem Akpınar and Civil Engin. (M.Sc.) Bilal Bingölbali for their unique friendship, supports and help.

I would like to express appreciations to my precious family at Boğaziçi University for their eternal friendship, support and faith in me.

I would thank my family for their endless love and support throughout my education life.

I would like to express my gratitude to my soulmate, Şükrü Olcay who is always there for me, for his patience for three years, endless support and love.

ABSTRACT

THE EFFECTS OF CLIMATE CHANGE ON SEA WATER INTAKE AND OUTFALL SYSTEMS IN THE CASPIAN SEA

Climate change affects sea level change which controls the wave and thermal mixing processes in the Caspian Sea (CS). The sea has been suffering from its unstable sea level due to climate change, which may be critical for the design and operation of Sea Water Intake Outfall (SWIO) systems. For the feasibility of a SWIO system, three processes are crucial: sea level, nearshore wave climate and thermal dilution. The scope of this thesis is the effects of climate change on sea level, nearshore wave climate and thermal dilution in the CS. The changes in the Caspian Sea Level (CSL) due to climate change are predicted for the next century by using an unsteady 2D vertically integrated circulation model (RMA2). At the end of 2100, a decrease of 10.67 m in the Caspian Sea level is predicted. The Garabogaz Ammonia and Urea Production Plant is chosen as a sample case to examine the effects of sea level change on SWIO systems in the CS. Nearshore wave climate and thermal dilution predictions are conducted using SWAN and CORMIX models for the same time periods, respectively. Operational problems are observed beginning in 2030 when there is intense wave breaking at the discharge location. Environmental constraints are jeopardized including the temperature difference at 100 m downstream exceeding $+3^0$C in 2051. As a consequence, the SWIO system may seriously harm the environment in 32 years after construction. This situation shows the importance of predictions of the sea level, wave climate and thermal mixing processes in addition to standard design checks for the project lifetime. One solution to this problem could be constructing such systems on coasts with steeper slopes. The southern coast, the middle part of the western coast and north-west coasts of the eastern coast of the CS have steeper slopes.

ÖZET

İKLİM DEĞİŞİKLİĞİNİN HAZAR DENİZİ'NDEKİ DENİZ SUYU ALMA VE BOŞALTMA SİSTEMLERİ ÜZERİNDEKİ ETKİLERİ

İklim değişikliği Hazar Denizi'ndeki dalga iklimini ve termal karışım sürecini kontrol eden su seviyesini etkiler. Bu deniz iklim değişikliğine bağlı olarak değişen su seviyesinden sıkıntı çekmektedir. Bu durum deniz suyu alma ve geri boşaltma sistemleri için kritik olabilir. Bu sistemlerin fizibilitesi için üç önemli süreç vardır: su seviyesi, yakın kıyı dalga iklimi ve termal seyrelme. Bu tezin kapsamı iklim değişikliğinin Hazar Denizi'ndeki su seviyesi, yakın kıyı dalga iklimi ve termal seyrelmesi üzerindeki etkileridir. İklim değişikliği sonucu oluşan Hazar Denizi su seviyesi değişikliği gelecek yüzyıl için kararsız, düşey integralli, iki boyutlu sirkülasyon modeli (RMA2) kullanılarak tahmin edilmiştir. Hazar Denizi'nin su seviyesinde, 2100 yılının sonunda, 10,67 m azalma öngörülmüştür. Hazar Denizi'ndeki su seviyesi değişiminin deniz suyu alma ve geri boşaltma sistemlerine etkisini incelemek için Karaboğaz Amonyak ve Üre Üretim Tesisi örnek olarak seçilmiştir. Aynı periyot için yakın kıyı dalga iklimi ve termal seyrelme öngörüleri sırasıyla SWAN ve CORMIX modelleri kullanılarak yapılmıştır. Su alım yerinin üzerinde yoğun dalga kırılmasının olduğu 2030 yılında operasyonel sorunların başladığı gözlemlenmiştir. 2051 yılında akıntı yönündeki 100 metrede sıcaklık farkı $+3^0$C'yi aşarak çevresel kısıtlama tehlikeye atılmıştır. Sonuç olarak bu deniz suyu alma ve geri boşaltma sistemi çevreye kurulduktan sonra 32 yıl içinde ciddi bir şekilde zarar verebilir. Bu durum proje ömrü için standart dizayn kontrollerine ek olarak su seviyesi, dalga iklimi ve termal karışım süreçlerinin öngörüsünün önemini gösterir. Bu probleme bir çözüm, bu tip sistemleri Hazar Denizi'nin daha dik eğimleri olan kıyılarına inşaa etmek olabilir. Hazar Denizi'nin güney kıyısı, batı kıyısının orta kısmı ve doğu kıyısının kuzeybatıya bakan kıyıları daha dik eğimlere sahiptir.

TABLE OF CONTENTS

LIST OF FIGURES

LIST OF TABLES

LIST OF SYMBOLS

a	Bottom elevation
A_L	Land area
A_S	Sea area
CO_2	Carbon dioxide
D	Discharge to Kara Bogaz Gol
$D0$	Beginning of discharge pipeline
D_o	Discharge mouth
E	Evaporation
E_L	Evaporation over land
E_S	Evaporation over sea
E_{xx}	Eddy viscosity coefficient for normal direction on x surface
E_{xy}	Eddy viscosity coefficient for shear direction on x surface
E_{yx}	Eddy viscosity coefficient for shear direction on y surface
E_{yy}	Eddy viscosity coefficient for normal direction on y surface
fl	Fraction of the loss in precipitation over land
g	Gravity acceleration
h	Water depth
h_b	Breaking wave depth
H	Sea level
H_b	Breaking wave height
H_s	Significant wave height
$I0$	Beginning of discharge pipeline
I_o	Intake mouth
n	Manning's roughness coefficient
Q_KBG	Discharge to Kara Bogaz Gol
Q_V	Volga River runoff
P	Precipitation
P_L	Precipitation over land
P_S	Precipitation over sea

r	Downstream distance from diffuser line
R	River runoff
t	Time
T_m	Mean wave period
T_p	Peak wave period
u	Velocity in x direction
v	Velocity in y direction
V_a	Wind speed
x	Cartesian coordinate
y	Cartesian coordinate
β	Angle between diffuser line and port centerline
γ	Angle between ambient current to diffuser line
ΔCSL	Annual Caspian Sea level change
Δt	Time step
ΔT	Temperature difference
ζ	Empirical wind shear coefficient
θ	Wave direction, angle between port centerline and horizontal
ρ	Density of fluid
σ	Angle between ambient current and port centerline
ϕ	Local latitude
ψ	Wind direction
ω	Rate of Earth's angular rotation

LIST OF ACRONYMS/ABBREVIATIONS

ARFIMA	Autoregressive Fractionally Moving Average
ARIMA	Autoregressive Integrated Moving Average
ARMA	Autoregressive-Moving Average
BSL	Baltic Sea Level
BUCEL	Boğaziçi University Coastal Engineering Laboratory
CASPCOM	Coordinating Committee on Hydrometeorology of the Caspian Sea
CEC	Coastal and Environmental Engineering and Consultancy
CORMIX	Cornell Mixing Zone Model
CORMIX2	Cornell Mixing Zone Model for submerged multiport diffuser
CS	Caspian Sea
CSL	Caspian Sea Level
ECMWF	The European Centre for Medium-Range Weather Forecasts
GAUPP	Garabogaz Ammonia and Urea Production Plant
H	the Hurst number
HA	The averaged water depth
HD	The depth at the port
KBG	Kara Bogaz Gol
LWL	Local water level
MHI	Mitsubishi Heavy Industries
MSL	Mean Sea Level
NOPEN	Number of openings
PER	Precipitation-Evaporation+Runoff
RMA2	Two-dimensional hydraulic model
SSW	South-South-West
SWAN	Simulating Waves Nearshore
SWIO	Sea Water Intake Outfall
TL-ARFIMA	Trend line combined with ARFIMA
VRD	Volga River discharge

YB1	Distance from shoreline to the first point of the diffuser line
YB2	Distance from shoreline to the second point of the diffuser line

1. INTRODUCTION

Sea water intake outfall (SWIO) systems are commonly used to supply cooling and/or fresh water to residential or industrial developments on the coast. In power-plants, most of the water is used for cooling and some are used for desalination. For this reason, there are a lot of projects that take water from the sea, lake or river and discharge the used water back to its original source. When using the sea water, long-term prediction of sea level, wave climate and thermal mixing process according to foreseen project lifetime may be helpful for the environment and SWIO system itself. Examining the possible changes in any of these processes may be crucial.

This prediction is very important because coastal engineering facilities may be impacted due to changes in sea level which consequently changes the wave climate, current intensities and mixing processes. As a result of that impact, the facility may face operational problems. Furthermore, it may harm the environment.

One of the water bodies that house large SWIO systems due to water shortages in its hinterland, is the Caspian Sea (CS). The CS is an enclosed water body and has no outflow. Rivers and precipitation feed the CS whereas the CS loses its water only to Kara Bogaz Gol (KBG) and by evaporation. There are serious concerns that the CS may dry out in the future like the Aral Sea because of increasing temperatures due to climate change (Huseynov, 2011). These concerns are painted by a ten years old Azerbaijani girl in Figure 1.1. In this picture, the children being aware of pollution and the decreasing water level, want to refill the CS with tap water. Unfortunately, they do not realize that tap water is not independent of the CS water. This picture suggests that not only the changing sea level affects the SWIO systems but the SWIO systems affect the sea level change by taking large amounts of sea water through desalination plants. For cooling water, there is no net loss of sea water, but water is heated up and pumped back to its original source. One thing in the painting is true; by nature or by humans, the evaporation processes speed up, and eventually the sea level drops.

Figure 1.1. Children supply clean water to the Caspian Sea to fight with the decreasing water level and pollution (Huseynov, 2011).

Five countries, Russia, Kazakhstan, Turkmenistan, Iran, and Azerbaijan neighboring the CS, take advantage of the CS for desalination and cooling purposes. The SWIO system of Lukoil on the Russian coast, the Garabogaz Ammonia and Urea Production Plant on Turkmen coast using cooling water and the desalination plant on the Kazakh coast of the Caspian Sea are some examples. Furthermore, the Caspian region oil and natural gas infrastructures are shown in Figure 1.2. Most of the oil refinery and power plants use cooling water. In addition to that, these countries suffer from lack of fresh water which led them to build severe desalination plants. Turkmenbashi Desalination Plants built in 2010 and 2016 produce 35,000 m^3 and 50,000 m^3 fresh water per day using the CS water (Polimeks, 2019) To produce 85,000 m^3 fresh water, 170,000 m^3 sea water is needed. The eastern Caspian is mainly dependent on desalination plants. There are Turkmenistan's Balkan, Esenguly, Turkmenbashi and Garabogaz provinces and the coastal provinces of Kazakhstan. The MAEK Desalination Plant in Aktav supplies 50% of drinking water (UNEP *et al.*, 2008) to Kazakhstan. The Uzen oilfield in Kazakhstan (UNEP *et al.*, 2008) and Parre Sar Combined Cycle Power Plant in the

southern Caspian coastline using 151,000 m^3 cooling water per hour (SPI, 2019) can be given as examples.

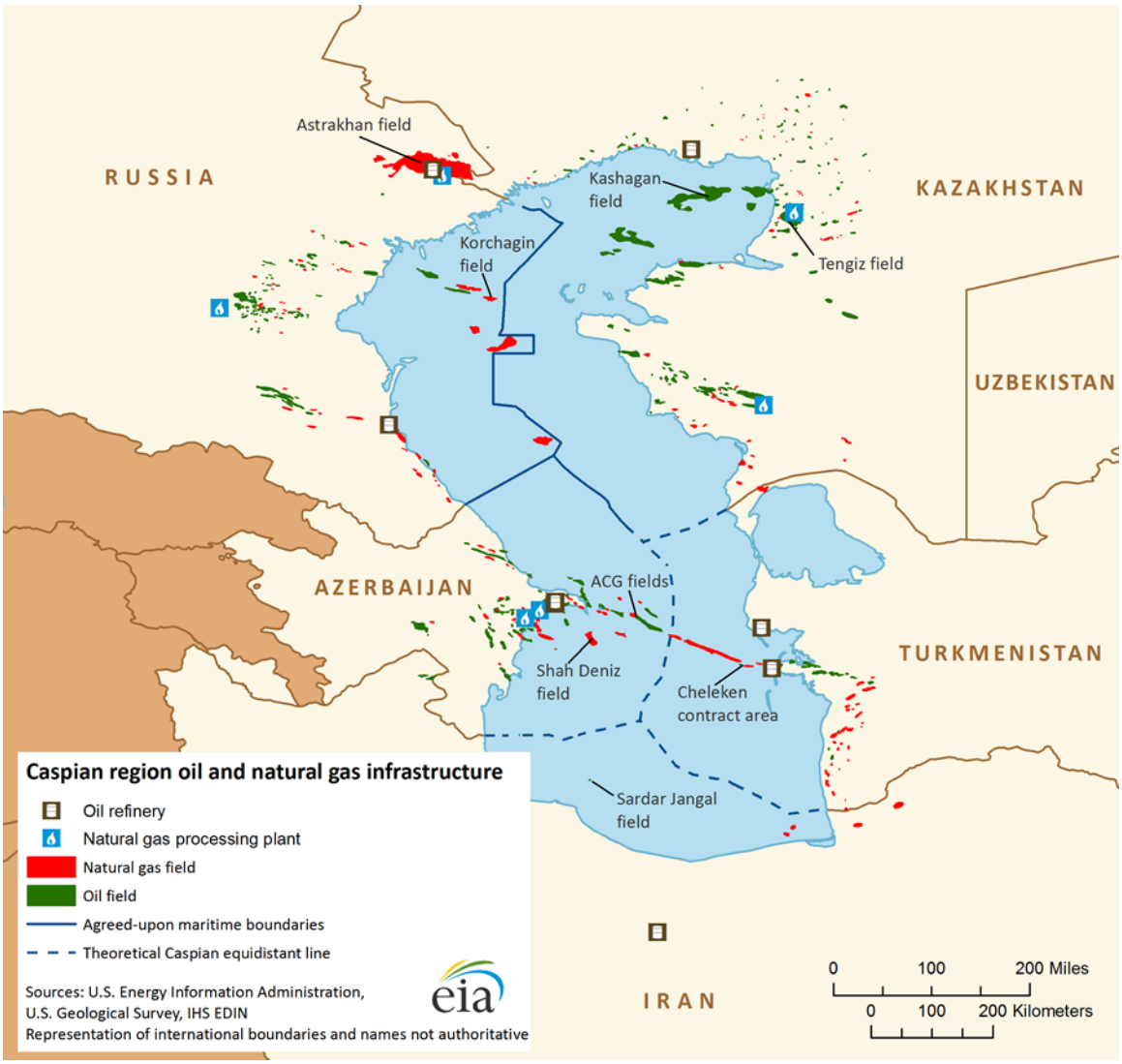

Figure 1.2. Caspian region oil and natural gas infrastructures (EIA, 2019).

While these projects are in proposal or construction stages, their feasibility and designs are usually based on the present or near future conditions derived from, daily, seasonal or short-term changes. But, especially for the CS, long-term changes may be totally different. The Caspian Sea level (CSL) has been seriously changing for centuries, which leads to environmental and engineering problems for SWIO systems. There are few separate studies considering the CSL change and feasibility of SWIO systems. Feasibility of SWIO systems should incorporate the sea level change. One should combine the sea level change and the feasibility of these systems and examine

these two processes together to reach what will happen in the future.

The main objective of this thesis is the effects of climate change on sea level, nearshore wave climate and thermal dilution of SWIO systems in the Caspian Sea. In this thesis, the Garabogaz Ammonia and Urea Production Plant on the Turkmen coast of the Caspian Sea near Kara Bogaz Gol is used as a test case of how sensitive water depths might be on wave agitation and thermal mixing for a SWIO system. Its location is shown in Figure 1.3.

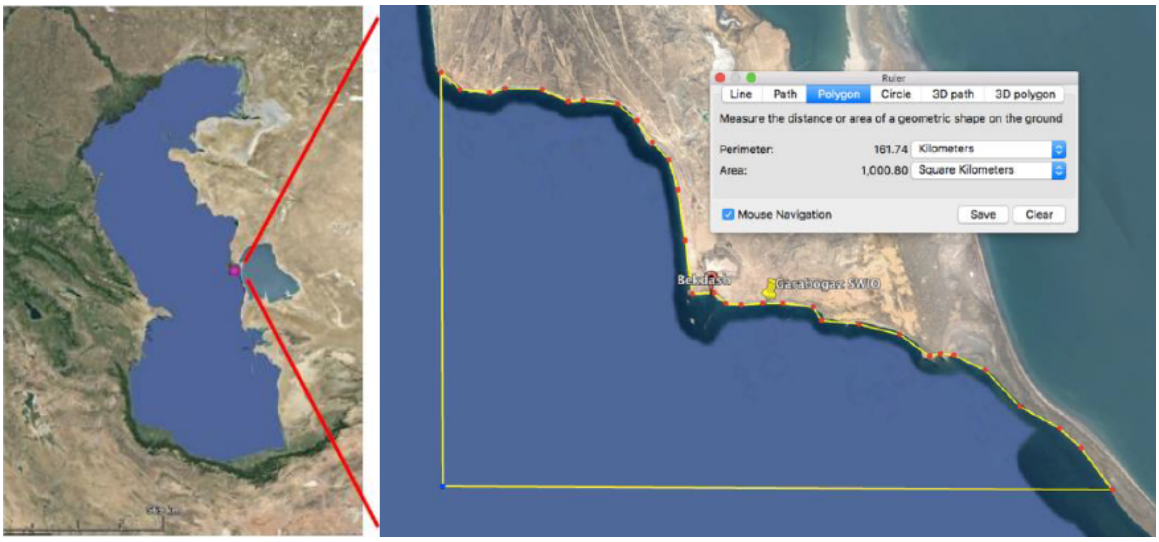

Figure 1.3. Location map of the model area. (Google Earth, 2018).

RMA2 model is used to predict the Caspian Sea level change until 2100. Precipitation, evaporation and wind data are taken from ECMWF. The Volga River runoff and the discharge to the Kara Bogaz Gol data are taken from CASPCOM (2018) and Aladin *et al.* (2012), respectively. According to the sea level change, SWAN and CORMIX models are run to predict nearshore wave climate and thermal dilution in the next century, respectively.

A nested grid is employed to account both for the effect of the far field deep water conditions and the local bathymetric features near the SWIO. Regular computational grid with Cartesian coordinates and stationary mode of SWAN are used. Bathymetry data is taken from Navionics Sonar Chart (2018).

CORMIX Mixing Zone Model is used to model near-field thermal dilution. submerged multiport diffuser version of CORMIX (CORMIX2) is used with unidirectional diffuser type. For the worst-case scenario, summer is selected due to high sea water temperatures which decrease the dilution rates.

In the next chapter, a literature review of the Caspian Sea level change, wave climate and thermal dilution studies are given. After that chapter, methodology and results are discussed. Finally, summary, conclusion and recommendation for future work are given.

2. LITERATURE REVIEW

The problem in this study is how climate change affects the CSL, and consequently, wave agitation and thermal dilution of heated water discharged from an SWIO system. Wave and thermal dilution models are needed to observe the effect of the change of the CSL. For wave and thermal dilution modeling, SWAN and CORMIX are used, respectively. The reliability of these models and their usage areas have been studied in the literature.

Furthermore, the long term prediction of the CSL due to climate change is a critical part of this study. For the SWAN and CORMIX models, the future CSL as a model input is a game changer process. To see the effects on wave agitation and thermal dilution, reliable input sea level data for SWAN and CORMIX predictions are needed. That is why literature survey on the CSL is very crucial.

In this chapter, literature review of the Caspian Sea level prediction, wave climate modeling with SWAN and thermal mixing modeling with CORMIX are discussed.

2.1. The Caspian Sea Level

The Caspian Sea is the largest lake on Earth. It is an endorheic (no outflow to open water bodies) basin between Europe and Asia neighboring Russia, Kazakhstan, Turkmenistan, Iran, and Azerbaijan. Its perimeter and surface area are shown in Figure 2.1. The CSL has varied between -26 m and -29 m below the Baltic Sea Level (BSL) in the last 85 years (Figure 2.2). The CS has several inlets including Volga, Ural, Kura, Terek, and Sefidrud rivers, but no outlet to open water bodies. Volga is the largest river feeding into the Caspian Sea and plays an important role in controlling the CSL.

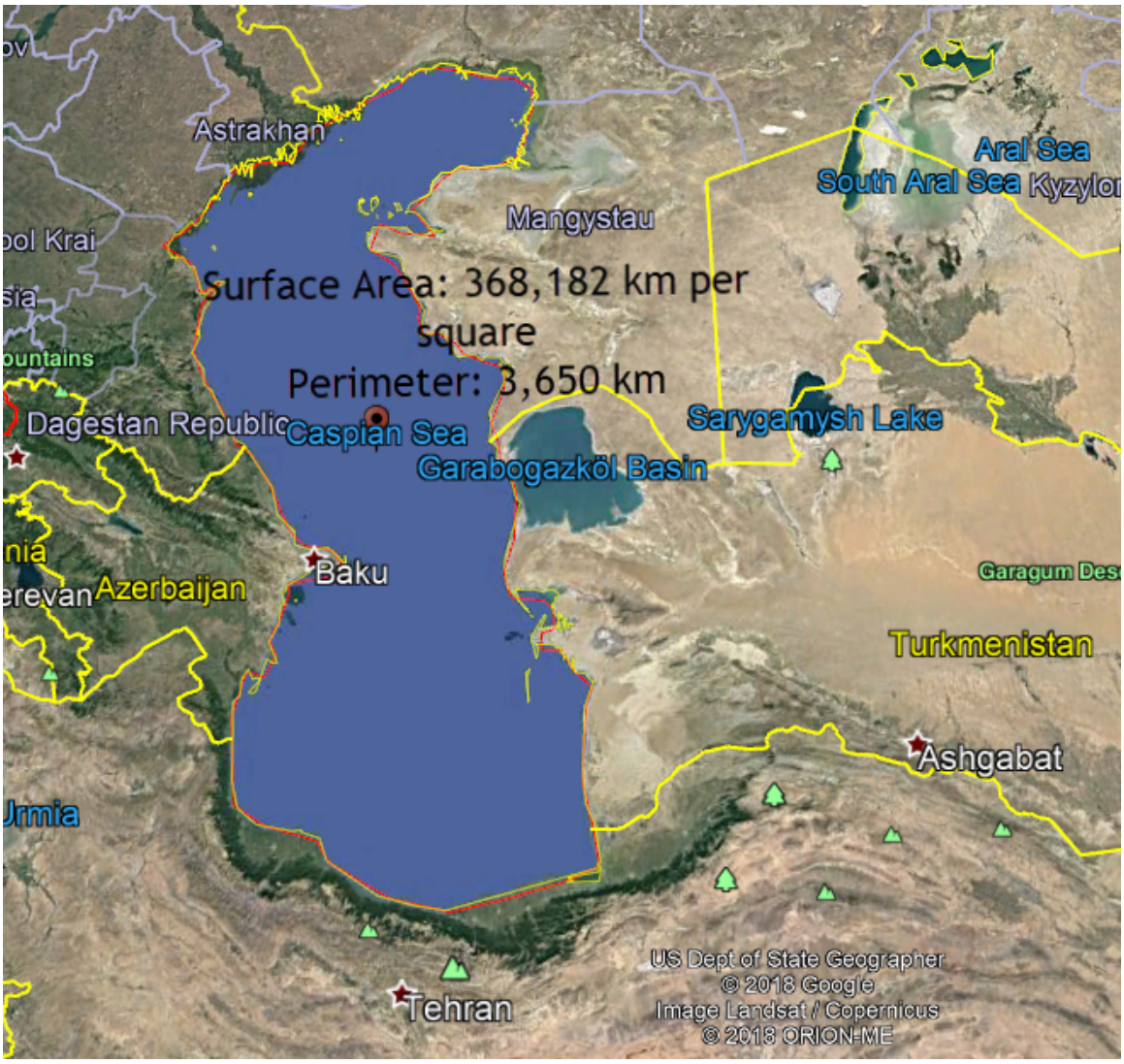

Figure 2.1. The Caspian Sea. (Google Earth, 2018).

Arpe *et al.* (2014) studied the water budget between inflow to the CS and outflow from the CS to predict the CSL. They used the European Centre for Medium-Range Weather Forecasts interim reanalysis and seasonal forecasts, which were needed due to continuous fluctuation of the CSL. The rate they found for the CSL change is 100 times faster than that of the global ocean sea level over the last century. This result has environmental, social and economic effects. For the hydrological budget of the CS, they included precipitation minus evaporation (P-E) over the CS and Volga River discharge (VRD). Besides, Ural, Sefidrud and Kura Rivers are added as boundary conditions for the CSL.

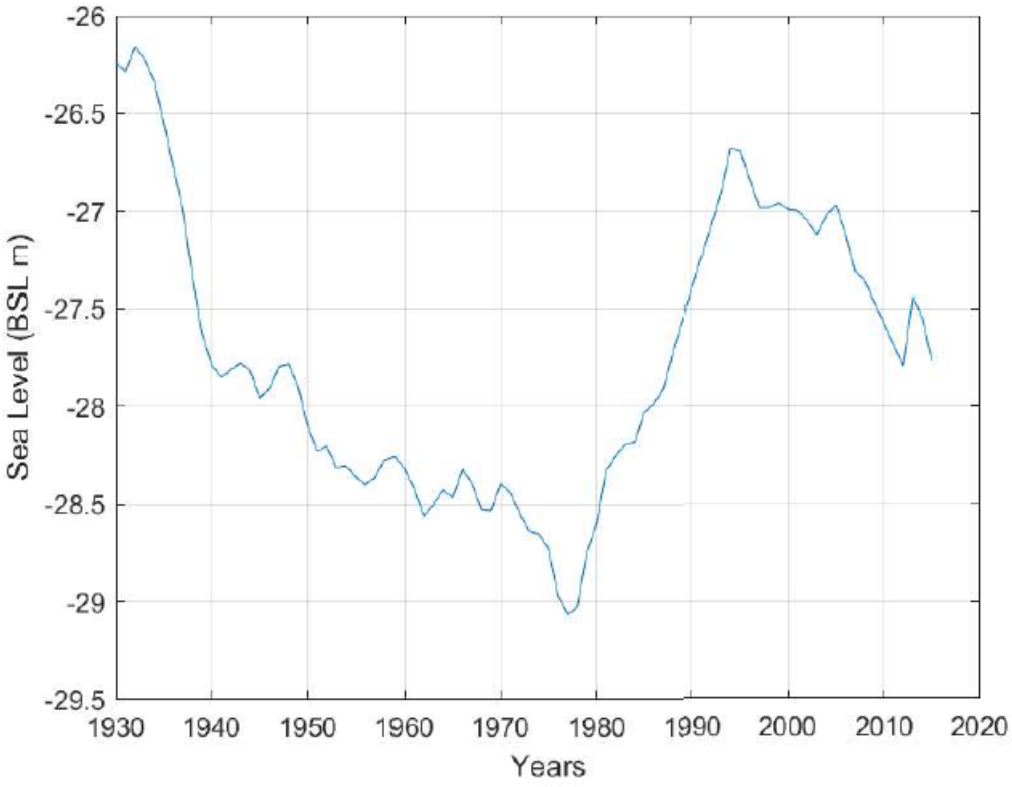

Figure 2.2. Yearly CSL changes between 1930 and 2015. Data is taken from Coordinating Committee on Hydrometeorology of the Caspian Sea (CASPCOM), Bekdash Station.

Furthermore, it is modeled that there is a delay of the water in the Volga basin due to groundwater reservoir and ice and snow in winter (Figure 2.3). When all parameters are included, and four months delay is parameterized, the model complied with observations.

There were different results according to various combinations of data such as the weather forecast interim reanalysis data with and without the groundwater parametrization, and both weather forecast interim reanalysis data and seasonal forecast data. This study has shown that forecast using both Volga basin and seasonal forecasts gives satisfying results when predicted and observed data are compared. With the storage of Volga basin data and seasonal forecast, a few months more prediction of the CSL can be reached. This is an important contribution to environmental, social and economic

issues around the CS and needs to be developed by considering the discharge to KGB, evaporation, greenhouse gases, etc.

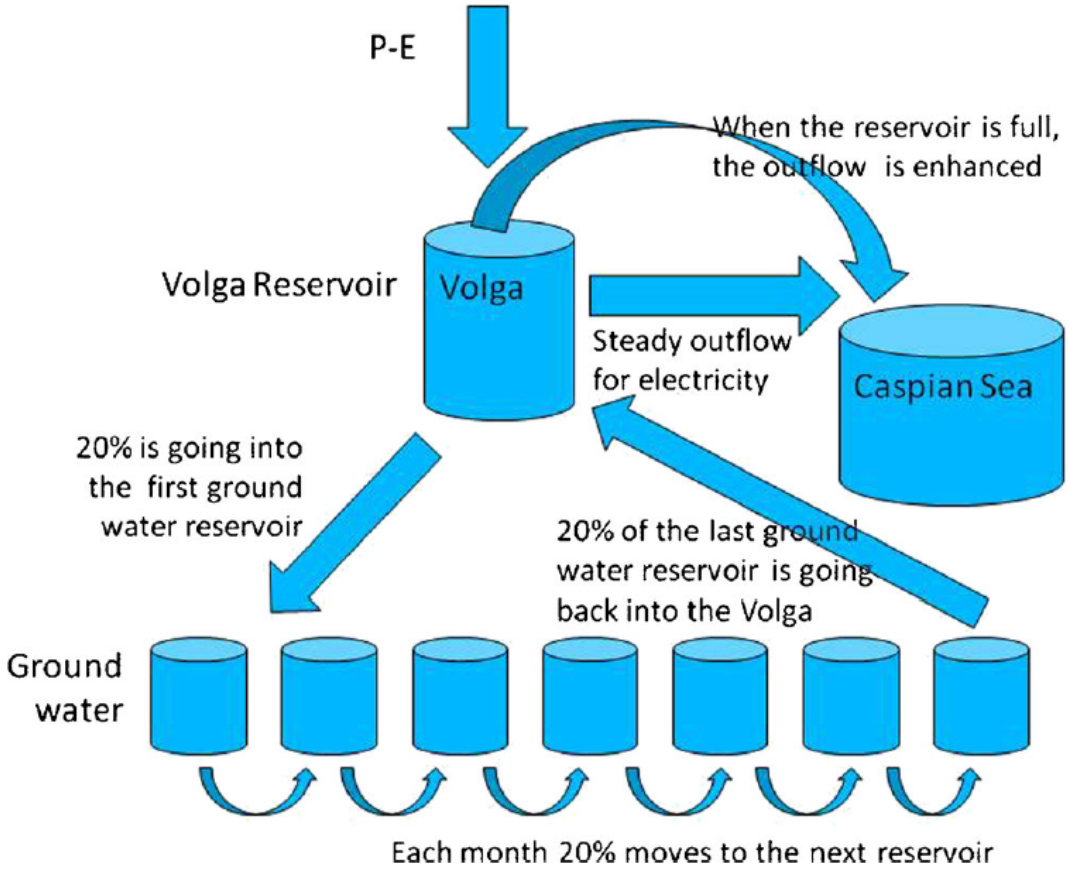

Figure 2.3. Schematic of the parameters that affect the Caspian Sea level (Arpe *et al.*, 2014).

Elguindi and Giorgi (2006) have studied the CSL because enclosed water bodies are seriously affected by climatic changes and variability and that situation has its consequences which interest particularly people living around the CS. This study aims to predict possible changes of the CSL until the end of the 21st century under different greenhouse gas emission scenarios. In order to simulate surface air temperature, precipitation, and evaporation over the CS, they used General Circulation Models covering the years between 1905 and 1999 and 2000 and 2099. The half degree global data sets produced by the Climatic Research Unit of the University of East Anglia were compared with the 20th century simulations of precipitation and temperature (New *et al.*, 2002).

Simple hydrologic balance equation developed by Elguindi and Giorgi (2005) was used to predict changes in the CSL. The equation is

$$\Delta CSL = \left[\frac{A_L}{A_S}[P_L(1-fl) - E_L] + P_S + D - E_S\right] \tag{2.1}$$

where ΔCSL is the annual CSL changes, $\frac{A_L}{A_S}$ is the proportion of land area to sea area, P_L and E_L are precipitation and evaporation over land, respectively and P_S and E_S are precipitation and evaporation over sea, respectively. The parameter of fl represents the fraction of the loss in P_L that cannot be included in the model. D is the discharge to KGB, but it is neglected. There are two scenarios for different fl and number of realizations to simulate the CSL. For both two scenarios, the model predicts that the CSL at the end of the 21st century will drop by 9 m (Figure 2.4). But there will not be a sharp decrease or stable period. Estimated precipitation is increasing but evaporation has a larger rise. The vulnerability of the CSL and its environment to climatic changes has been proved.

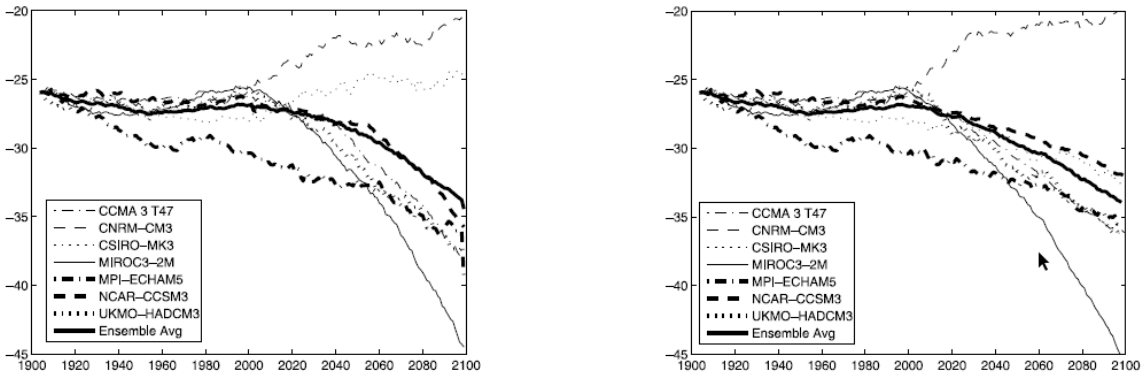

Figure 2.4. Predicted mean sea level of the CS for the 21st century. Graphs at left and right are for scenario A2 and A1b, respectively (Elguindi and Giorgi, 2006).

Renssen *et al.* (2007) have tried to understand the relationship between climate change and the Caspian Sea level considering very long time. They used a climate-hydrological-sea level model using historical, measured and geological data. Thus, they have prediction of the Caspian Sea level, evaporation, precipitation, the Volga River

runoff and discharge to Kara Bogaz Gol. As a result, a dramatic drop to below -30 m-BSL is expected in the Caspian Sea level at the late 21^{st} century.

Roshan *et al.* (2012) have studied the effect of CO_2 increases on the CSL considering 1951 - 2006 and 2025 - 2100 periods. The reason for studying the CO_2 effect is that temperature and climate change mostly depend on CO_2 level. They have considered five different scenarios of the CO_2 level. The necessary data was generated and used to predict the future CSL using the MAGICC SCENGEN Model software (version 5.3). The past and future mean CSL are shown in Figure 2.5. Results show that temperature and the CSL are more related to each other than precipitation and the CSL. Despite the weak relationship between CO_2 and evaporation, it increases when CO_2 rises. Furthermore, there is a direct proportion between CO_2 and the CSL. 86 cm and 163 cm rise of the CSL are expected in 2017 and 2100, respectively (Figure 2.5).

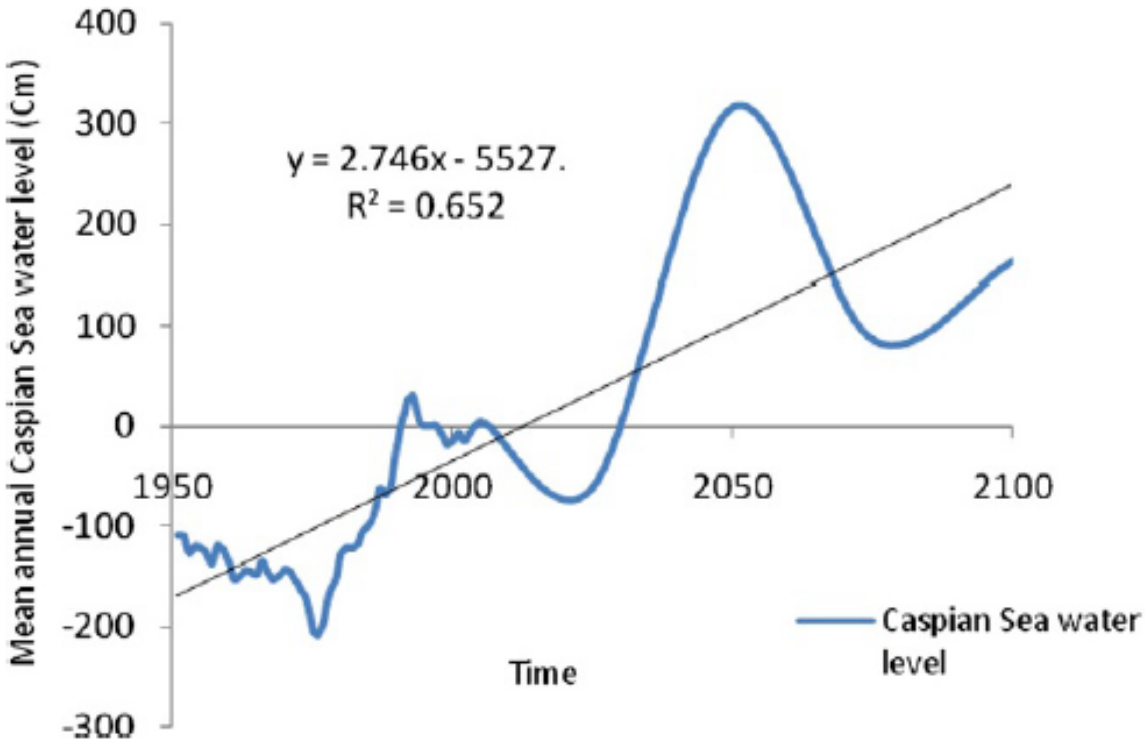

Figure 2.5. The past and future annual mean CSL (Roshan *et al.*, 2012).

Beni *et al.* (2013) have aimed to put together historical documents and geological records to recreate the CSL changes using numerical modeling during the last millennium. They wanted to emphasize the importance of a multidisciplinary approach in recreating the CSL changes. The results show that solar activity features in the main CSL fluctuations. Even though the primary reason for the CSL changes is climatic changes, seismic events also have an important role. Because they change the local base level. This study has proved that the multidisciplinary approach is a useful method for such studies.

Ercan *et al.* (2013) have aimed to forecast the future CSL changes, determine the long-term dependence of the CSL and determine confidence band for the CSL changes. Firstly, the long-term dependence and linear trend of the CSL were studied. For long-term dependence, they used the Hurst number (H) which is an index of long-term memory. If H is between 0.5 and 1, the process has a long-term dependence. It is concluded that the signal of the CSL time series has a long-term memory. In addition to that, the CSL has not a linear trend until 1995 and after that, it has a linear trend. To forecast the CSL in the future, ARFIMA models are used. Four different models which are Mixed Autoregressive-Moving Average process (ARMA), Autoregressive Integrated Moving Average process (ARIMA), Autoregressive Fractionally Moving Average process (ARFIMA) and trend line combined with ARFIMA (TL-ARFIMA) were compared. It turned out to be that ARFIMA model can adapt the abrupt sea level changes more quickly and easily than the ARMA and ARIMA models which are not good at the forecast. TL-ARFIMA is better than ARFIMA with the exclusion of updating performance. The variance of the forecast error generates the confidence band. In other word, it considers the uncertainty in forecasting. That is why it is a significant parameter in order to trust the results. They found the confidence band estimated using ARFIMA as 13.3 m in 2039. Besides, they also realized that the time period is a crucial factor for forecast performance when modeling is used.

Chen *et al.* (2017) have predicted the CSL changes between 1979 and 2015. The inputs of the model were climate model predicted precipitation (P), evaporation (E) and the observed river runoff (R). Volga River is the largest contributor in R. They

called that system PER (P-E+R) flux prediction. The water balance equation below is used to reconstruct the CSL:

$$\frac{dH}{dt} = P - E + R \tag{2.2}$$

where t is time and H is the sea level. Modeling result is shown in Figure 2.6. The result is satisfying. The model found the significant rise in period 1979 - 1995 and drop in period 1996 -2015 as +12.38 cm/yr and -6.79 cm/yr and these values are 12.74 cm/yr and -6.72 cm/yr in the observed data, respectively. The game changer was the increased evaporation rate over the CS. That was why the increasing trend in the CSL was reversed by the increased evaporation rate. This new decreasing trend is thought to continue due to global warming scenarios.

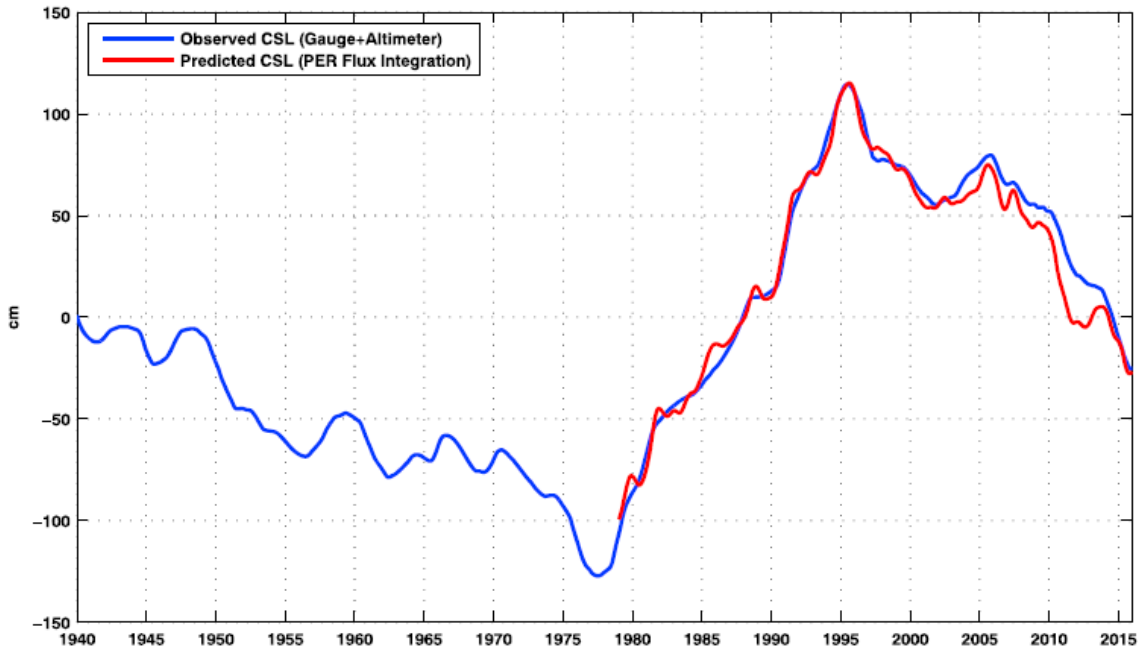

Figure 2.6. The CSL change from tide gauge, satellite altimeter and PER flux integration between 1940 and 2015 (Chen *et al.*, 2017).

Due to its depth (around 5 m), the northern part of the CS is vulnerable and continued warming in the northern hemisphere needs precaution. Because evaporation is related to the surface temperature. The example of Aral Sea shows the importance

of the balance of the water.

2.2. Wave Modeling

As mentioned before, wave modeling has a crucial place in SWIO systems. Waves can damage pipe systems, especially intake part of pipes. One must consider whether wave breaking point is at an intake mouth or not. Because when waves break, there is turbulence which is an unwanted situation for an intake mouth. Wave modeling is needed to decide where the pipeline should be. At this point, the depth of water is the most important factor for wave propagation. Besides, breaking point also depends on the depth of water. That is why wave modeling is needed to simulate the effects of change of the CSL on SWIO systems.

SWAN (Simulating Waves Nearshore) is a third-generation wave model developed at Delft University of Technology to compute random, short-crested wind-generated waves in coastal regions. The SWAN model simulates depth-induced wave refraction and shoaling, current induced refraction and shoaling, depth and steepness induced wave breaking, diffraction, bottom friction, wind-wave growth, wave-induced set-up, wave-wave interaction and white capping that redistribute and dissipate energy in a growing wave field (SWAN User Manual, 2006). The formulation of SWAN is based on the spectral wave action balance equation. Reliability of SWAN is proved in many instances some of which are Hadadpour *et al.* (2013), Hadadpour *et al.* (2014), Rusu and Onea (2013), Mai *et al.* (1999), Booij *et al.* (1996), Rusu (2011) and Kamranzad *et al.* (2016).

Mai *et al.* (1999) have compared the numerical models with the experimental data and the field data for water waves in shallow coastal areas. SWAN is among the numerical models. According to results, the numerical models are in good agreement with the experimental data but there is a difference up to 30% between the field data and SWAN model because of the tidal currents.

The wave modeling with the addition of the ambient current was studied and compared with the field data by Booij *et al.* (1996). As shown in Figure 2.7, despite the underestimation of the mean period (T_m) by using SWAN, there is a good agreement between the field data and the numerical results. Furthermore, when the ambient current is considered, the results are better than the case without current.

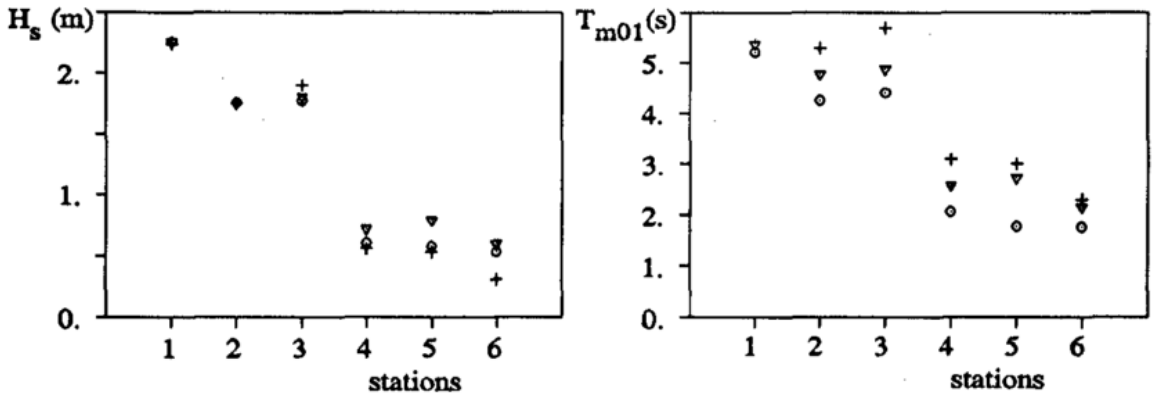

Figure 2.7. Computed and observed significant wave height (left panel) and mean wave period (right panel) at the observation stations for the flood current case in the Friesche Zeegat: (+) observations, (o) SWAN results, (∇) SWAN results without currents (Booij *et al.*, 1996).

Hadadpour *et al.* (2014) have predicted the wave parameters in Anzali, Caspian Sea using the SWAN model. After comparison with the field data, calibration and validation were done. Finally, linear transfer function and artificial neural network (ANN) were used to improve the modeled waves. The results showed that ANN is better than linear transfer function and SWAN is skilled to model the wave characteristics. Furthermore, Hadadpour *et al.* (2014) have used SWAN model wave characteristics to measure wave energy and to locate hot spots in Anzali, Caspian Sea. The comparison was made between the field data and the numerical model. Providing energy is generally harmful to the environment and renewable energy is a solution to this problem. Wave energy is one of the renewable energy resources. According to the results, they could specify the wave energy and hotspots using the SWAN. winter is found the most energetic season.

Rusu (2011) showed the performances of the numerical models for water waves, including SWAN. For this study, ocean (deep) and coastal (shallow) waters were considered. Numerical model results compared with the field data. In general, numerical models provide a good prediction of the wave characteristics in both deep and shallow water. One of this paper's results is shown in Figure 2.8. to illustrate the similarity between the numerical results and the field data. The best result is given by the simulation of the significant wave height.

Figure 2.8. Direct comparisons SWAN against B5 (H_s, T_m and mean wave direction), day 1-1996/11/01- day 98-1996/02/06, (TI-1) (Rusu, 2011).

Rusu and Onea (2013) and Kamranzad *et al.* (2016) have studied wave energy using the SWAN model in the Caspian Sea. Rusu and Onea (2013) also studied wind energy and validated the SWAN model with the satellite data. They found that the central part of the Caspian Sea is the most energetic part (Figure 2.9). Kamranzad *et al.* (2016) took the field data at 4 stations in the southern part. They compared the SWAN model results with these data. As a result, the central part of the southern Caspian Sea was found as the most suitable part for energy harvesting.

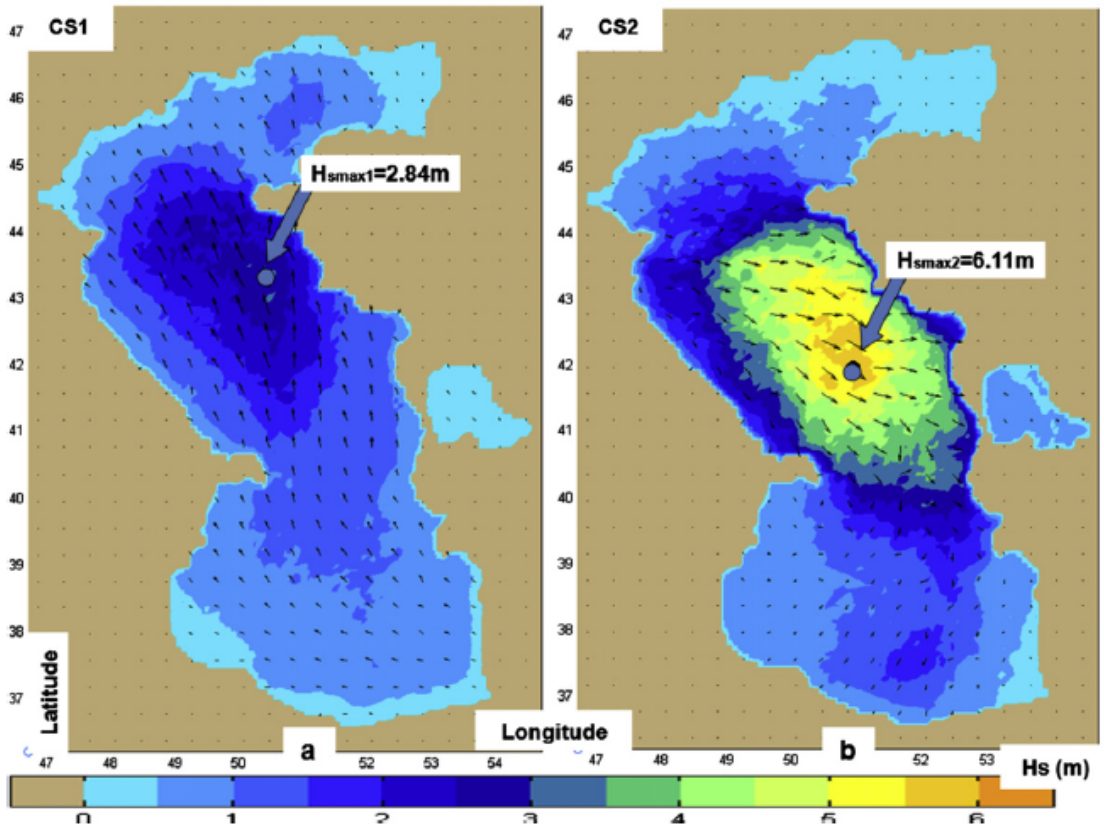

Figure 2.9. H_s analysis in the Caspian Sea for average energy case (left) and high energy case (right) (Rusu and Onea, 2013).

2.3. Thermal Dilution

Thermal dilution is conditioned by fluctuations of the CSL. When heated water is discharged to shallow water, thermal dilution may not be enough to meet regulations

because there will be less water which mixes with heated water. For this point of view, the decreasing CSL is a restrictor for thermal dilution. That is why one must simulate thermal dilution for the possible worst-case scenario.

Bath *et al.* (2004) have studied thermal discharge criteria from an evaporative cooling system of a large industrial project in King Bay, Australia. Regulation for such projects is generally strict due to environmental concerns. In this case, the temperature difference between the discharge and the ambient water must be less than 2^0C at the end of the outlet pipe but the system could not meet this criterion. That is why they studied what happens when the temperature difference is 6^0C. For this study, they considered near field (plume dispersion model) and far field (EFDC model) modeling of the discharged water with the additional cost analysis of the cooling towers. Besides, they researched for the most suitable diffuser design. Results showed that for the two different temperature criteria, there is the 0.2^0C difference at the end of the initial mixing zone where near-field modeling ends. Previous studies show that the fauna and infauna can tolerate temperature difference up to 2^0C above the ambient. For far fields modeling, the difference is less than 0.1^0C. As a conclusion, the biota in King Bay will not be affected by the discharge which has temperature 6^0C above the ambient.

Fossati *et al.* (2011) have modeled the thermal dilution of a power plant cooling water discharge in the Montevideo Bay. For the numerical model, they used RMA-10 (2D vertical integrated mode) which is based on finite elements. Calibration of the model was done with field data after the numerical modeling. They also considered the effect of the discharge on the intake and the effect of the currents. The study area is very shallow and there is no stratification so that 2D vertically integrated method works very well. After a comparison between the numerical model and the field data, it was clear that there is no need for hydrodynamic, thermal and power plant calibrations. As a result, the numerical modeling was satisfying.

CORMIX is a mixing zone model and decision support system for environmental impact assessment of regulatory mixing zones. In CORMIX, the importance of boundary interaction to provide steady-state mixing behavior and plume geometry

is emphasized (CORMIX User Manual, 1996). Reliability of CORMIX is approved in many articles some of which are Buvaneshwari *et al.* (2014), Al-Ghamdi (2010), Bleninger and Jirka (2004), Morelissen *et al.* (2013), Bleninger *et al.* (2010), Purnama and Bleninger (2011), Jirka *et al.* (1991) and Roberts (2011).

Buvaneshwari *et al.* (2014) have studied thermal dilution modeling of cooling water discharge into the closed Ennore creek located in Ennore, Chennai along the Coromandel Coast of the Bay of Bengal. In the study area, there is two strong types of flow: the ebb and flood flow. These are making changes for the study area such as closed creek mouth. Considering that situation, near-field modeling with CORMIX3 (surface discharge), far-field modeling with MIKE21 and diffuser design with Visual Plumes were studied. After numerical modeling, calibration was done. The temperature difference between the effluent and the ambient is found 4^0C at the Buckingham canal during flood tide and 5^0C during ebb tide at the creek mouth which is similar to the model results and temperature plots.

Al-Ghamdi (2010) has simulated Jeddah multiport sea outfall in the Red Sea using CORMIX (submerged multiport discharge mode) with average ambient conditions. It is found that when the effluent meets the regulations, the system with high dilution by high exit momentum and the convenient cross current does not harm the environment.

Bleninger and Jirka (2004) and Morelissen *et al.* (2013) have studied the dynamic coupling of the near field and far field models of wastewater discharge. CORMIX for the near-field model and DELFT3D for the far-field model were used in both two studies. Besides, Morelissen *et al.* (2013) have proved the numerical modeling with laboratory experiments. They have concluded that dynamic coupling gives reliable results and CORMIX is favorable for the near-field model.

Bleninger *et al.* (2010) have studied desalination plant discharges. Reducing environmental impact was based on the study. The multiport diffuser is found the most suitable way to increase initial dilution. CORMIX and DELFT3D are considered

as effective ways for the near-field model and far-field model, respectively. Dynamic coupling of these two numerical models is found significant to evaluate the effect of discharge beyond the initial mixing zone.

Purnama and Bleninger (2011) have simulated the brine discharge of Barka Plant, Oman using CORMIX for two scenarios. Because discharges of brine water and heated water from two different plants are united. According to CORMIX results, they found that the regulations are met with this method.

Roberts (2011) has studied diffusers for thermal discharges using numerical modeling and laboratory experiment. The momentum and the buoyancy of the discharge considerably affect dilution. The momentum of the discharge depends on the diffuser configuration. It is found that diffusers can easily mix the heated discharge with the ambient water and help the mixed water meet the regulations.

Jirka *et al.* (1991) have considered the hydrodynamic classification of submerged multiport diffuser discharges. To achieve high initial dilution and meet the regulations, the hydrodynamic classification of submerged multiport diffuser system with respect to flow type, density, and temperature stratifications and type of wastewater is important. This research is valid for CORMIX2. Figure 2.10. shows three major diffuser types. One can find the best diffuser type considering the conditions of his/her case to reach high dilution.

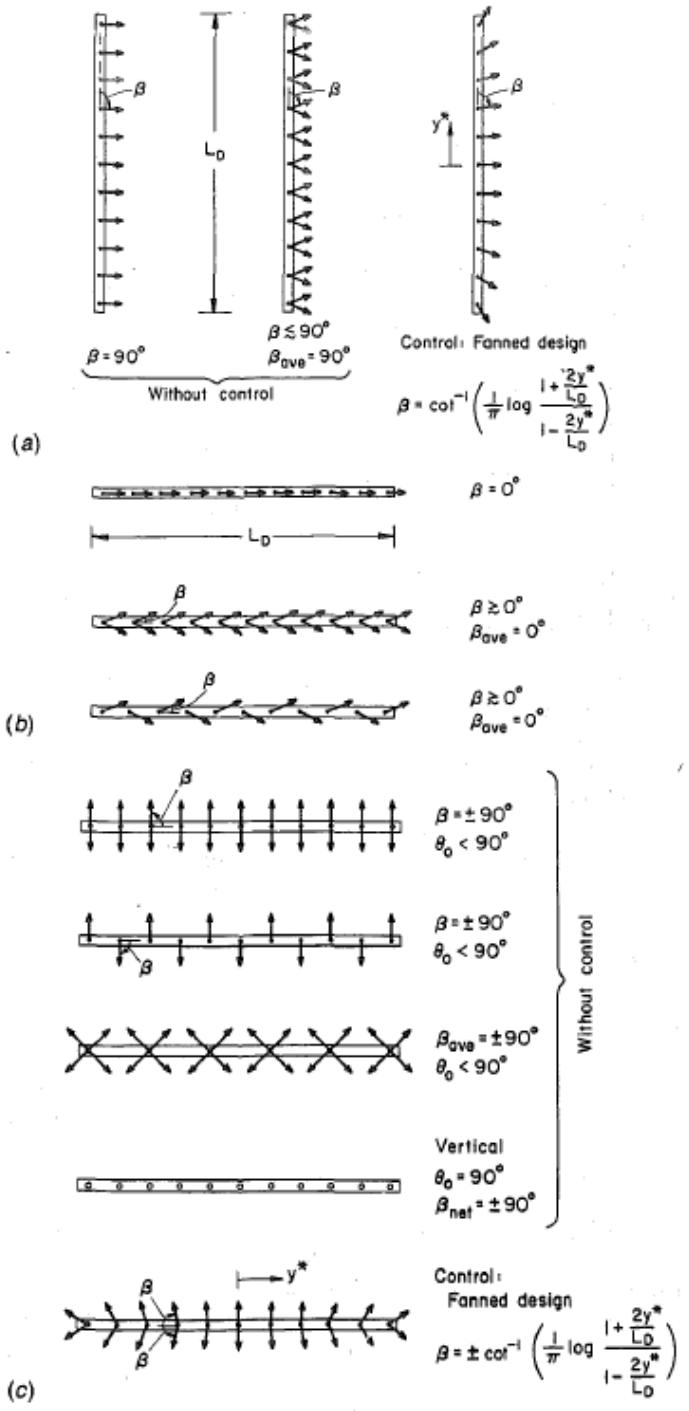

Figure 2.10. Three major diffuser types for multiport diffusers: (a) Unidirectional; (b) Staged; (c) Alternating (Jirka *et al.*, 1991).

3. METHODOLOGY

To predict the feasibility of the SWIO system and its effect on the CS, firstly, the CSL change over a monthly time interval is predicted between 2016 and 2100 with a ten-year interval using RMA2 model with the monthly Volga River discharge, precipitation, evaporation, discharge to KBG and wind data. After that, SWAN and CORMIX models are run using the yearly averaged local CSL to predict nearshore wave climate and thermal dilution with a ten-year time step at the project area, respectively. Because there are some criteria for safe operation which are wave breaking at discharge or intake points and exceeding 3^0C temperature rise at 100 m downstream. Furthermore, the plume should not touch the shoreline because it will cause the accumulation of heated water. Besides, if there is a serious decrease in the sea level, the system will be exposed.

This chapter gives the CSL change analysis for the past 85 years, the input data for the RMA2, SWAN and CORMIX models and the methodology applied to predict sea level change, nearshore wave climate and thermal mixing in the next century. In the end, a brief chart and time loop chart summarize the methodology and the connection between the models.

3.1. Prediction of Sea Level Change in the Next Century

The yearly CSL changes in terms of m-BSL between 1930 and 2015 are shown in Figure 2.2. According to this figure, the average value is -27.80 m-BSL. Maximum and minimum values are -26.16 m-BSL in 1932 and -29.07 m-BSL in 1977, respectively. The range of the variation is 2.91 m for 85 years, which is a critical amount. The choice of Bekdash Station is because it is the closest station with a century long historical data.

Monthly CSL changes between 1930 and 2015 are shown in Figure 3.1. According to this figure, the CS has its maximum value in summers and the minimum value in winters. The maximum and minimum differences summer and winter levels within the

same year are in 1932 and 2001 with the differences of 54 cm and 2 cm, respectively. The yearly and monthly data are merged into one data set to better understand the time scales in CSL changes (Figure 3.2). This new data set shows that the sea level indicates both seasonal but also episodic (long-term) variations of the CSL. The maximum and minimum levels are recorded in July 1932 and in November 1977, respectively. In general, the highest water level occurs in summer and the lowest level occurs in winter.

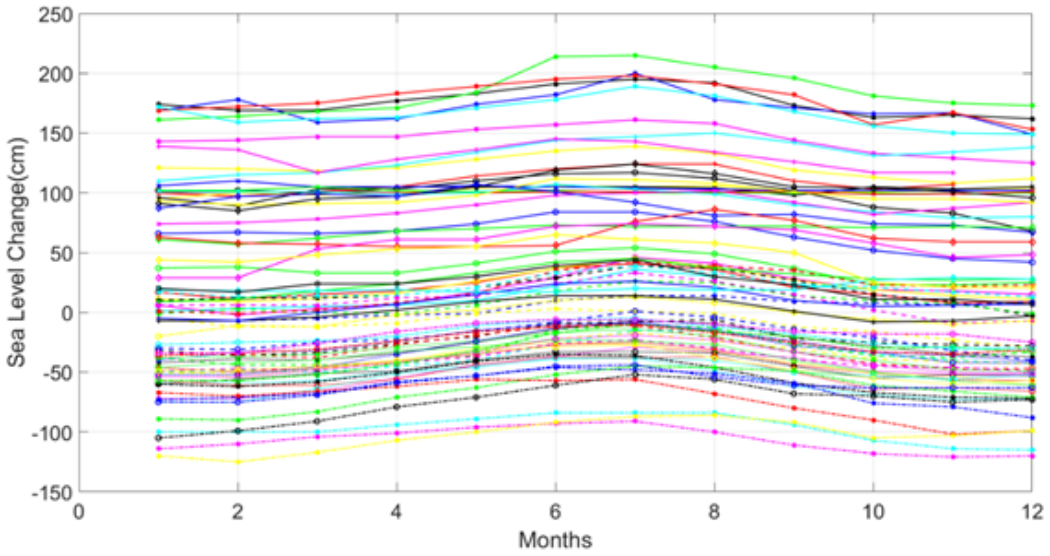

Figure 3.1. The monthly CSL changes between 1930 and 2015. Data is taken from Coordinating Committee on Hydrometeorology of the Caspian Sea (CASPCOM), Bekdash Station.

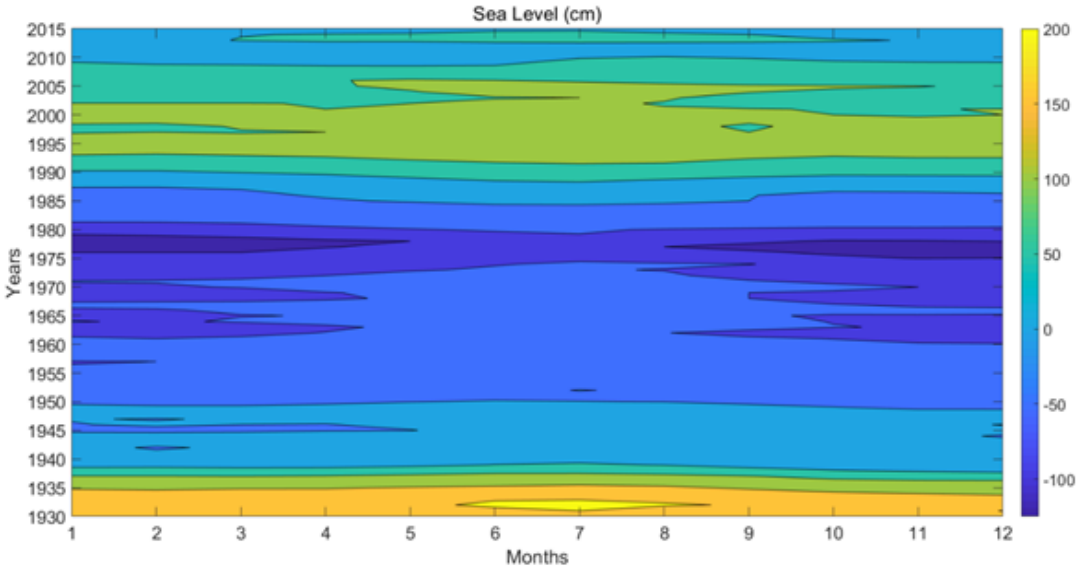

Figure 3.2. The combination of the yearly and monthly CSL changes. Data is taken from Coordinating Committee on Hydrometeorology of the Caspian Sea (CASPCOM), Bekdash Station.

As mentioned before, climate change will seriously affect the Caspian Sea level (Elguindi and Giorgi 2006; Renssen *et al.* 2007; Roshan*et al.* 2012). To predict the sea level change, RMA2, a two-dimensional depth-integrated finite element hydrodynamic numerical model (Users Guide for RMA2 Version 4.5, 2011), is used in this thesis. RMA2 solves the equations of mass and momentum conservation in two horizontal directions. To define turbulence characteristics and bottom friction, eddy viscosity coefficients and Manning's equation are used, respectively. RMA2 can solve both steady and dynamic problems. In this thesis, dynamic mode is used. The governing equations are the momentum conservation in x direction Equation 3.1, the momentum conservation in y direction Equation 3.2 and the mass conservation Equation 3.3.

$$h\frac{\partial u}{\partial t} + hu\frac{\partial u}{\partial x} + hv\frac{\partial u}{\partial y} - \frac{h}{\rho}\left[E_{xx}\frac{\partial^2 u}{\partial x^2} + E_{xy}\frac{\partial^2 u}{\partial y^2}\right] + gh\left[\frac{\partial a}{\partial x}\frac{\partial h}{\partial x}\right] + \frac{gun^2}{\left(1.486h^{\frac{1}{6}}\right)^2}\left(u^2+v^2\right)^{\frac{1}{2}} - \varsigma V_a^2 cos\psi + 2hvwsin\Phi = 0 \tag{3.1}$$

$$h\frac{\partial v}{\partial t} + hu\frac{\partial v}{\partial x} + hv\frac{\partial v}{\partial y} - \frac{h}{\rho}\left[E_{yx}\frac{\partial^2 v}{\partial x^2} + E_{yy}\frac{\partial^2 v}{\partial y^2}\right] + gh\left[\frac{\partial a}{\partial y}\frac{\partial h}{\partial y}\right] + \frac{gvn^2}{\left(1.486h^{\frac{1}{6}}\right)^2}\left(u^2+v^2\right)^{\frac{1}{2}} - \varsigma V_a^2 sin\psi + 2huwsin\Phi = 0 \tag{3.2}$$

$$\frac{\partial h}{\partial t} + h\left(\frac{\partial u}{\partial x} + \frac{\partial v}{\partial y}\right) + u\frac{\partial h}{\partial x} + v\frac{\partial h}{\partial y} = 0 \tag{3.3}$$

where h is water depth, x and y are Cartesian coordinates, t is time, u and v are velocities in the x and y directions, ρ is the density of the fluid, E_{xx}, E_{yy}, E_{xy}, and E_{yx} are respectively eddy viscosity coefficients for normal direction on x surface, normal direction on y surface and shear direction on each surface, g is the gravity acceleration, a is bottom elevation, n is the Manning's roughness n-values, 1.486 is the coefficient to convert from SI units to non-SI units, ζ is empirical wind shear coefficient, V_a is wind speed, ψ is wind direction, ω is rate of Earth's angular rotation, and Φ is local latitude.

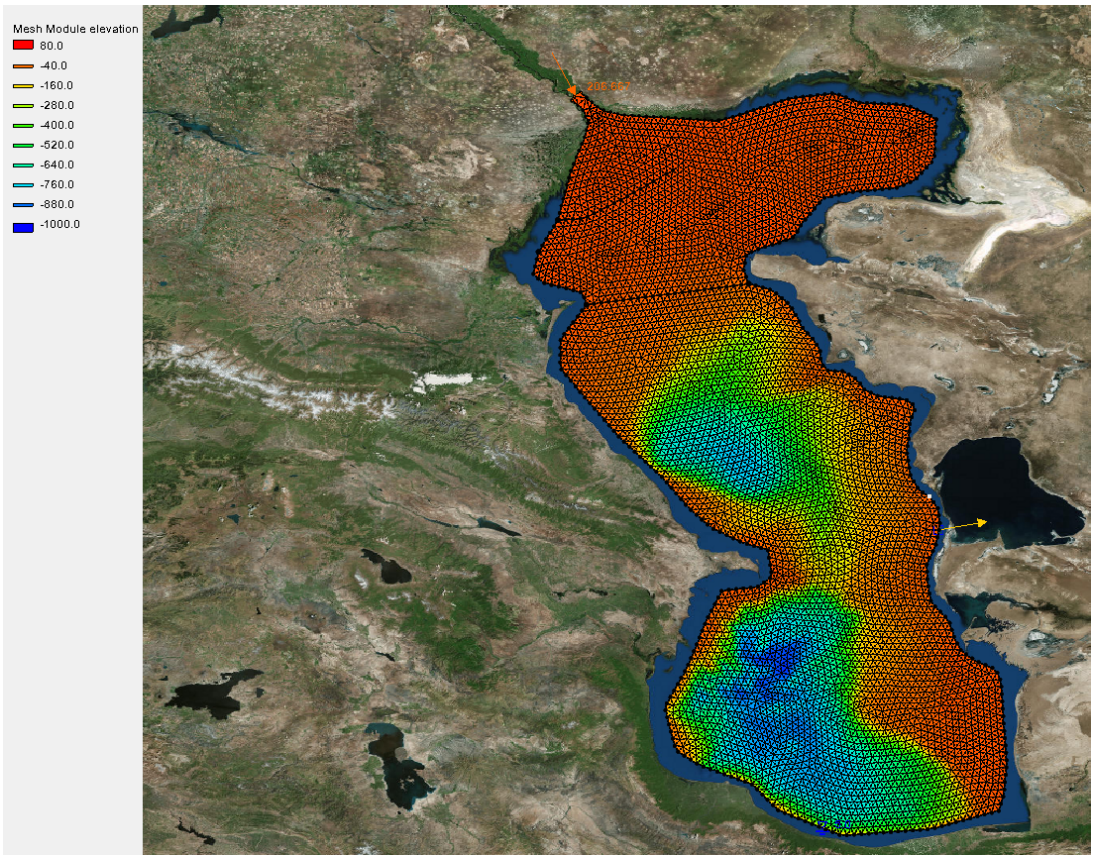

Figure 3.3. RMA2 model of The Caspian Sea.

The RMA2 model of the Caspian Sea consists of triangular mesh type with 8204 quadratic elements and 16759 nodes. Bathymetry data is taken from Satellite Geodesy (Satellite Geodesy, 2019). Its spacing is 1.002' for West-East direction and 0.684' for North-South direction. The minimum elevation is -959.02 m and the maximum is 4.93 m (Figure 3.3). The reason for taking 4.93 meters as the maximum value is the consideration of the Volga River in the model mesh area. RMA2 allows taking the maximum value as the possible minimum value for water elevation head. Therefore, the water elevation head is taken as 5 m at the south part of the Caspian Sea. Otherwise, the solution does not converge because of the possible dry conditions.

The annual water discharge to the Bay of Kara-Bogaz-Gol is taken from Aladin *et al.* (2012). The European Center for Medium-Range Weather Forecasts (ECMWF, 2019) ERA-Interim monthly data set is used to take wind speeds u and v at 10 m above the sea surface, and precipitation and evaporation data for 2016. To obtain the Volga River runoff data for 2016, CASPCOM (CASPCOM, 2018) is used.

Before the sea level prediction for the next century, an eleven-year prediction with 2005 data for 2016 is conducted to obtain the percentage of error in RMA2. Sources for the data is the same as indicated above except the annual discharge to the Bay of Kara-Bogaz-Gol. It is taken as 264.27 m^3/s (Renssen *et al.*, 2007). According to the recorded data by ECMWF, there is 10.5 cm decrease in the Caspian Sea level per year between 2005 and 2016 (Figure 2.2). It is found that there is 11.2 cm/yr decrease for the same period in the model results. Therefore, there is 6.7% error in the RMA2 model results.

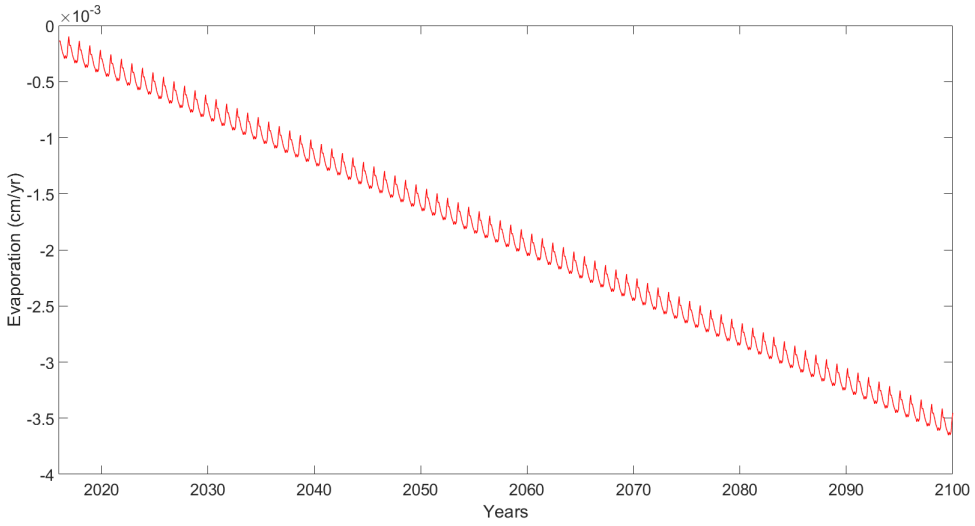

Figure 3.4. Evaporation input data for RMA2 based on Roshan *et al.* (2012) and ECMWF (2019).

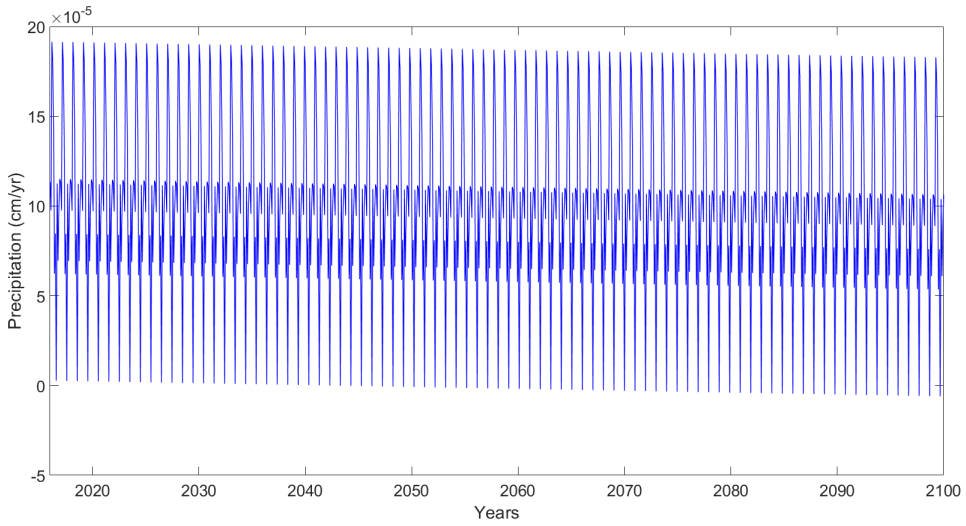

Figure 3.5. Precipitation input data for RMA2 based on Roshan *et al.* (2012) and ECMWF (2019).

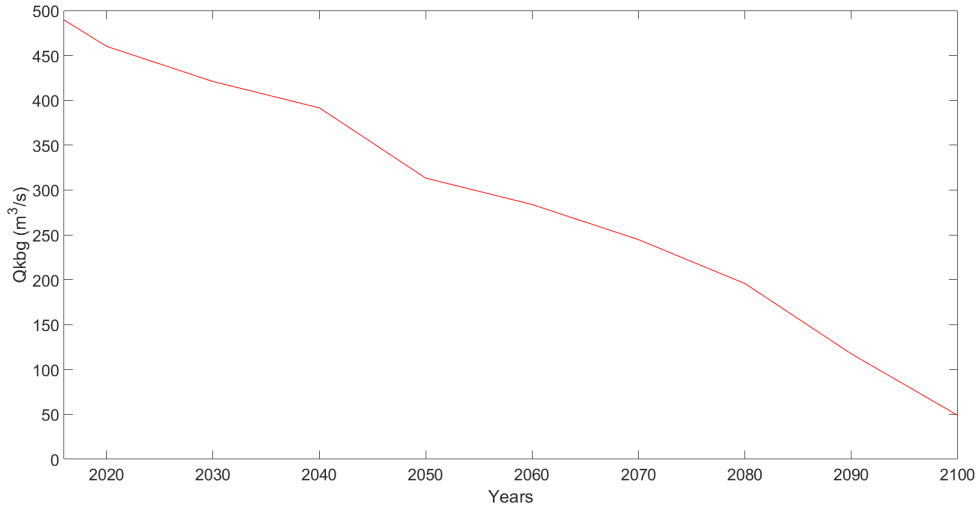

Figure 3.6. Discharge input data to the Bay of Kara-Bogaz-Gol for RMA2 based on Aladin *et al.* (2012).

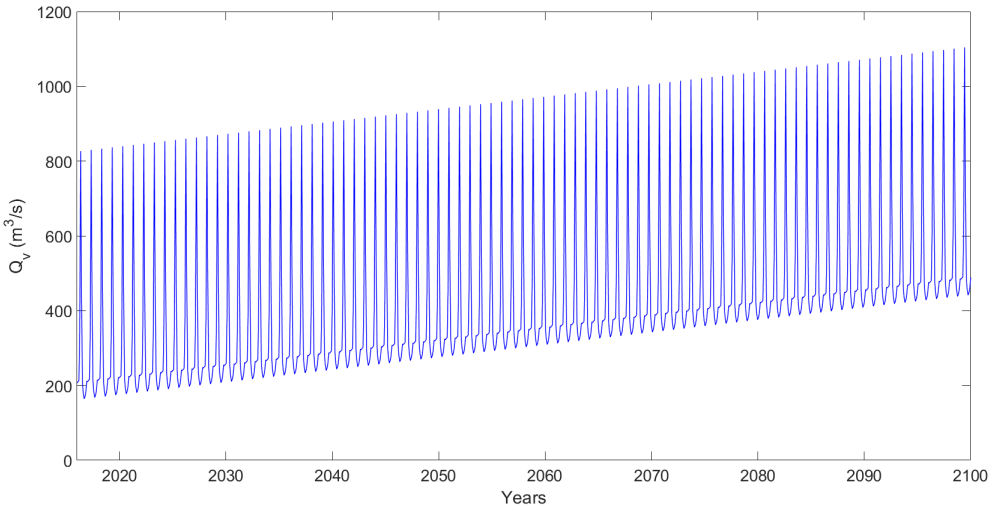

Figure 3.7. Volga River runoff input data for RMA2 based on CASPCOM (2018) and Renssen *et al.* (2007).

For the analysis of the next century's sea level, wind climate is assumed to be the same. Precipitation and evaporation data, the Volga River runoff data, and the annual discharge to the Bay of Kara-Bogaz-Gol are analyzed according to Roshan *et al.* (2012), Renssen *et al.* (2007) and Aladin *et al.* (2012), respectively. Figure 3.4 to 3.7 show the input data used for the years between 2016 and 2100.

RMA2 is run for 2016, 2020, 2030, 2040, 2050, 2060, 2070, 2080, 2090, and 2100. The sea level changes between these years are kept the same. For example, the sea level change for 2016 is assumed valid for 2017, 2018, and 2019.

3.2. Prediction of Nearshore Wave Climate in the Next Century

In the previous section, it is seen that climate change leads to a dramatic decrease in the Caspian Sea level, which consequently affects the wave climate. When it comes to coastal structures, wave parameters such as wave height, breaking wave point, etc., have the most important role in the sustainability of coastal structures. For that reason, it must be considered that in the future, these structures may not be feasible regarding to the wave climate at these structures' site. To examine this threat, the sample case of the Garabogaz Ammonia and Urea Production Plant is discussed according to the results of RMA2 modeling.

A consortium of GAP Construction Co. (GAP) and Mitsubishi Heavy Industries (MHI) has constructed a Seawater Intake Outfall (SWIO) system to provide cooling water to the Garabogaz Ammonia and Urea Production Plant from the Caspian Sea. For this project, numerical wave modeling was conducted by Boğaziçi University Coastal Engineering Laboratory (BUCEL) to study wave agitation along the SWIO according to the given data for the hydraulic and structural design, construction methods, wind, wave and soil conditions by MHI, GAP, STFA, MCG, CEC and ERBAŞI.

SWAN (2006), a third-generation wave model, developed at Delft University of Technology to compute random, short-crested wind-generated waves in coastal regions, is used. To see both the effect of the far field deep water conditions referred as the coarse mesh and near field bathymetric conditions referred as the fine mesh, a nested grid is employed by BUCEL (Otay and Uzun, 2018). For the coarse mesh, a grid area of 50 km x 30 km with a bathymetric grid resolution of 500 m x 500 m a computational grid resolution of 100 m x 100 m is used. For the fine mesh, a grid area of 7 km x 5 km with a bathymetric grid resolution of 50 m x 50 m a computational grid resolution of 25 m x 25 m is used.

The bathymetry data shown in Figure 3.8 is taken from Navionics (2018). To conceive the worst case scenario, the offshore extreme wind and wave conditions given by the companies are used and it is seen that the worst scenario among eleven scenarios is SSW wind and wave directions, 23.7 m/s wind speed, 5.7 m significant wave height and 10 s peak wave period which is the 100 year return period extreme wave characteristics at the BMT Argoss (2014) data point. After all, in today's conditions, the design wave height of 3 m is not exceeded and wave breaking points are not at the intake or discharge points for all scenarios.

Table 3.1. Fine mesh SWAN wave input data

Years	H_s (m)	T_p (s)	θ (CCW form x axis)
2016	3.42	10	48.94
2020	3.23	10	45.39
2030	2.54	10	46.09
2040	1.93	10	46.29
2050	1.29	10	48.48
2060	0.75	10	48.20
2070	0.22	10	52.18

In this thesis, the worst case scenario for wave characteristics is taken into account with different sea level conditions resulted from the RMA2 model for 2020, 2030, 2040, 2050, 2060 and 2070. For these years, both the coarse and fine meshes are used to obtain the nearshore wave climate. The reason for the absence of the SWAN models of the years 2080, 2090 and 2100 is that the intake and discharge pipelines will be no longer in the sea according to the results of RMA2. The water level for 2016 is considered as mean sea level (MSL) which is -28 m-BSL because the predicted averaged sea level values are used for the next century. Fine mesh wave input data for all years resulted from the coarse mesh SWAN models are shown in Table 3.1.

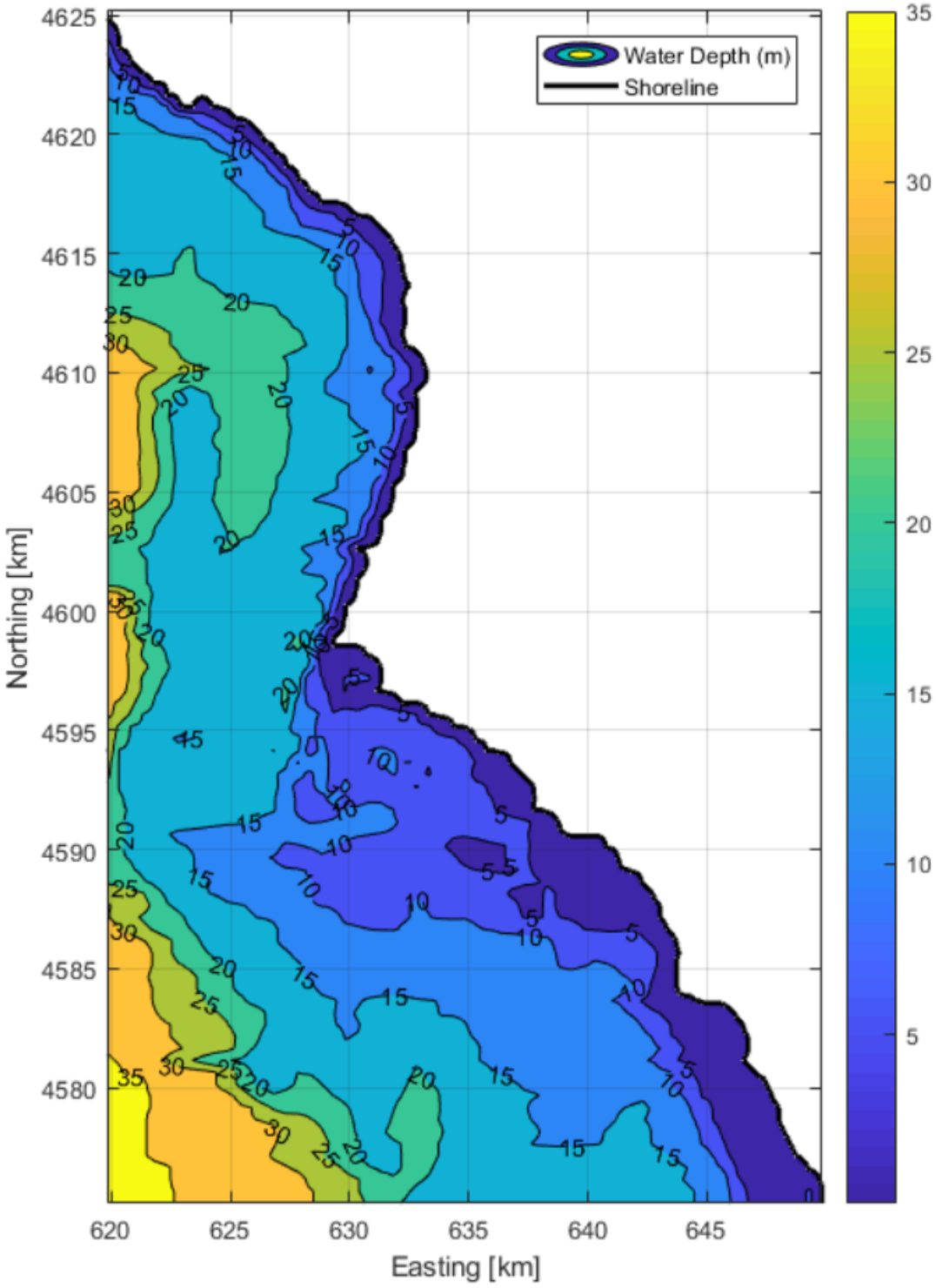

Figure 3.8. Bathymetry data for 2016 (Otay and Uzun, 2018).

3.3. Prediction of Thermal Mixing in the Next Century

Thermal dilution modeling has to be done when there is a SWIO system. It is important for the flora and fauna around the SWIO site. The thermal dilution analysis for the SWIO system is conducted by BUCEL (Otay and Uzun, 2018) to study the excess temperature due to the discharge of heated water and the mixing processes. After modeling all possible diffuser angles, tidal water levels, and ambient current velocities, it is seen that the design criteria for thermal dilution at the discharge location are satisfied in today's condition. CORMIX (Jirka *et al.* ,1996) is used to model thermal dilution. However, decreasing sea level seriously affects thermal mixing process, which must be considered when there is a SWIO system. To examine the effect of the sea level decrease, CORMIX model submerged multiport diffuser mode (CORMIX2) is run with the predicted average sea levels for the next century.

Summer conditions are taken into account to examine the worst case scenario because of the highest water temperature. The ambient water temperature and the discharged water temperature are taken as 28^0C and 38^0C, respectively. The diffuser line and port alignment, the number of ports, the ambient current direction taken as the positive x axis, the diffuser length and the distance from the shoreline for 2016 are shown in Figure 3.9. The ambient current direction is 330.5^0 counterclockwise from x axis for all years. The ambient current magnitudes resulted from RMA2 model for all years are shown in Table 3.2 where HA is average water depth, HD is the depth at the port, YB1 and YB2 are the distances from shoreline to the nearest and furthest points of the diffuser line, θ is the angle between port centerline and horizontal, σ is the angle measured counterclockwise from the ambient current direction to the plan projection of the port centerlines, β is the angle between the diffuser line and the port centerline, γ is the angle measured counterclockwise from the ambient current direction to the diffuser line and NOPEN is the number of the ports.

For the CORMIX models, wind magnitude as an input data is taken as 9.48 m/s which is the averaged value resulted from RMA2 models at the construction site. Considering the decreasing water level and its effects on the distance between the diffuser

axis and the shoreline, CORMIX is run for 2016, 2020, 2030, 2040, and 2050 because the system does not satisfy a submerged multiport diffuser criterion for the other years until 2100. After 2060, it becomes a surface discharge. Furthermore, there must be done some changes in parameters such as average depth and port height for 2040 and 2050 because CORMIX2 can run in two conditions which are deeply submerged discharge or slightly submerged discharge. To meet this criterion of CORMIX2, the averaged depth is taken as 2.2 m instead of 3.3 m for 2050 and the averaged depth and the port height are taken as 3.5 m and 1 m instead of 4.9 m and 1.5 m for 2040, respectively. Thus, the system satisfies the slightly submerged discharge criterion because parameters must be far away from the real values of those parameters to make the system a deeply submerged discharge again. Besides, making it a deeply submerged discharge causes a decrease in the factor of safety and makes the effect of the decreasing water level diminished.

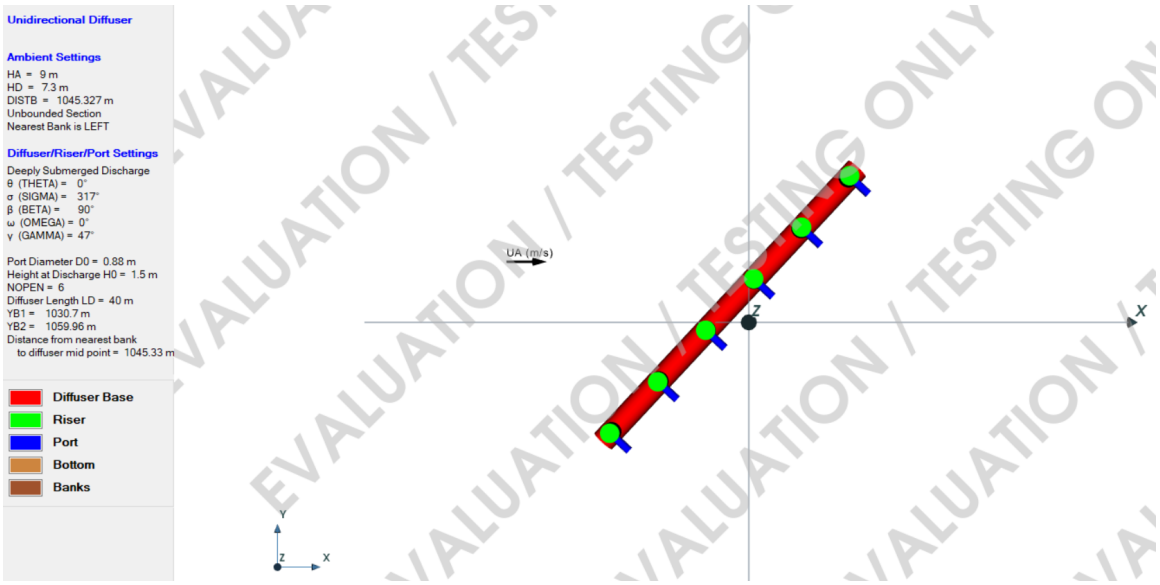

Figure 3.9. The diffuser alignment for 2016.

Table 3.2. The ambient current magnitudes for all years

Years	**Ambient Current Magnitude** m/s
2016	0.20
2020	0.19
2030	0.18
2040	0.15
2050	0.17
2060	0.18

3.4. Summary Chart of the Methodology

A brief chart of the methodology is given in Figure 3.10. Climate change affects the CSL in the future. That is why, the CSL is predicted using RMA2 and its result is imported as an input data to both SWAN and CORMIX. Finally, the feasibility of the system in terms of both operational and environmental aspects is discussed.

A summary chart indicating time steps is shown in Figure 3.11. Using interpolation, decadal climate change data (precipitation, evaporation, the Volga River runoff and outfall to the KBG) from big model (Renssen et al., 2007; Aladin et al., 2012; Roshan et al., 2012) are applied to monthly hydrodynamic model (RMA2) once every decade. Thus, the monthly CSL change in one year is found and the yearly averaged CSL change is calculated. After that, the yearly averaged CSL change is assumed to be the same for the years between the predicted years and the new CSL is calculated to use in the wave model (SWAN) and thermal mixing model (CORMIX). This process is repeated for every ten years between 2016 and 2100.

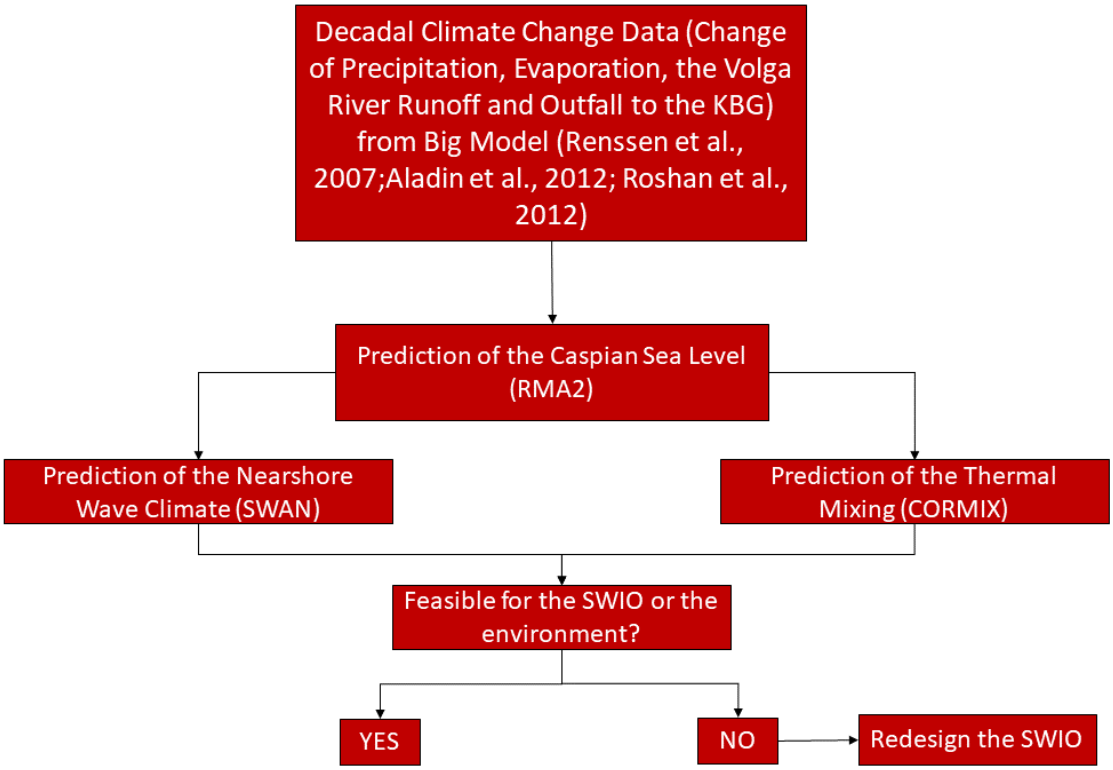

Figure 3.10. Summary Chart of Methodology.

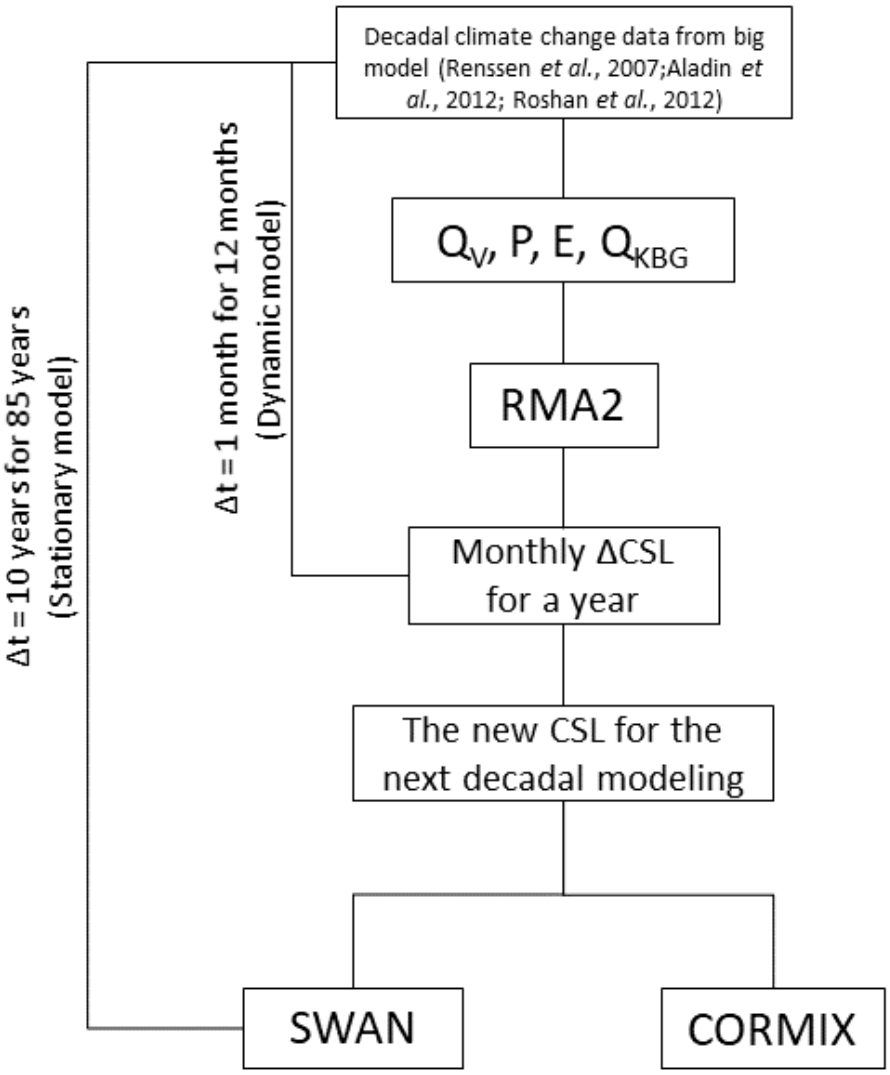

Figure 3.11. Summary chart with time steps.

4. RESULTS AND DISCUSSION

This chapter gives the results of RMA2, SWAN and CORMIX models and what is expected to happen due to climate change in the next century. It also gives a brief discussion about the process of the decrease in the sea level and its effects on nearshore wave climate and thermal mixing.

4.1. The Caspian Sea Level Results and Comparison

After modeling the mentioned ten years, the predicted Caspian Sea levels at the end of these years are shown in Table 4.1. While calculating the new sea level for another run, it is assumed that the change will be the same for the ten years between two modeled years but the rate of decrease is getting smaller due to an the increase in the Volga River runoff and decrease in the outflow to the KBG.

Table 4.1. RMA2 model results

Years	LWL Change (cm)	CSL Change (cm)	LWL (m-BSL)	CSL (m-BSL)
2016	-18.4	-18.2	-28.18	-28.18
2020	-17.5	-17.2	-28.92	-28.91
2030	-16.5	-16.3	-30.67	-30.63
2040	-15.7	-15.5	-32.32	-32.26
2050	-13.0	-12.9	-33.89	-33.81
2060	-12.	-11.7	-35.19	-35.10
2070	-10.5	-10.4	-36.39	-36.27
2080	-8.4	-8.3	-37.44	-37.31
2090	-4.9	-5.1	-38.28	-38.14
2100	-1.8	-2.0	-38.79	-38.67

It is concluded that melting ice covers and rise of the precipitation rate over the Volga River due to the climate change will lead to a rise in the Volga River runoff to the Caspian Sea (Roshan *et al.*, 2012). It is observed that as the Caspian Sea level decreases, the outflow to the KBG also decreases (Aladin *et al.*, 2012). Because evaporation over the KBG is big and the Caspian Sea feeds it as it loses its water. Therefore, the water resource for the KBG is the Caspian Sea and the more water the Caspian Sea has, the more water the KBG gets.

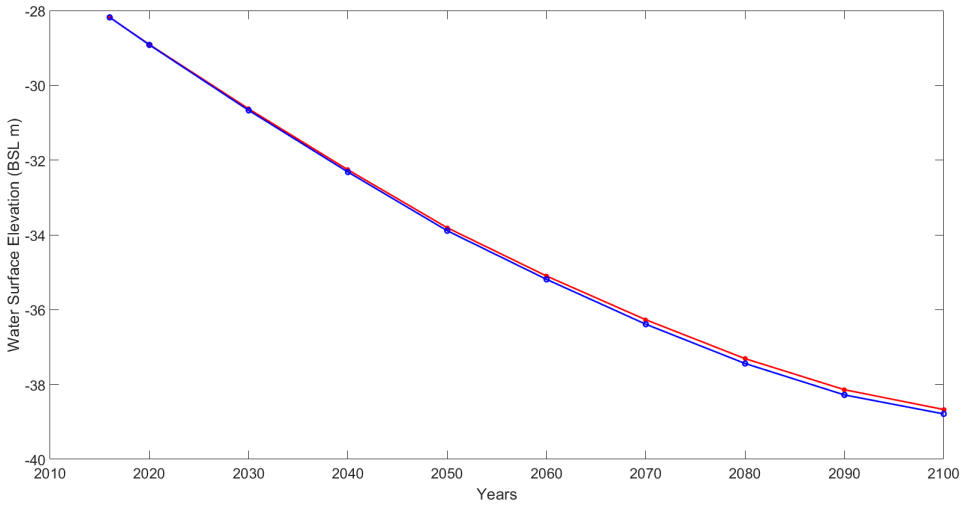

Figure 4.1. CSL and LWL from 2016 to 2100.

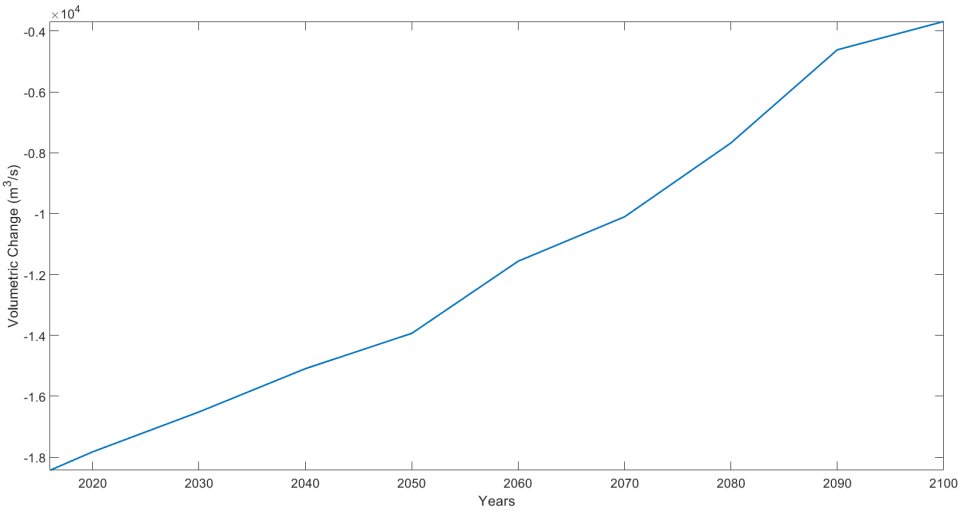

Figure 4.2. The yearly averaged total volumetric change in the CS.

As shown in Figure 4.2, the yearly averaged total volumetric change in the CS indicates a decreasing decrease trend. Because as the surface area of the CS decreases, the area affected by evaporation is getting smaller, which causes less volumetric loss due to evaporation decreases. Furthermore, discharge to the KBG is dependent of the CSL. As the CSL falls, discharge to the KBG also decreases. It may be concluded that, after a while, the CSL may start rising in the future.

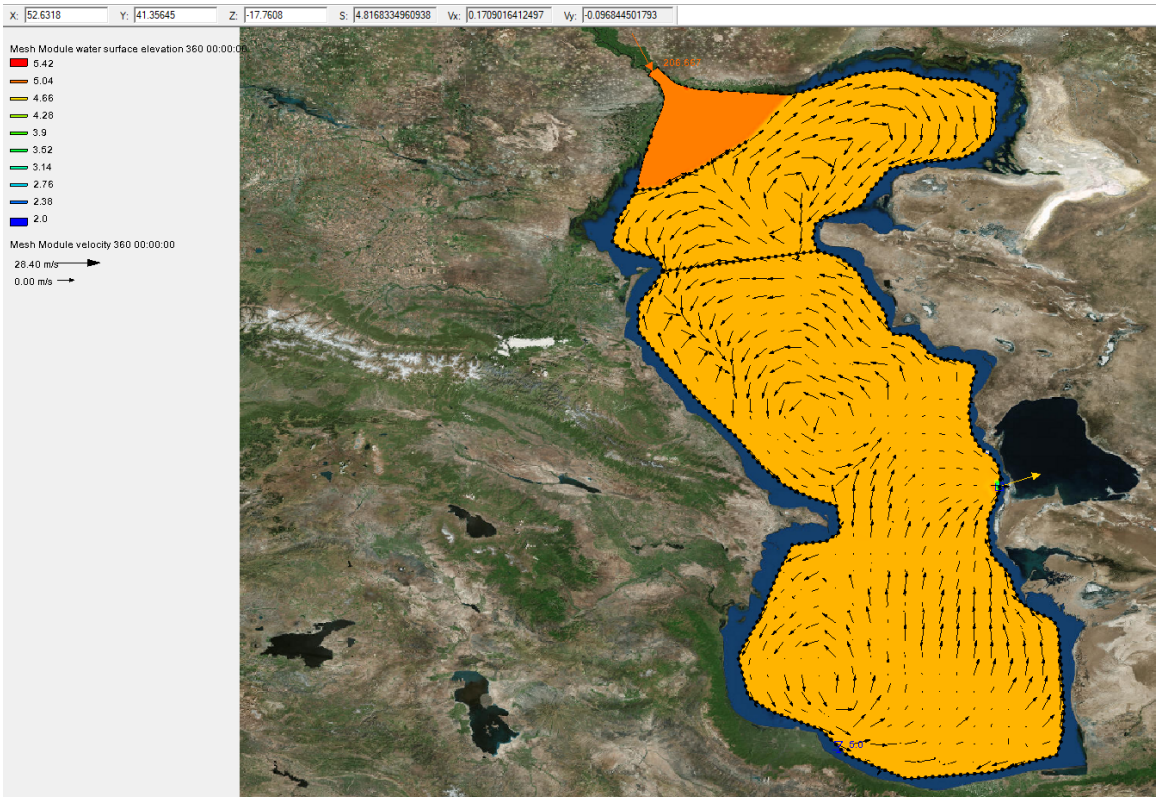

Figure 4.3. The predicted Caspian Sea level at the end of 2016 and the SWIO location.

As it is seen, a dramatic 10.67 m decrease in the Caspian Sea level is predicted at the end of 2100. To be more clear, it is also shown in Figure 4.1. To show the RMA2 output image for 2016, Figure 4.3 is used. the RMA2 output images of the other years are similar with 2016 except the decrease values which are indicated in Table 4.1. Furthermore, the predicted CS depth in 2100 is shown in Figure 4.4.

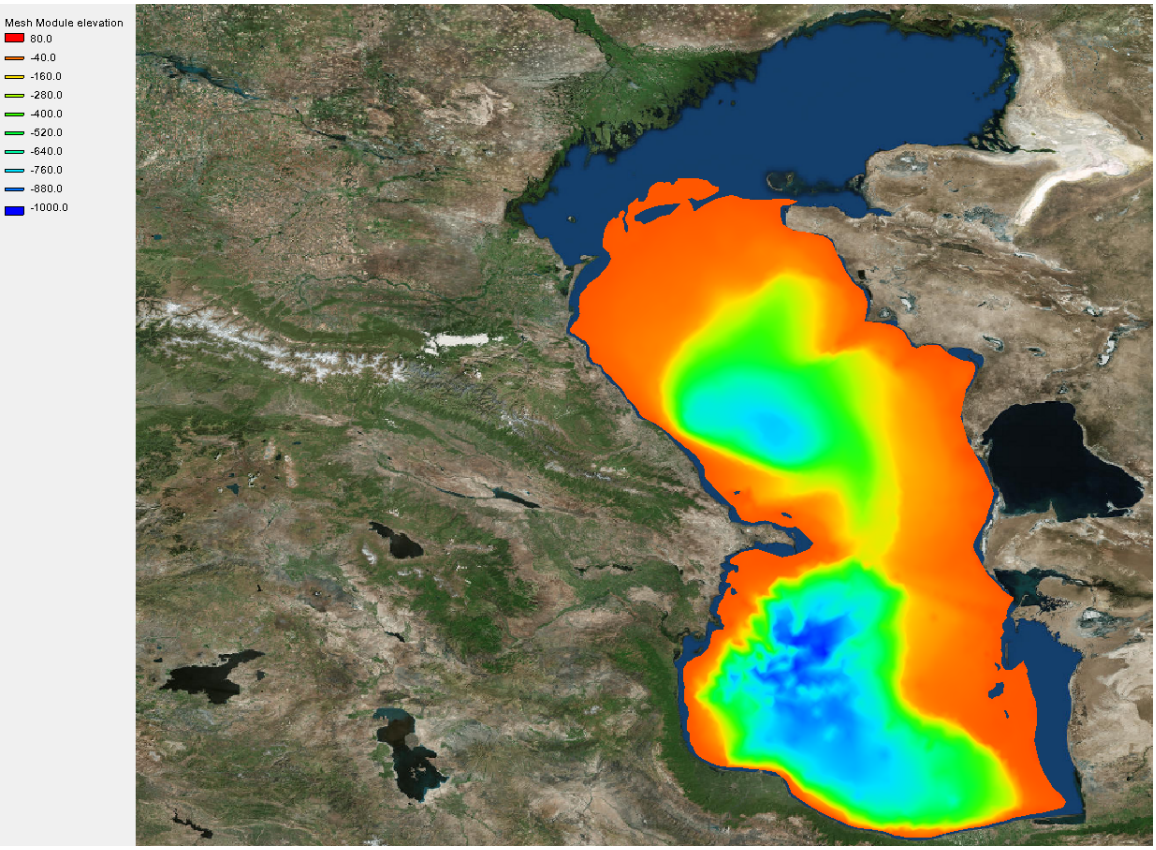

Figure 4.4. The predicted Caspian Sea depth in 2100.

Months of December, May and August are chosen and shown in Figure 4.5 for the monthly mean surface currents in order to compare with Figure 4.6. The models are quite similar. There are some discrepancies among the east coast current pattern. The reason for that may be the magnitude of outflow to the KGB because the data between 1900 and 1990 (Aladin *et al.*, 2012) is taken into account and it is higher compared to the data of Figure (Ibrayev *et al.*, 2010). Due to this outflow, circulation is changing its direction on the middle of the east coast.

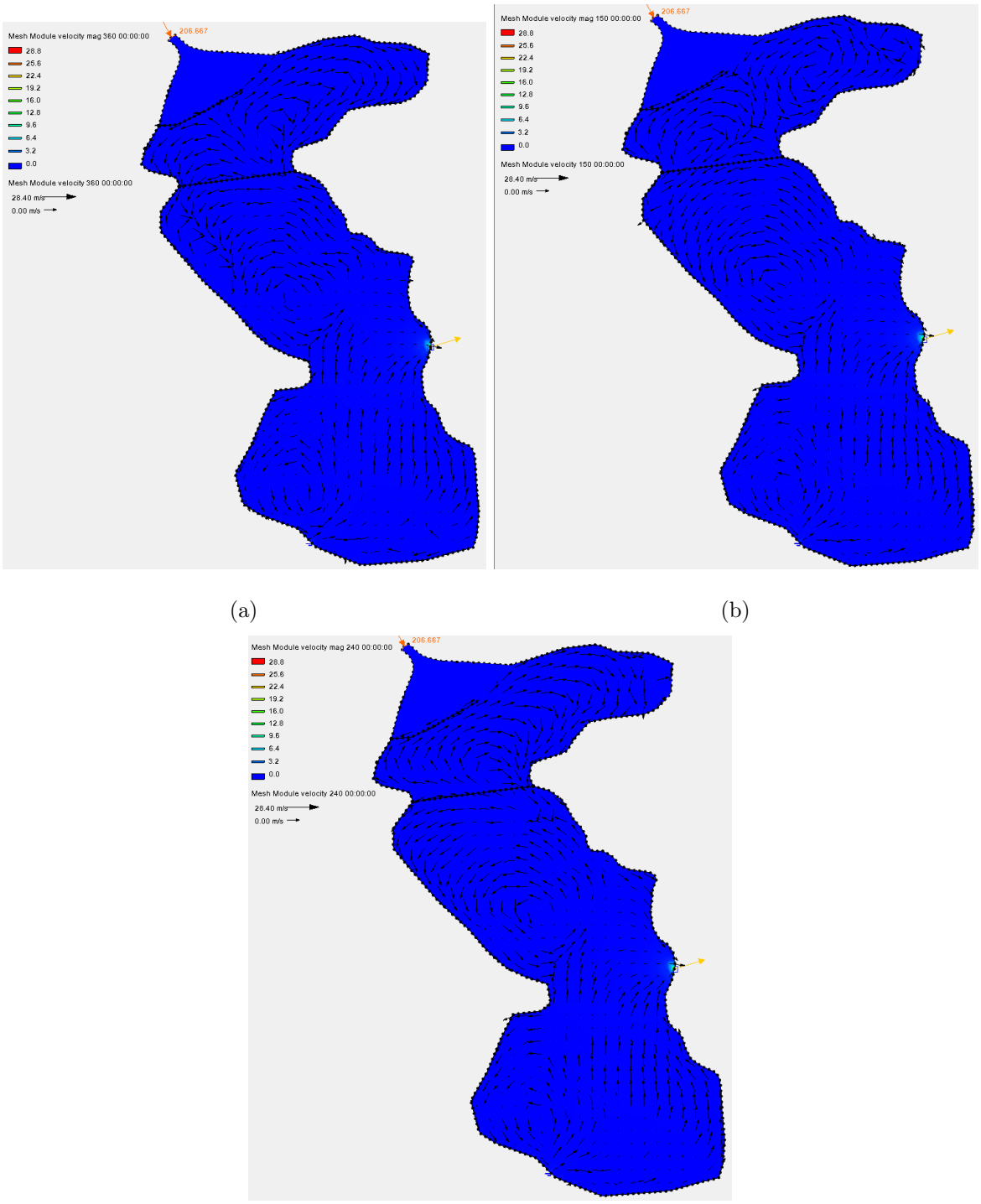

(a) (b)

(c)

Figure 4.5. Mean surface currents (m/s) for (a) December, (b) May and (c) August.

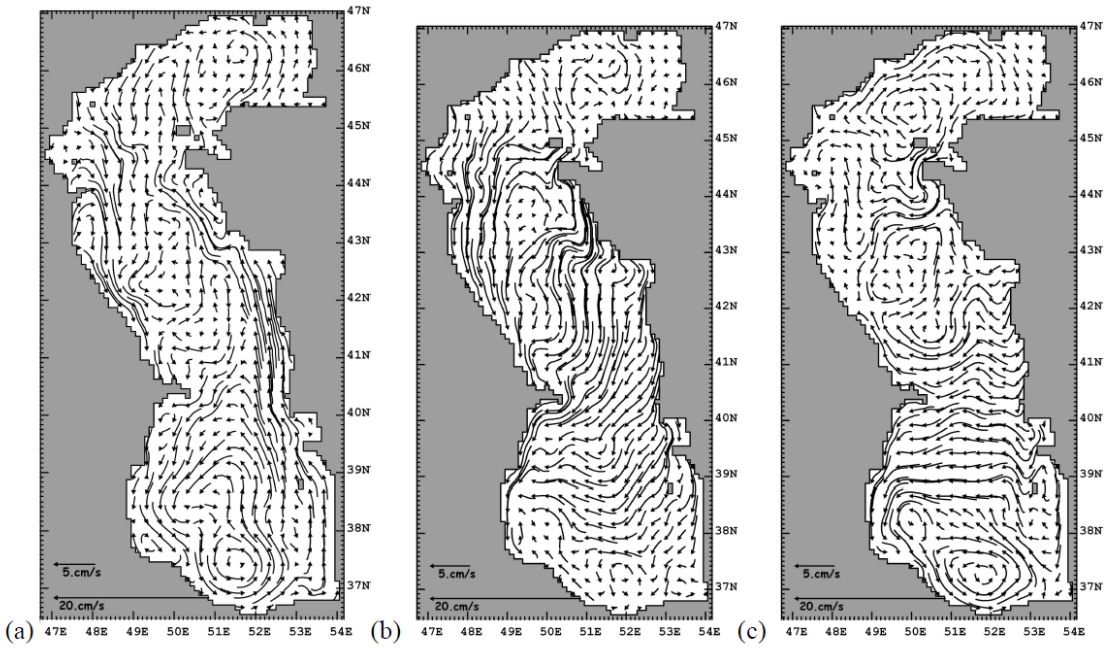

Figure 4.6. Mean surface currents (cm/s) for (a) December, (b) May and (c) August (Ibrayev *et al.*, 2010).

4.2. Nearshore Wave Climate Results and Comparison

Nearshore wave climate at the SWIO area is modeled for all years except 2080, 2090 and 2100. Because the area where the SWIO pipes are placed will dry out. Even if the pipeline seems to be in the sea, in fact, the pipes will be in a place that has become a pond without a connection with the sea in 2070. So that, the SWIO system will have a serious problem before 2070. Figure 4.7 shows the fine mesh SWAN results for the years of 2050, 2060 and 2070 to illustrate the location of the pipeline and the beginning of the dry process. Blue and red lines indicate intake and outfall pipes, respectively. In 2060, the outfall mouth is very close to the shoreline which is indicated with a black line along the coast and in 2070 it is not in the sea anymore. It cannot be said that the intake mouth is in the sea because it is in a shallow pond apart from the sea. The wave characteristics are dependent only on the wind input in 2070.

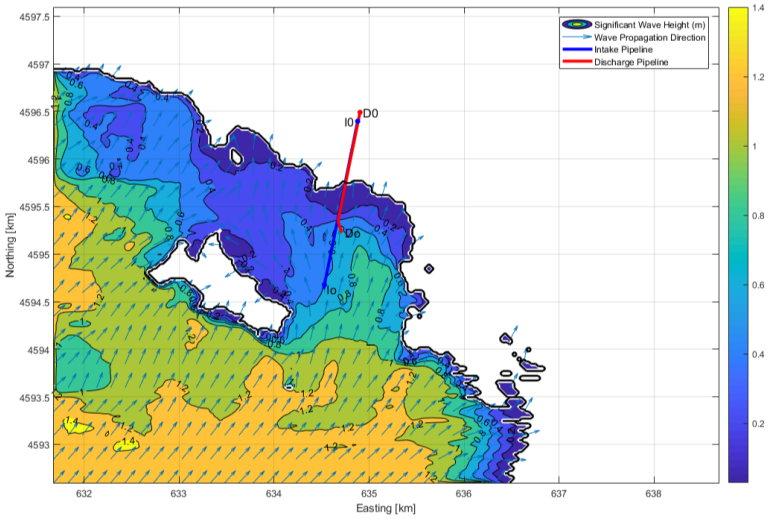

(a)

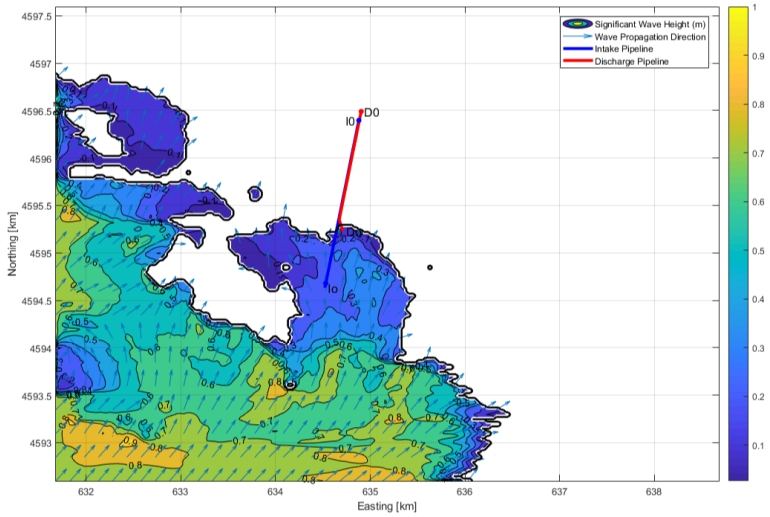

(b)

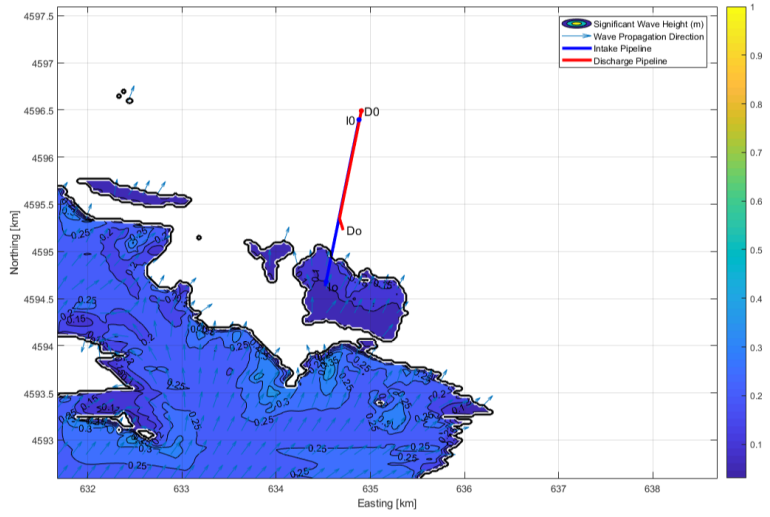

(c)

Figure 4.7. Fine mesh SWAN results for (a) 2050, (b) 2060 and (c) 2070.

Wave heights never exceed the design wave height because the pipe area is very shallow. But this criterion is for the main pipe which is very stronger than the ports. The ports are eventually damaged by smaller wave heights and wave breaking. That is why, the normalized source term magnitudes for energy dissipation due to surf breaking which are effective in shallow areas (Akpınar *et al.*, 2012) are examined for all years. Figure 4.8 and 4.9 show the normalized source term magnitude for energy dissipation due to surf breaking in 2030 and 2060, respectively. Table 4.2 shows these magnitudes at the intake and discharge location for the modeled years. In 2030, there is an intense energy dissipation due to surf breaking at the intake location. After 2030, energy dissipation intensity is decreasing. This will cause cavitation in the pipe, which is devastating for the system. Thus, operational problems are observed beginning in 2030. For the discharge location, energy dissipation due to surf breaking is intense in 2060. But considering the height of the ports, the ports will already be exposed and become a surface discharge because the depth at discharge location in 2060 is 0.2 m and the port height is 1.5 m (Figure 4.10 and 4.11). In 2050, the port height and the depth at the discharge location are 1.5 m. Thus, the first impact of the breaking will directly reach the ports, which is also dangerous.

Table 4.2. The normalized source term magnitude for energy dissipation due to surf breaking on the intake (I_o) and the outfall mouths (D_o).

Years	at I_o (m)	at D_o (m)
2016	-6.2	-3.6
2020	-6.9	-3.8
2030	-9.0	-4.1
2040	-	-4.3
2050	-	-4.0
2060	-	-6.0
2070	-	-

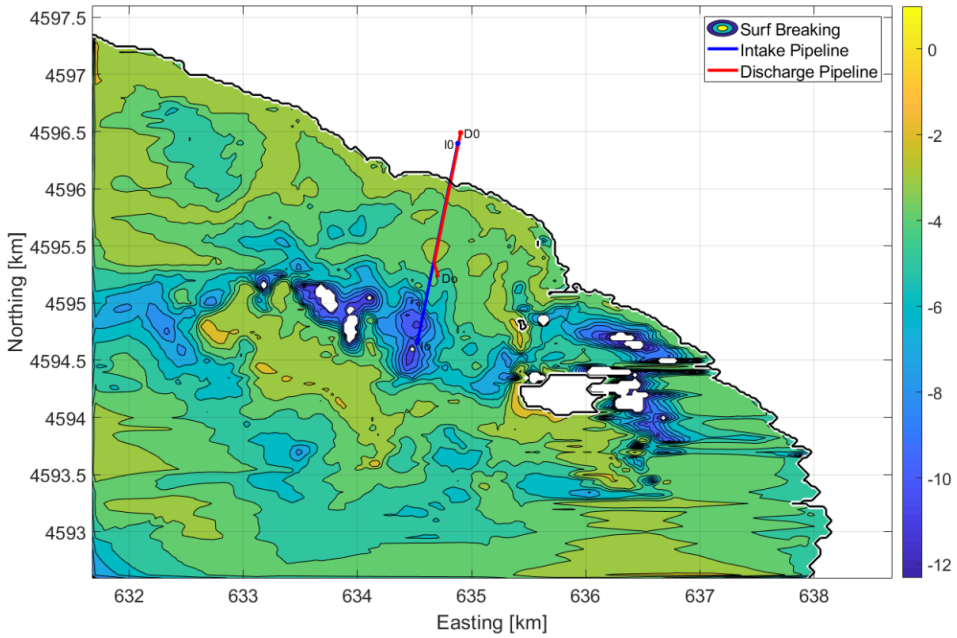

Figure 4.8. The normalized source term magnitude for energy dissipation due to surf breaking for 2030.

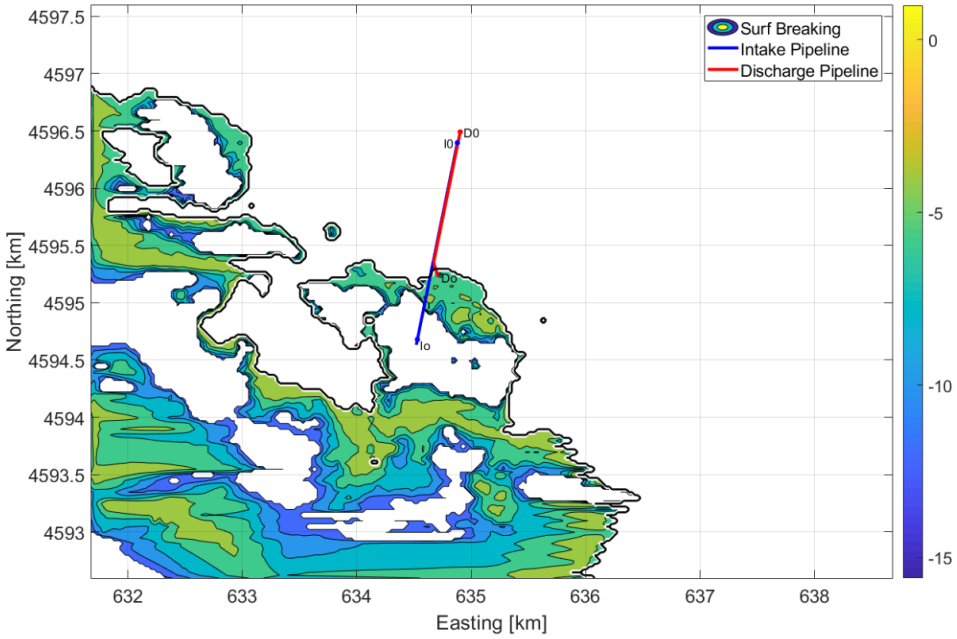

Figure 4.9. The normalized source term magnitude for energy dissipation due to surf breaking for 2060.

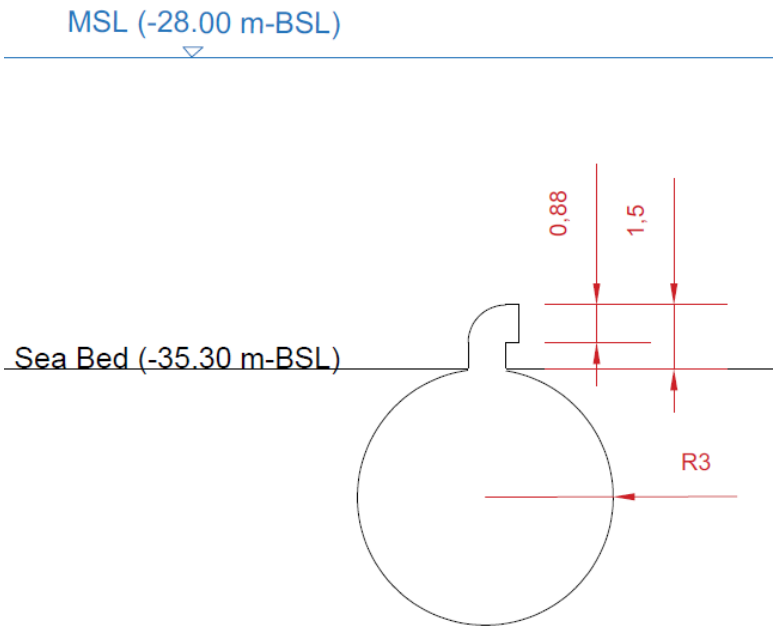

Figure 4.10. Side view of the diffuser and mean sea level in 2016.

Figure 4.11. Photograph of the diffuser. Photograph is taken from Murat Cenk Gerdanlı - MCG Mühendislik.

4.3. Thermal Mixing Results and Comparison

Thermal mixing criteria are that temperature difference at 100 m downstream must be smaller than 3^0C and the plume should not reach the shore. It seems that smaller than 3^0C criterion is not exceeded for the modeled years but touching the shore-

line occurs in 2030, 2040 and 2050 at 4200, 2100 and 1450 m downstream, respectively. The discharge part of the system is slightly submerged after 2050. At the beginning of 2052, the system will be surface discharge in a very shallow location. For the years of 2060, 2070, 2080, 2090 and 2100, the pipe will completely be exposed. To catch where operational hazards begin, some extra CORMIX runs are conducted. Between 2050 and 2060, there is a 12.9 cm/yr decrease in the sea level. Considering this amount of decrease, CORMIX model is run for the years of 2051 and 2052 assuming the same current, the temperature difference will be 3^0C in 2051 and operational hazards will occur (Table 4.3). In 2052, the temperature difference will reach 3.13^0C.

Table 4.3. CORMIX model results

Years	$\triangle T$ (^{0}C) at $r = 100$ m
2016	1.37
2020	1.36
2030	1.60
2040	1.88
2050	2.81
2051	3.01
2052	3.13

Figure 4.12 shows thermal dilution result and the distance to touch the shoreline for 2040. The plume centerline which has the highest concentration of the plume is becoming the bank after touching the shoreline. That is why touching the shoreline is a severe issue. Besides, the water depth near the shoreline is very small, which may cause the accumulated hot water to reduce the temperature difference between the ambient water and the discharged water. Thus, the concentration will be higher at the downstream distance of 100 m. Figure 4.13 shows that the situation is getting worse in 2050 and operational problems will be in 2051 (Figure H.2).

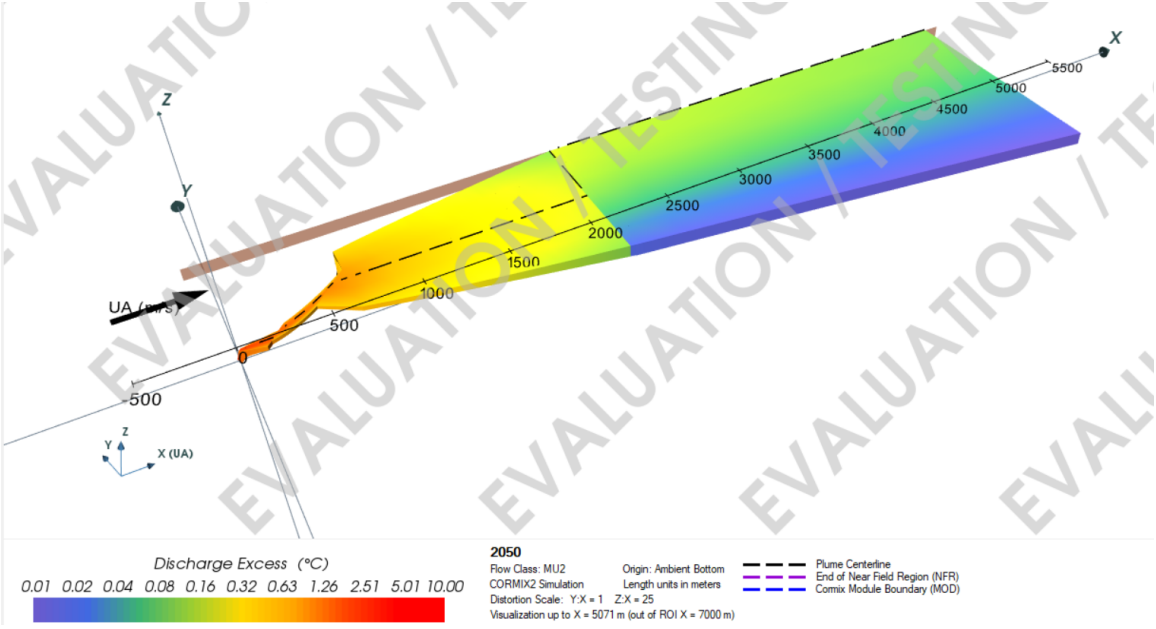

Figure 4.12. Thermal dilution result for 2040.

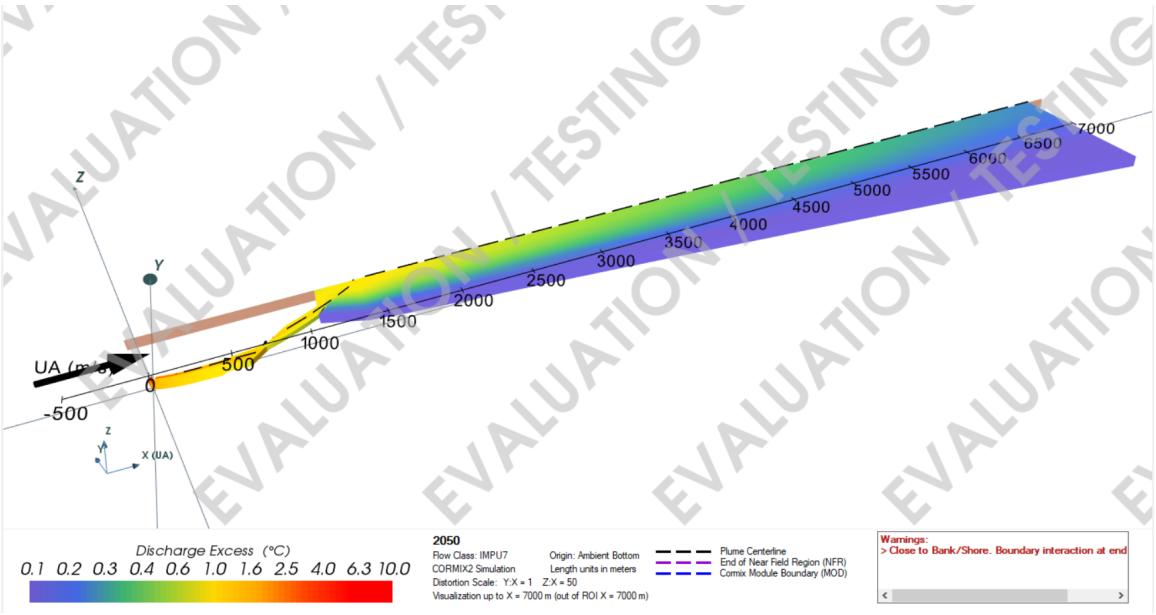

Figure 4.13. Thermal dilution result for 2050.

5. SUMMARY AND CONCLUSION

The Caspian Sea is a closed basin without a connection with the other water bodies. It does not have an outflow but has several inflows, especially the Volga River. Its sea level has dramatically changed for centuries because it is very sensitive to climate change. This situation causes many problems for coastal structures and their effects on the environment. One of these structures is a SWIO system. The Garabogaz Ammonia and Urea Production Plant previously studied by BUCEL was taken as a sample case to examine a SWIO system condition with different sea levels.

As the first step, precipitation and evaporation data, the Volga River runoff data, and the annual discharge to the Bay of Kara-Bogaz-Gol are analyzed according to Roshan et al. (2012), Renssen et al. (2007) and Aladin et al. (2012), respectively. After that, the Caspian Sea level is predicted for the next century using a two-dimensional hydrodynamic mode (RMA2). It will decrease 0.91 m, 2.63 m, 4.26 m, 5.81 m, 7.10 m, 8.27 m, 9.31 m, 10.14 m and 10.67 m by the end of 2020, 2030, 2040, 2050, 2060, 2070, 2080, 2090 and 2100, respectively. It follows a decreasing decrease rate because the increasing evaporation approaches the sum of the increasing Volga River runoff and decreasing precipitation. At that point, the CSL is mainly controlled by the outflow to the KBG which depends on the CSL and it is higher when the CSL is higher.

To predict the nearshore wave climate of the project area, a third generation wave model (SWAN) is used with the calculated sea level decreases. It is found that in 2030, operational problems will begin with wave breaking at the intake head of the SWIO which may cause cavitation in the pipe and eventually stop the operation. Furthermore, normalized energy dissipation magnitude due to wave breaking on the discharge location reaches its highest value in 2060. The main pipe is stronger than the ports. For that reason, wave breaking will eventually harm the ports which have a smaller diameter compared to the main pipe. Solution for this problem may be building a breakwater to break waves before they reach the discharge point. However, this may cost more than the SWIO. Besides, even the system properly operates, environmental

problems due to large temperature difference between water and discharged waters will start after a while. This process is mainly devastating in terms of the operational aspect.

CORMIX model is used to examine the prediction of the thermal mixing process of the heated discharge. It is concluded that the pipeline will partially be exposed in 2052. But before this happens, the operational hazards will begin in 2051 and the plume will touch the shoreline at 2100 m and 1450 m downstream in 2040 and 2050, respectively. After a while, the sea water temperature at the shoreline will increase because of the low water level. As long as the SWIO system works, the temperature difference between the ambient water and the heated discharge will decrease, which leads to decreasing dilution rate. According to additional CORMIX analysis conducted for yearly inrervals, the temperature difference will reach $+3.01^0$C in 2051. In this scenario, the habitat around the project site will seriously be affected. Besides, the evaporation rate of the CS will rise due to the higher temperature of the sea water. This consequence may have longterm environmental impacts. Considering different ambient current magnitude and directions, it may cause some environmental problems earlier. One of the solutions can be using more ports with a smaller diameter to increase the exit velocity or duck-bill nozzle to control the exit velocity. If the exit velocity is controlled according to the system working capacity, a devastating effect on the environment can be prevented for a long time. Because the exit velocity is the starting point for thermal dilution. Another solution to this problem can be constructing the system deeper location of the CS but it will cost more than the estimated or choosing the steeper slope locations which are less affected by the CSL change.

As a consequence, the CSL change is expected to start harming the SWIO system in 12 years and the SWIO system will harm the environment in 33 years (Table 5.1) if it continues to operate with an alternative intake location. It is crucial that the feasibility study must be conducted for not only current circumstance but also the future. The definition of the future depends on the project lifetime. All possibilities and processes must be examined in detail before taking action. This is a very important factor for the advantage of the system, the environment and the Caspian Sea which will face a

devastating future.

Table 5.1. Operational hazards

Years	Wave breaking point	Thermal dilution at 100 m downstream
2016	Wave breaking is at offshore.	1.37
2020	Wave breaking is at offshore.	1.36
2030	Wave breaking is at the intake head.	1.60
2040	Wave breaking is between the intake and discharge heads.	1.88
2050	Wave breaking is between the intake and discharge heads.	2.81
2051	Wave breaking is between the intake and discharge heads.	$+3.01^0$C
2052	Wave breaking is between the intake and discharge heads.	$+3.13^0$C
2060	Wave breaking is at the discharge head.	-

6. RECOMMENDATION FOR FUTURE WORK

In this thesis, the yearly averaged sea level is used after modeling the Caspian Sea level. SWAN and CORMIX models are run according to the results of RMA2 model and it is understood that seasonally or monthly averaged data may be more useful to specify when operational problems begin, and the design criteria are exceeded.

The thermal dilution for 2050 may exceed the allowable maximum temperature change of 3^0C when the monthly averaged sea level is considered. The results say that the ports are partially exposed in 2052. At this point, tidal and/or seasonal effects will play an important role in thermal dilution of the system especially between the years 2050 and 2055. Wave breaking point also fluctuates regarding to the sea level fluctuations. Even tidal fluctuations can play a role in when the operational problems occur.

In this thesis, it is also argued that when constructing SWIO systems, sea level prediction should be made in accordance with the project lifetime and feasibility studies should be carried out. Finally, the most suitable and feasible location should be chosen. There are some suggestions resulted from this thesis about possible SWIO system locations at the Caspian Sea coast.

The north side of the Caspian Sea is too shallow to construct a SWIO system. It will be the first part to dry out (Figure 4.4). The south side of the Caspian Sea is the most feasible one because it is the deepest part. The middle Caspian Sea is neither shallow nor deep but its bathymetric slope near the shore varies. Operational problems and environmental hazards can be prevented by placing the pipeline in steeper slope areas because taking the intake and discharge points to the offshore area will not be cost-efficient. The southern coast, the middle part of the western coast and north-west coasts of the eastern coast of the Caspian Sea have steeper slopes (Figure 6.1).

For a deep understanding, the effect of a discharge location to the intake location of the same system must be examined. If there are some sea water intake and discharge systems that are close to each other, their effects on each other and the environment should also be examined in a bigger scale rather than a local feasibility study. Because for the environment, it can be a double effect that there are many sea water intake and discharge systems. They can most probably harm the environment faster, which means their operational problems will begin sooner. The relationship between the environment and such systems is a cycle that will always affect each other and they bring their ends together.

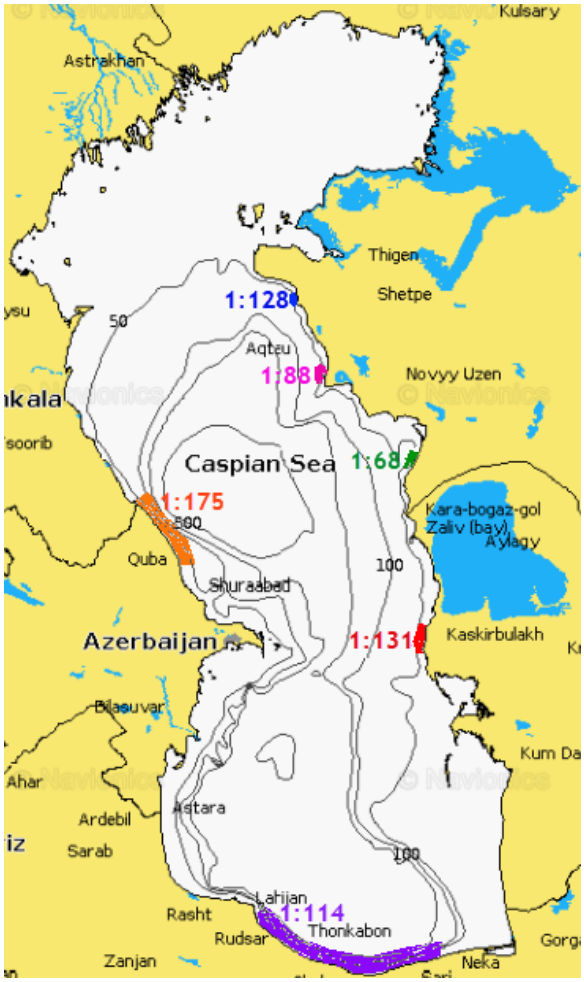

Figure 6.1. The slopes between the shoreline and 20 m contour. Data is taken from Navionics.

REFERENCES

Akpınar, A., G.Ph. van Vledder, M.İ. Kömürcü, and M. Özger, "Evaluation of the Numerical Wave Model (SWAN) for Wave Simulation in the Black Sea", *Continental Shelf Research*, Vol. 50-51, pp. 80-99, 2012.

Aladin, N., I. Plotnikov, and Y. Chuykov, "Sustainable Society for the Saving Unique Biodiversity and Very Rich Biological Resources of the Caspian Sea", *Journal of Coastal Conservation*, 2012.

Al-Ghamdi, A.S., "Simulation of Jeddah Multi-port Sea Outfall", *Journal of Coastal Conservation*, Vol. 14, pp. 63-69, 2010.

Arpe, K., S.A.G. Leroy, F. Wetterhall, V. Khan, S. Hagemann, and H. Lahijani, "Prediction of the Caspian Sea Level Using ECMWF Seasonal Forecasts and Reanalysis", *Theoretical and Applied Climatology*, Vol. 117(1-2), pp. 41-60, 2014.

Bath, A., B. Shackleton, and C. Botica, "Development of Temperature Criteria for Marine Discharge from a Large Industrial Seawater Supplies Project in Western Australia", *Water Institute of South Africa (WISA) Biennial Conference*, Cape Town, South Africa, May 2004, Water SA, 2004.

Beni, A.N., H. Lahijani, R.M. Harami, K. Arpe, S.A.G. Leroy, N. Marriner, M. Berberian, V. Andrieu-Ponel, M. Djamali, A. Mahboubi, and P.J. Reimer, "Caspian Sea-Level Changes During the Last Millennium: Historical and Geological Evidence from the South Caspian Sea", *Climate of the Past*, Vol. 9, pp. 1645-1665, 2013.

Bleninger, T., A. Niepelt, G.H. Jirka, S. Lattemann, A. Purnama, H.H. Al-Barwani, and R.L. Doneker, "Environmental Hydraulics Framework of the Design of Discharges from Desalination Plants", *6^{th} International Symposium on Environmental Hydraulics*, Athens, Greece, June 2010, Taylor & Francis Group, London, 2010.

Bleninger, T., and G.H. Jirka, "Near- and Far-Field Model Coupling Methodology for Wastewater Discharges", *14^{th} Congress of Asia and Pacific Division, International Association of Hydraulic Engineering and Research*, 2004.

Booij, N., L.H. Holthuijsen, and R.C. Ris, "The SWAN Wave Model for Shallow Water", *25^{th} International Conference on Coastal Engineering*, Orlando, Florida, 2-6 September, 1996, American Society of Civil Engineering, New York, pp. 668-676, 1996.

Buvaneshwari, S., V. Ravichandran, and B.V. Mudgal, "Thermal Pollution Modeling of Cooling Water Discharge into a Closed Creek System", *Indian Journal of Geo-Marine Sciences*, Vol. 43, pp. 1415-1421, 2014.

CASPCOM, *Coordinating Committee on Hydrometeorology of the Caspian Sea*, http:// www.caspcom.com/index.php?razd = sess & lang = 1&sess = 17&podsess = 61, accessed in June 2018.

Chen, J.L., T. Pekker, C.R. Wilson, B.D. Tapley, A.G. Kostianoy, J.F. Cretaux, and E.S. Safarov, "Long-Term Caspian Sea Level Change", *Geophysical Research Letters*, Vol. 44, pp. 6993-7001, 2017.

Claire, C., and L. Ingvar, "Metocean Data Provision, Caspian Sea", BMT Argoss, 2014.

ECMWF, *The European Centre for Medium-Range Weather Forecasts*, https://apps.ecmwf.int/datasets/data/interim-mdfa, accessed in March 2019.

Elguindi, N., and F. Giorgi, "Projected Changes in the Caspian Sea Level for the 21st Century Based on the Latest AOGCM Simulations", *Geophysical Research Letters*, Vol. 33, 2006.

Elguindi, N., and F. Giorgi, "Simulating Multi-Decadal Variability of Caspian Sea Level Changes Using Regional Climate Model Outputs", *Climate Dynamics*, Vol.

16, pp. 167-181, 2005.

Ercan, A., M.L. Kavvas, and R.K. Abbasov, "Long-Range Dependence and Sea Level Forecasting", *Springer Briefs in Statistics*, Springer Dordrecht Heidelberg London New York, 2013.

Fossati, M., P. Santoro, S. Urrestarazu, and I. Piedra-Cueva, "Numerical Study of the Effect of a Power Plant Cooling Water Discharge in the Montevideo Bay", *Journal of Applied Mathematics*, 2011.

Google Earth Pro, *The Caspian Sea*, https://www.google.com/earth, accessed in June 2018.

Hadadpour, S., A. Etemad-Shahidi, E. Jabbari, and B. Kamranzad, "Wave Energy and Hot Spots in Anzali Port", *Energy*, Vol. 74, pp. 529-536, 2014.

Hadadpour, S., H. Moshfeghi, E. Jabbari, and B. Kamranzad, "Wave Hindcasting in Anzali, Caspian Sea: A Hybrid Approach", *Journal of Coastal Research*, Special Issue No. 65, pp. 237-242, 2013.

Ibrayev, R.A., E. Özsoy, C. Schrum, and H.I. Sur, "Seasonal Variability of the Caspian Sea Three-Dimensional Circulation, Sea Level and Air-Sea Interaction", *Ocean Science*, Vol. 6, pp. 311-329, 2010.

Jirka, G.H., Fellow, ASCE, and P.J. Akar, "Hydrodynamic Classification of Submerged Multiport-Diffuser Discharges", *Journal of Hydraulic Engineering*, Vol. 117, pp. 1113-1128, 1991.

Jirka, G.H., R.L. Doneker, and S.W. Hinton, *User's Manual for CORMIX: A Hydrodynamic Mixing Zone Model and Decision Support System for Pollutant Discharges into Surface Waters*, Cornell University, New York, 1996.

Kamranzad, B., A. Etemad-Shahidi, V. Chegini, "Sustainability of Wave Energy Resources in Southern Caspian Sea", *Energy*, Vol. 97, pp. 549-559, 2016.

Mai, S., N. Ohle, and C. Zimmermann, "Applicability of Wave Models in Shallow Coastal Waters", *The 5th International COPEDEC*, Cape Town, South Africa, 1999.

Morelissen, R., T. van der Kaaij, and T. Bleninger, "Dynamic Coupling of Near Field and Far Field Models for Simulating Effluent Discharges", *Water Science & Technology*, Vol. 67.10, pp. 2210-2220, 2013.

Navionics Webapp.Sonar Chart, https://webapp.navionics.com/?lang=enboating@4&key=qa_bG%7Byq_I, accessed in January 2018.

New, M., D. Lister, M. Hulme, and I. Makin, "A High-Resolution Data Set of Surface Climate over Global Land Areas", *Climate Research*, Vol. 21, pp. 1-25, 2002.

Otay, N.E., and P. Uzun, "Numerical Model Study of Wave Agitation at Alternative Intake and Discharge Locations", 2018.

Otay, N.E., and P. Uzun, "Thermal Dilution Analysis for Alternative Discharge Locations", 2018.

Polimeks, http://polimeks.com/en/buildingdetail/49/5/turkmenbashi - desalination, accessed in July 2019.

Purnama, A., H.H. Al-Barwani, T. Bleninger, and R.L. Doneker, "CORMIX Simulations of Brine Discharges from Barka Plants, Oman", *Desalination and Water Treatment*, Vol. 32:1-3, pp. 329-338, 2011.

Renssen, H., B.C. Lougheed, J.C.J.H. Aerts, H. de Moel, P.J. Ward, and J.C.J. Kwadijk, "Simulating Long-term Caspian Sea Level Changes: The Impact of Holocene and Future Climate Conditions", *Earth and Planetary Science Letters*, Vol. 261, pp. 685-693, 2007.

Roberts, P.J.W., "Diffusers for Heated Water Disposal from Power Plants", *The 2011 Georgia Water Resources Conference*, University of Georgia, April 2011.

Roshan, G., M. Moghbel, and S. Grab, "Modeling Caspian Sea Water Level Oscillations Under Different Scenarios of Increasing Atmospheric Carbon Dioxide Concentrations", *Iranian Journal of Environmental Health Science & Engineering*, Vol. 9, pp. 24-33, 2012.

Rusu, E., "Strategies in Using Numerical Wave Models in Ocean/Coastal Applications", *Journal of Marine Science and Technology*, Vol. 19, No. 1, pp. 58-75, 2011.

Rusu, E., and F. Onea, "Evaluation of the wind and wave energy along the Caspian Sea", *Energy*, Vol. 50, pp. 1-14, 2013.

Sazeh Pardazi Iran (SPI) Consulting Engineers Co., http://sazehpardazi.ir/water-intake-outfall-system-of-parehsar-combined-cycle-power-plant/, accessed in July 2019.

The SWAN team, *SWAN User Manual*, Delft University of Technology, Deltares, The Netherlands, 2017.

UNEP, UNDP, UNECE, OSCE, REC, and NATO, 2008, "Environment and Security Transforming Risks into Cooperation-The case of the Eastern Caspian Region", Imprimerie Nouvelle Gonnet, F-01303 Belley, France.

U.S. Energy Information Administration (EIA), https://www.eia.gov/beta/international/regions-topics.php?RegionTopicID=CSR, accessed in July 2019.

APPENDIX A: WIND INPUT DATA FOR RMA2

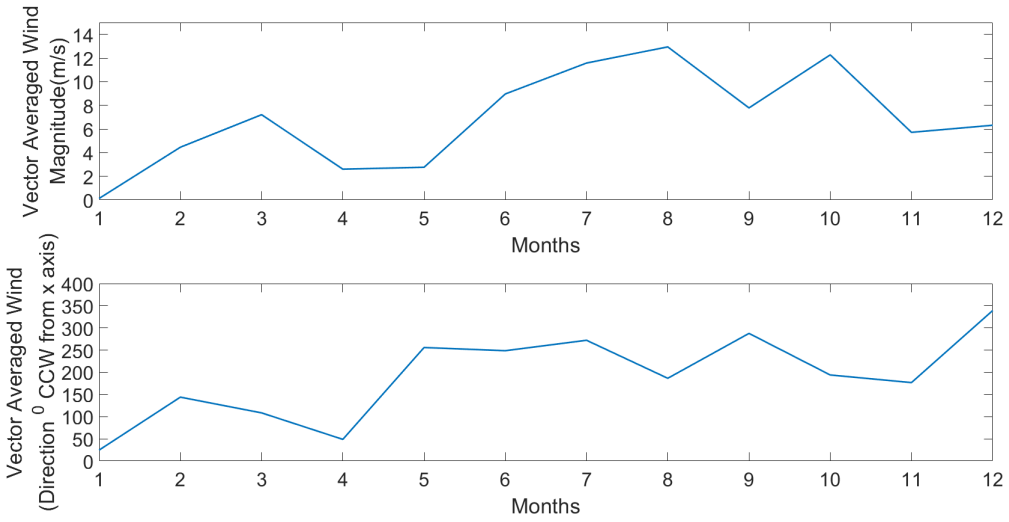

Figure A.1. Vector averaged wind input data for RMA2. Data is taken from ECMWF.

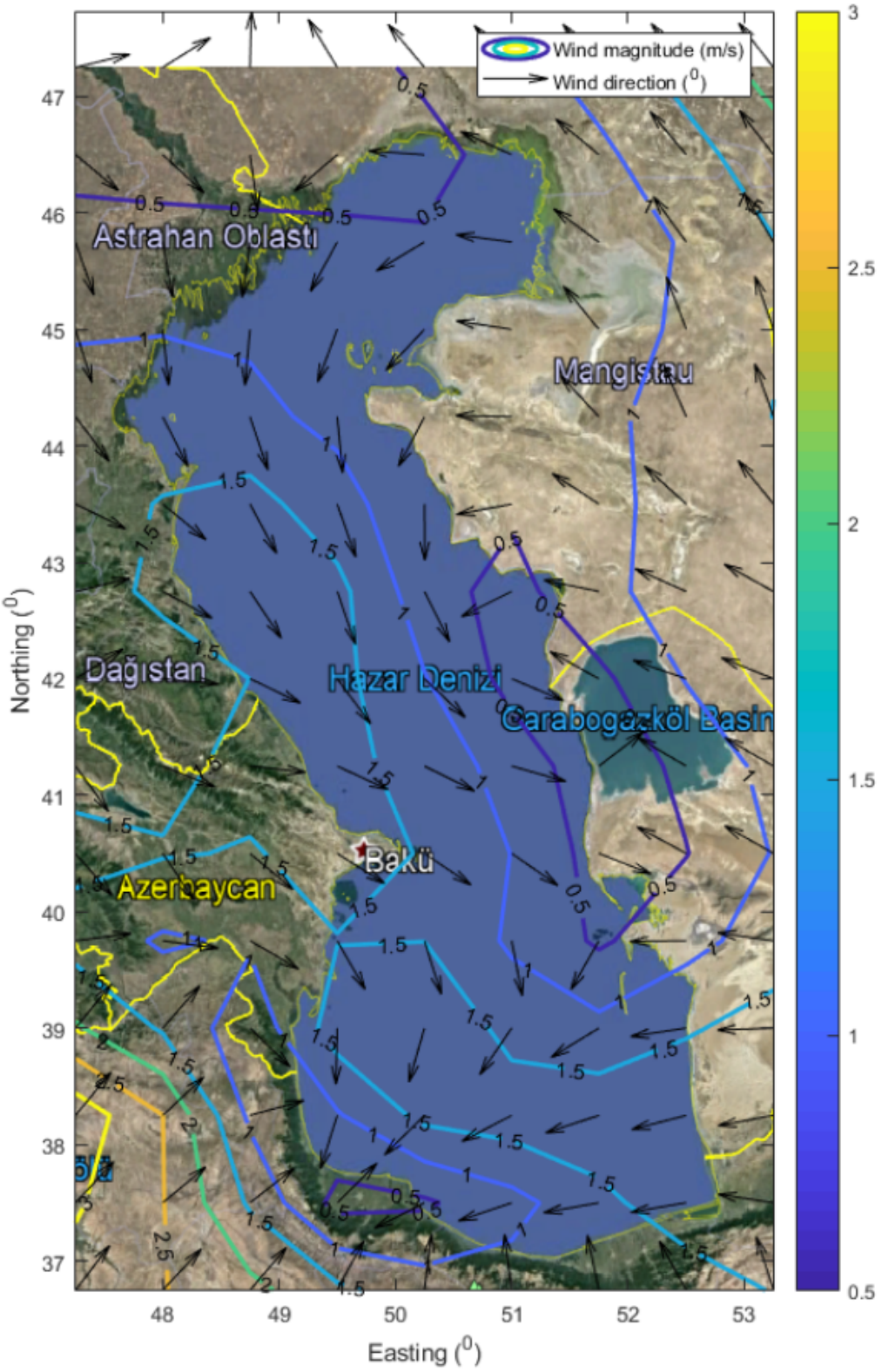

Figure A.2. Wind input data for January. Data is taken from ECMWF.

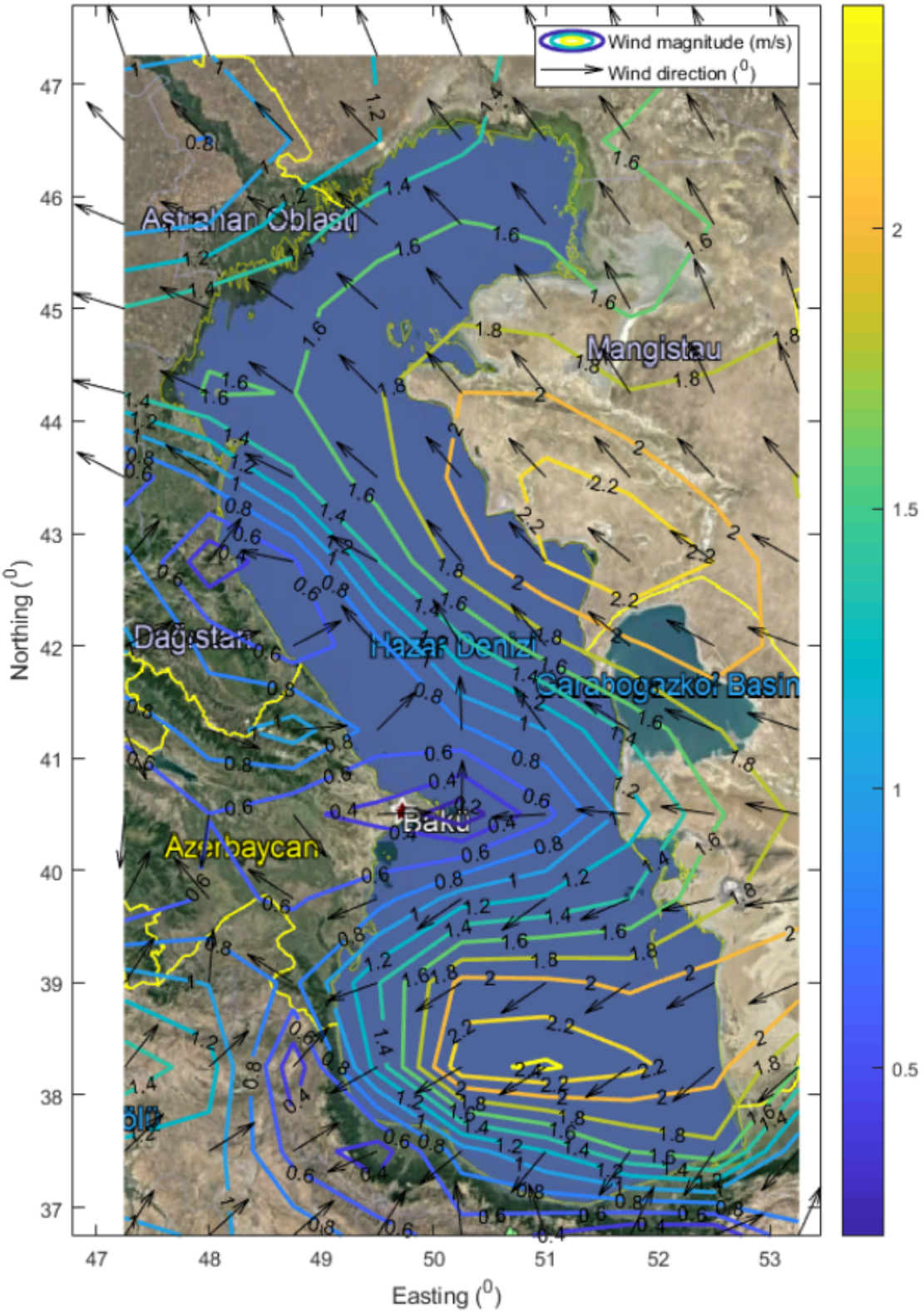

Figure A.3. Wind input data for February. Data is taken from ECMWF.

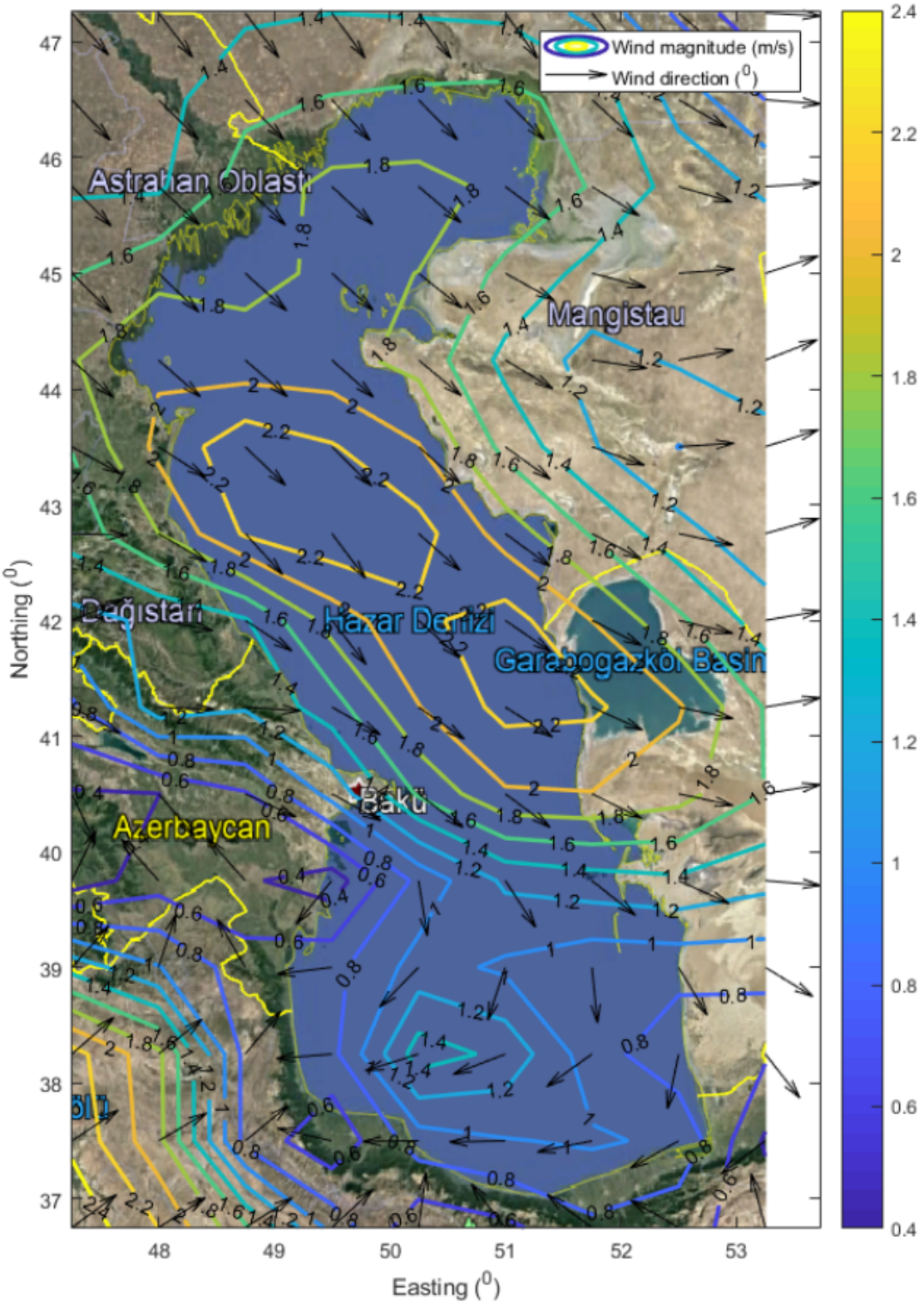

Figure A.4. Wind input data for March. Data is taken from ECMWF.

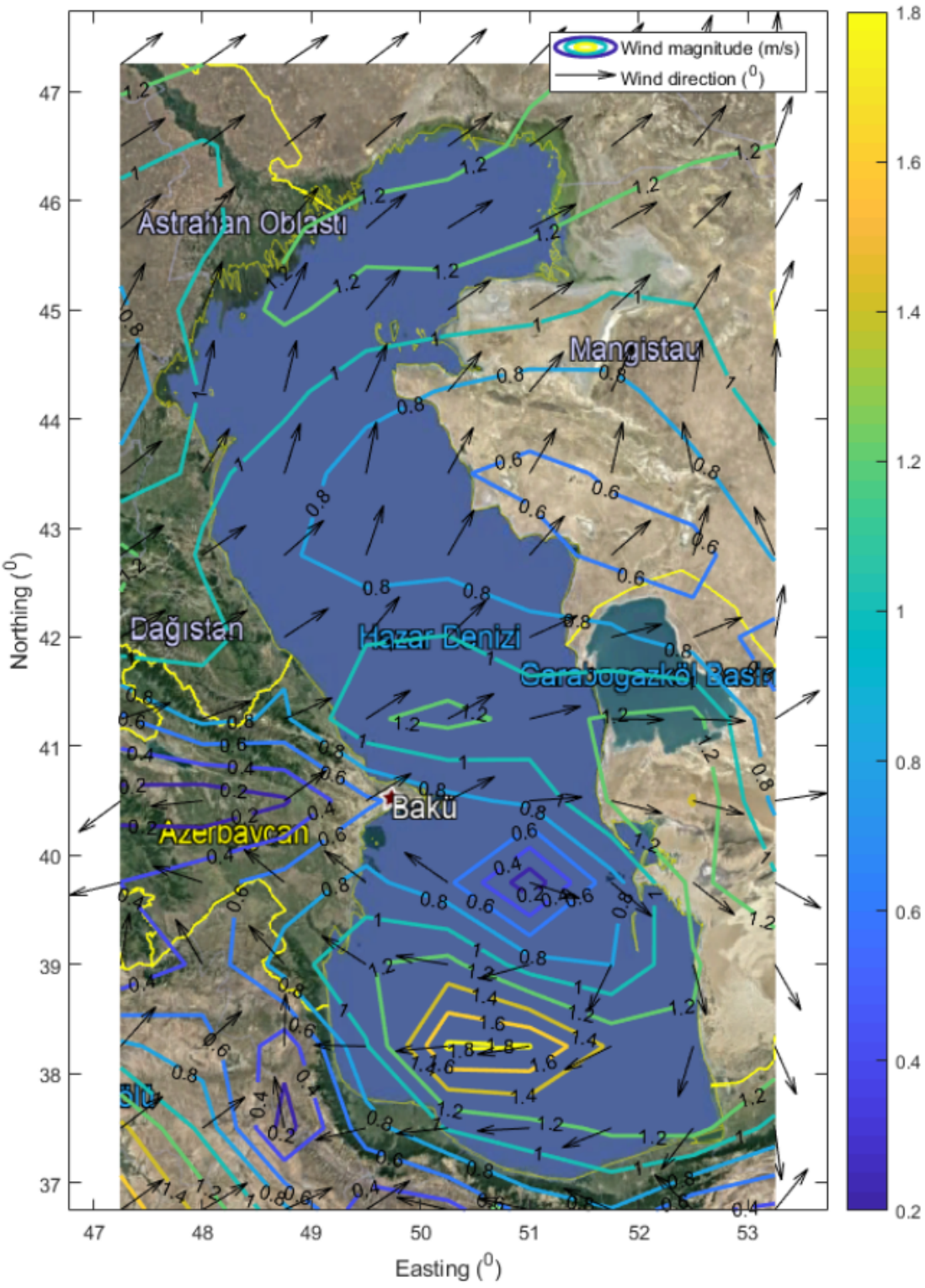

Figure A.5. Wind input data for April. Data is taken from ECMWF.

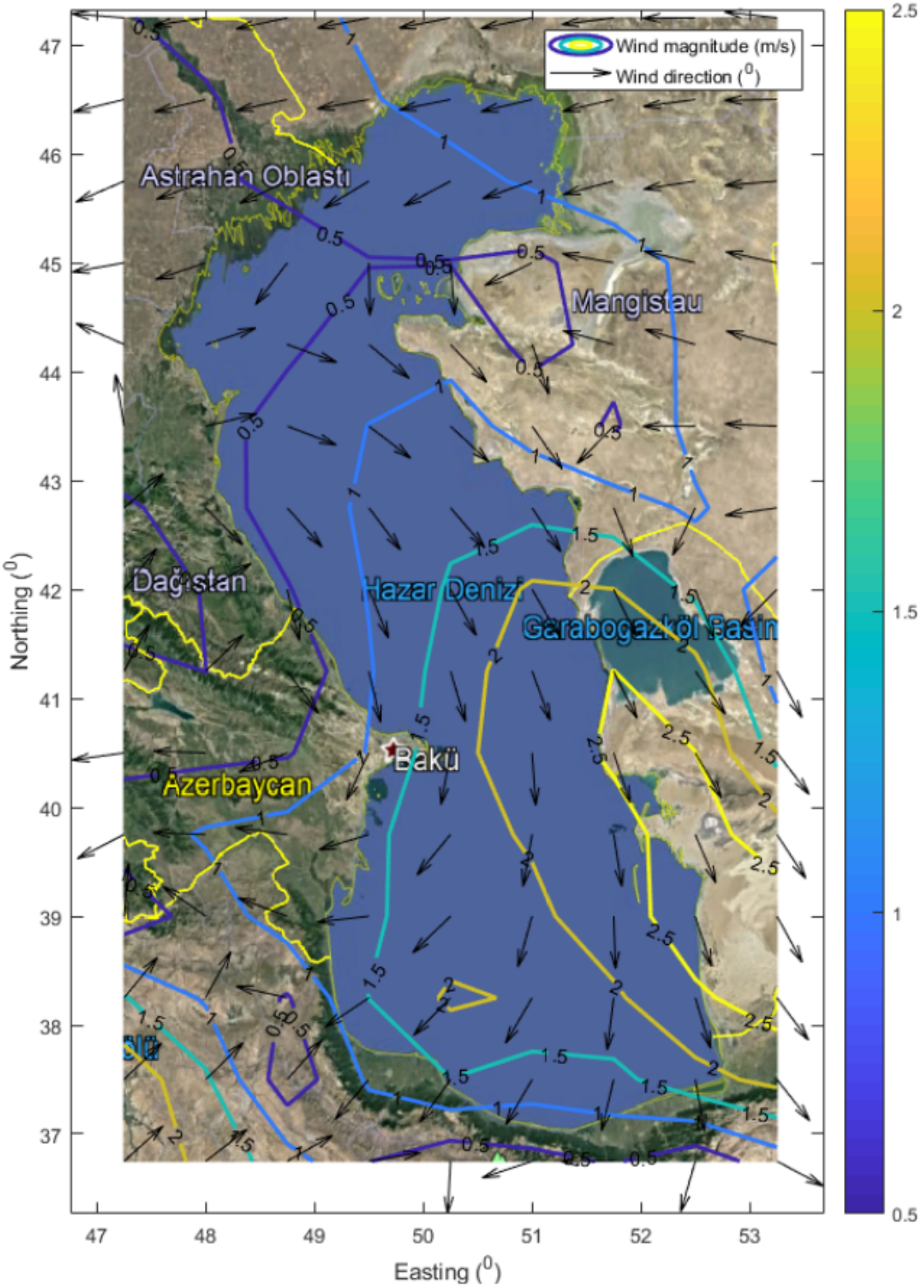

Figure A.6. Wind input data for May. Data is taken from ECMWF.

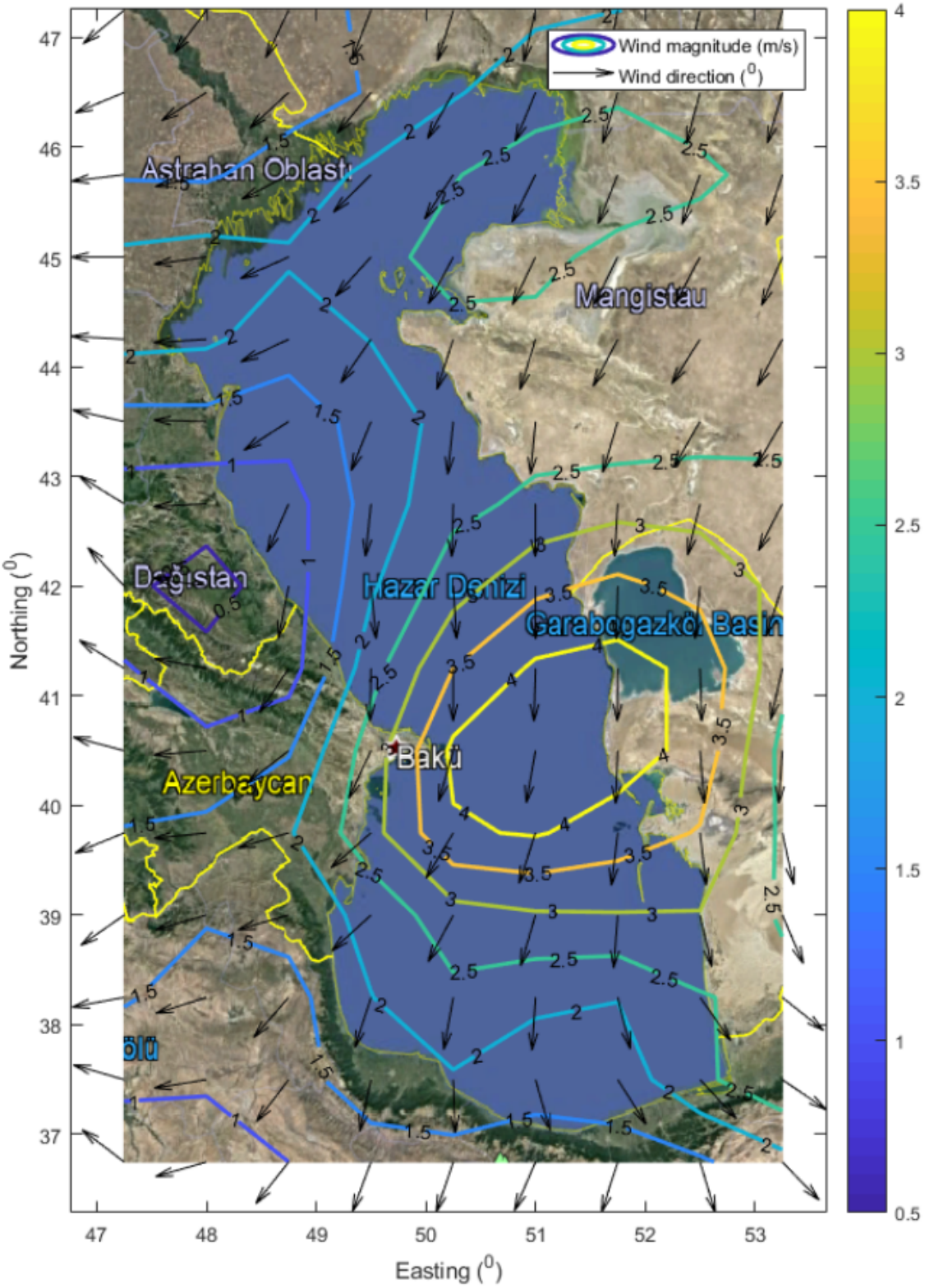

Figure A.7. Wind input data for June. Data is taken from ECMWF.

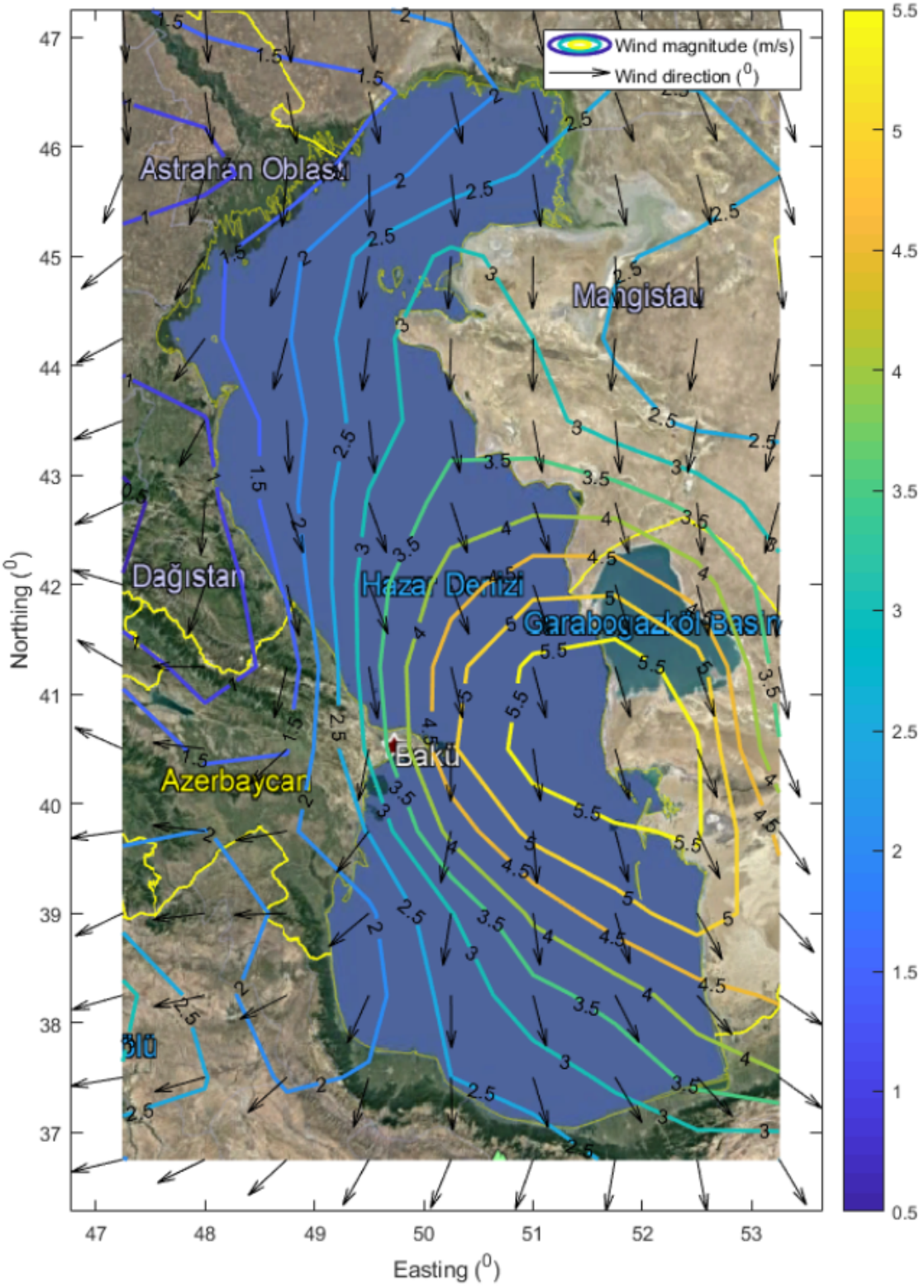

Figure A.8. Wind input data for July. Data is taken from ECMWF.

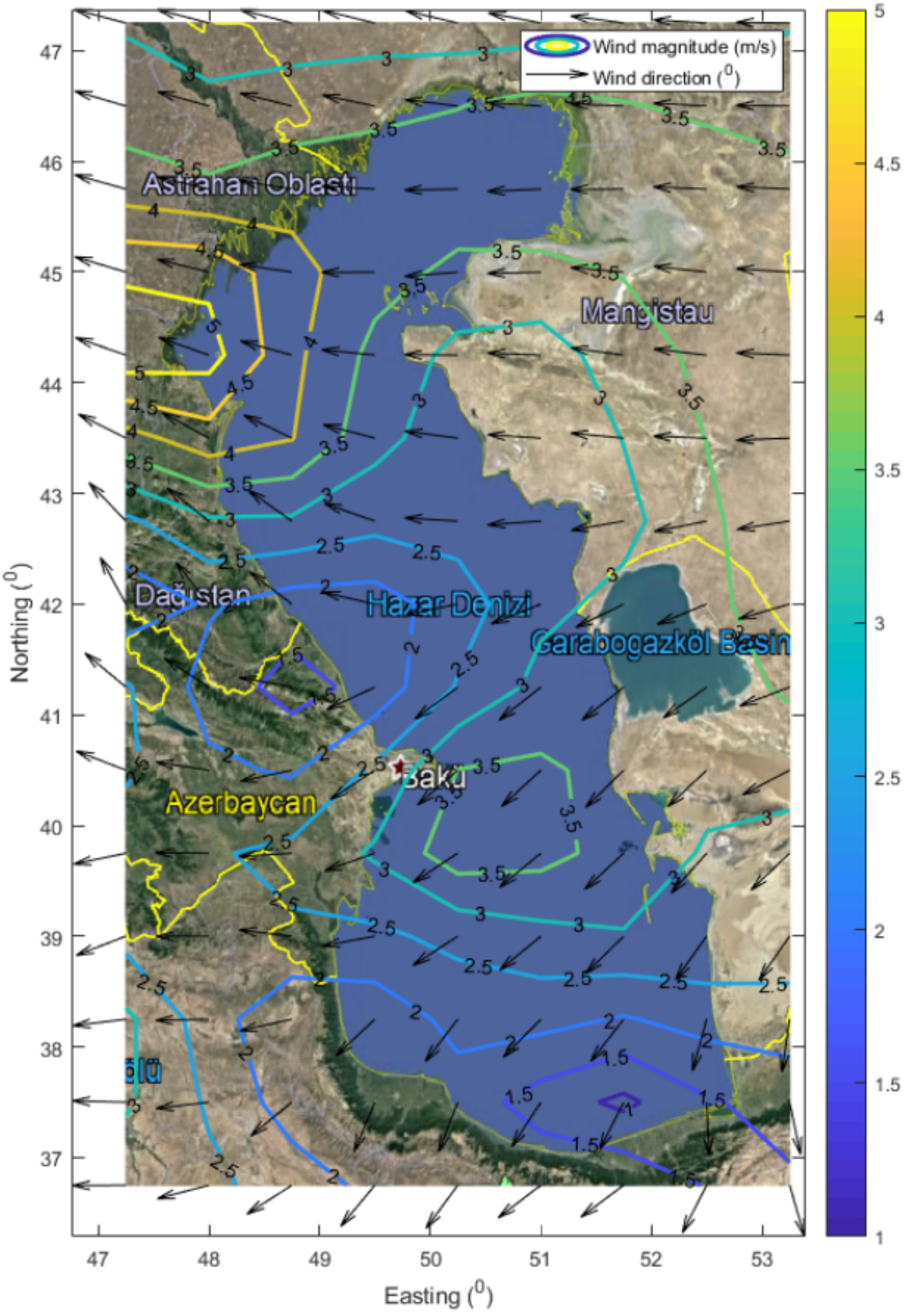

Figure A.9. Wind input data for August. Data is taken from ECMWF.

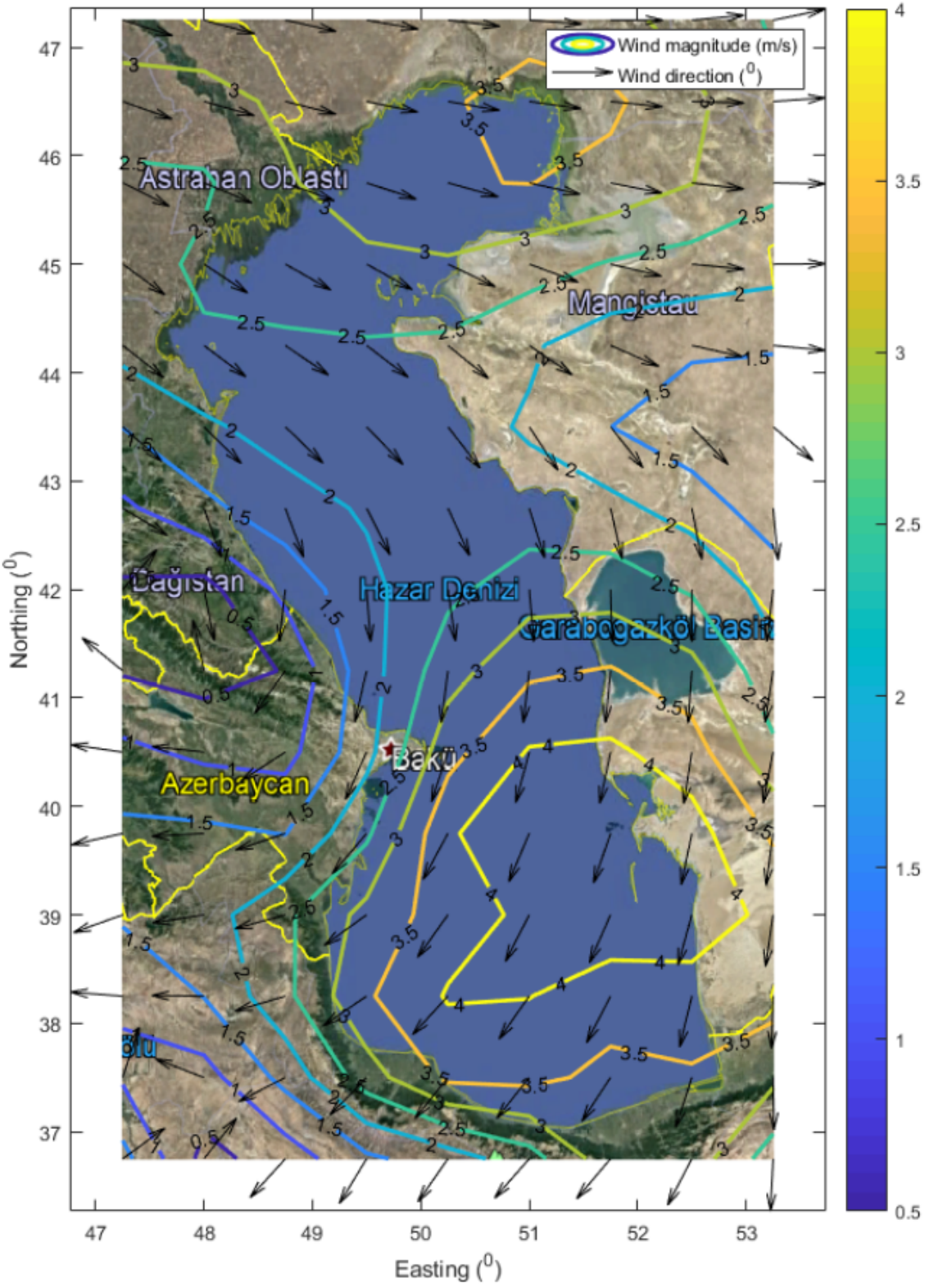

Figure A.10. Wind input data for September. Data is taken from ECMWF.

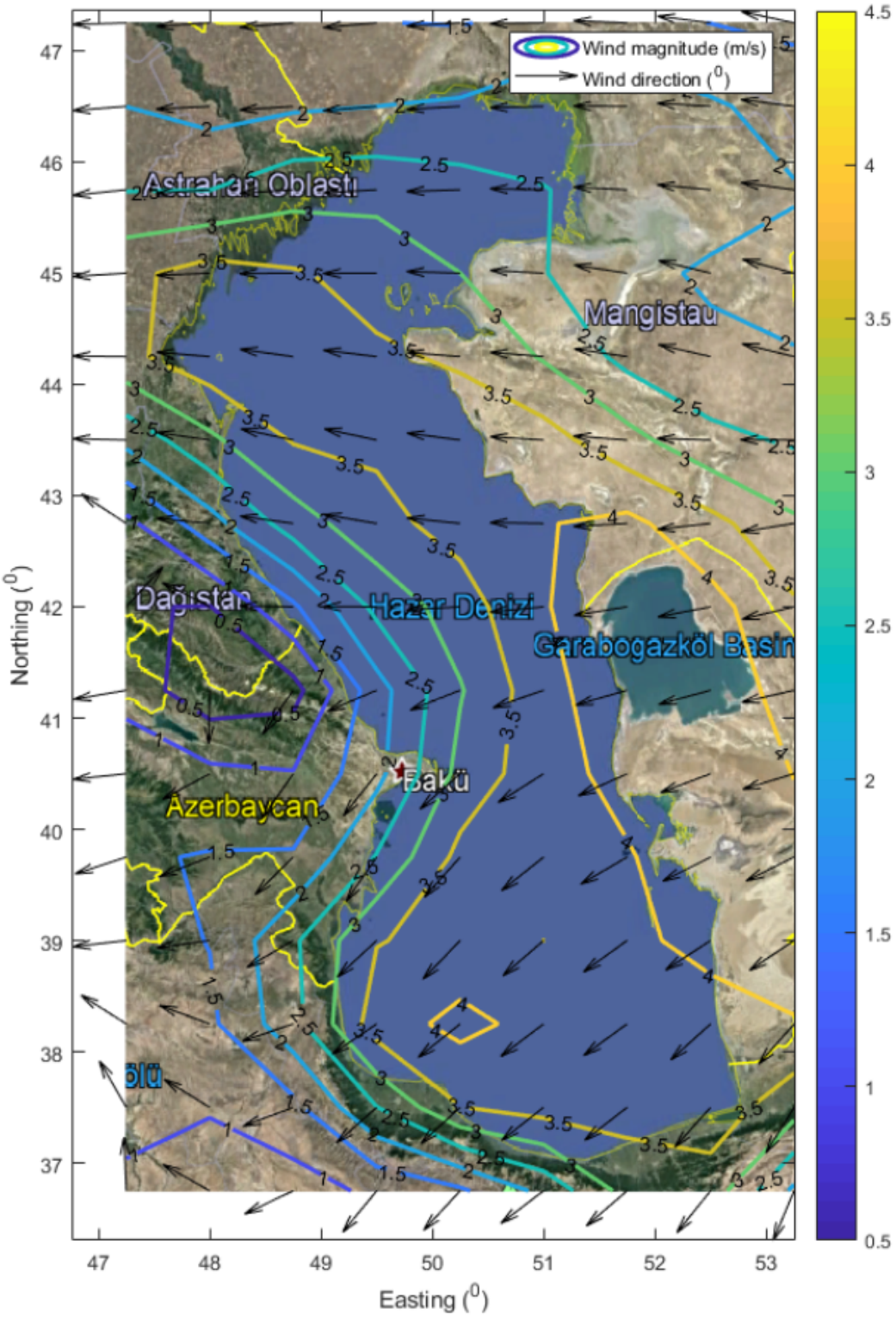

Figure A.11. Wind input data for October. Data is taken from ECMWF.

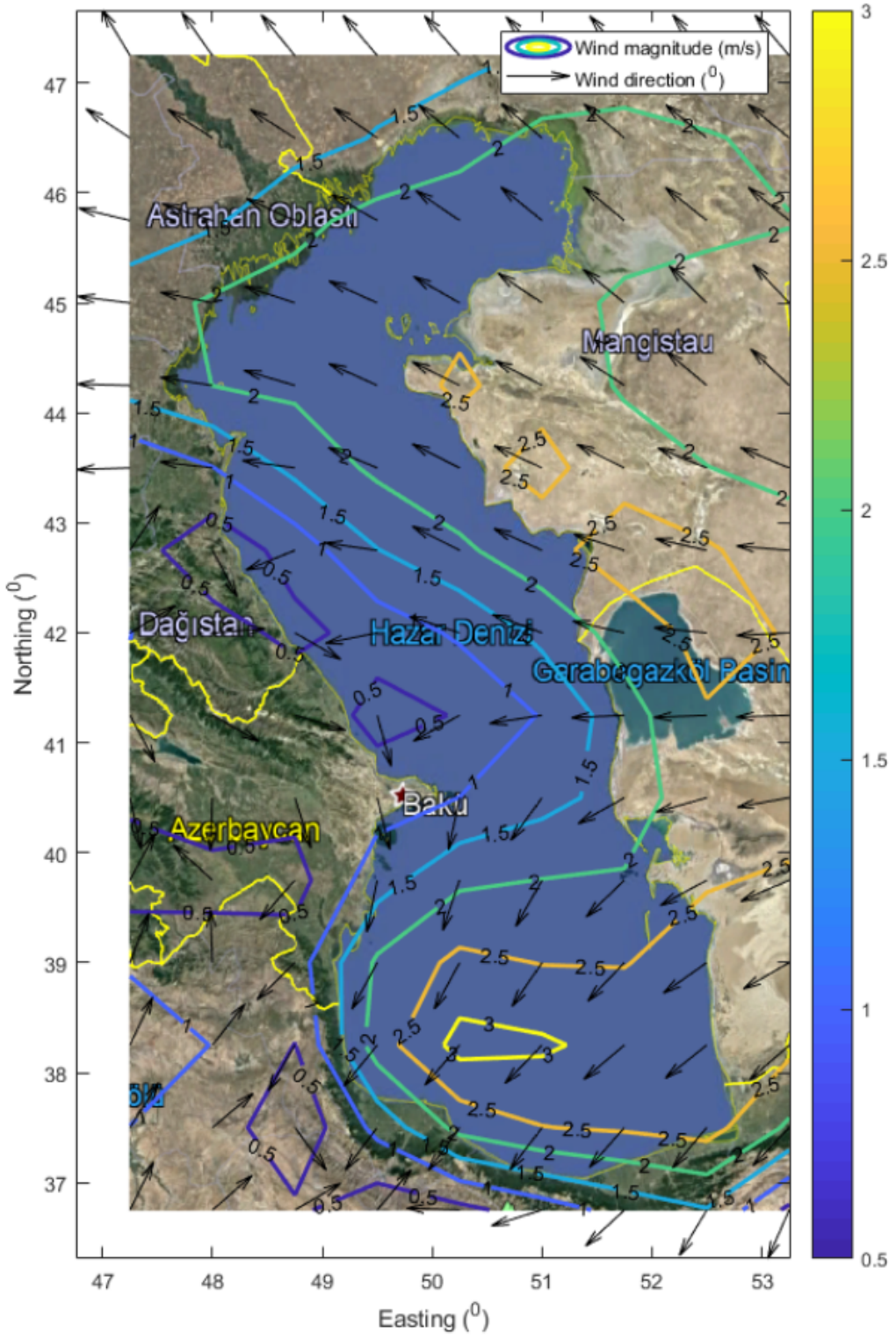

Figure A.12. Wind input data for November. Data is taken from ECMWF.

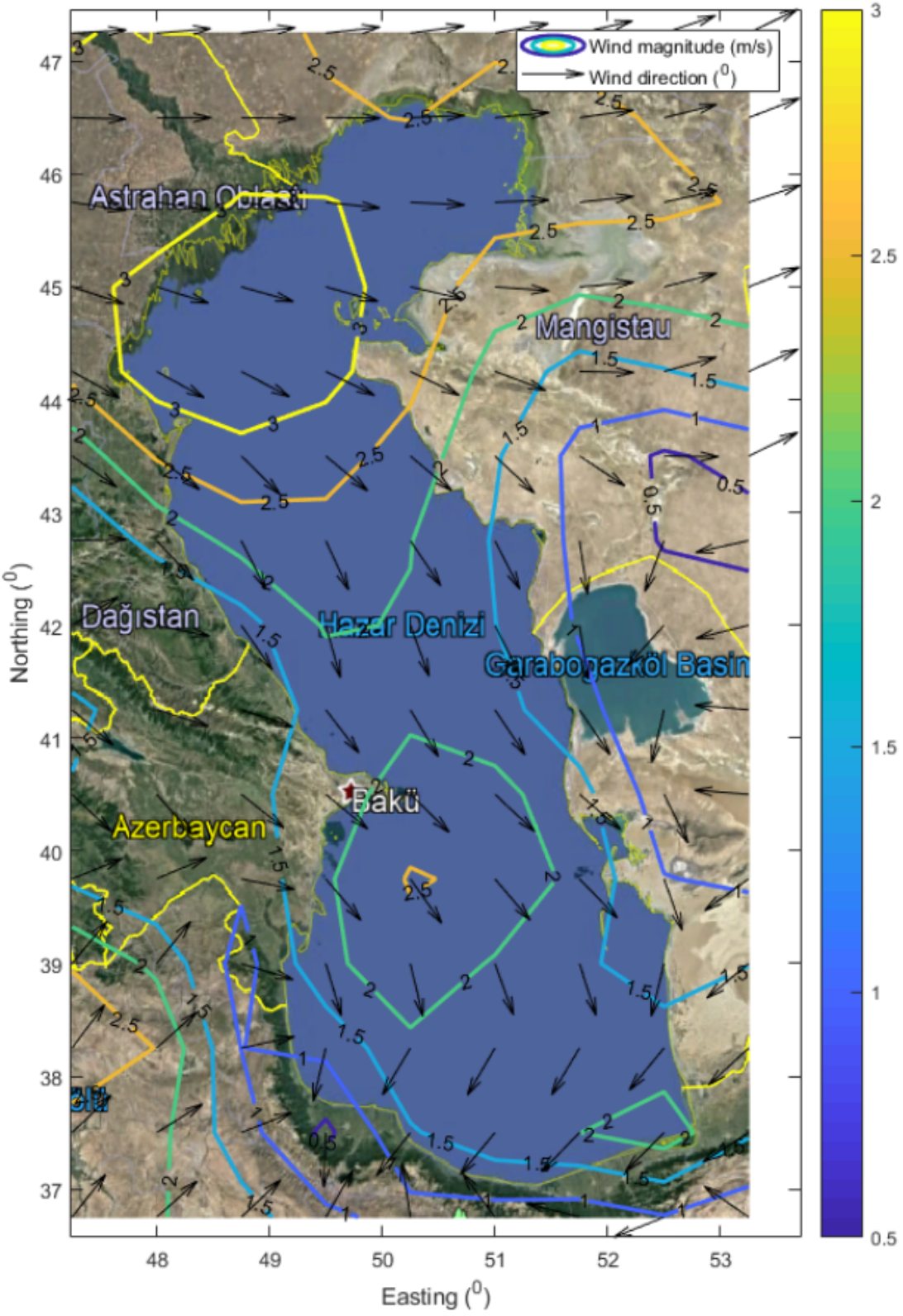

Figure A.13. Wind input data for December. Data is taken from ECMWF.

APPENDIX B: COARSE MESH SWAN BATHYMETRY DATA

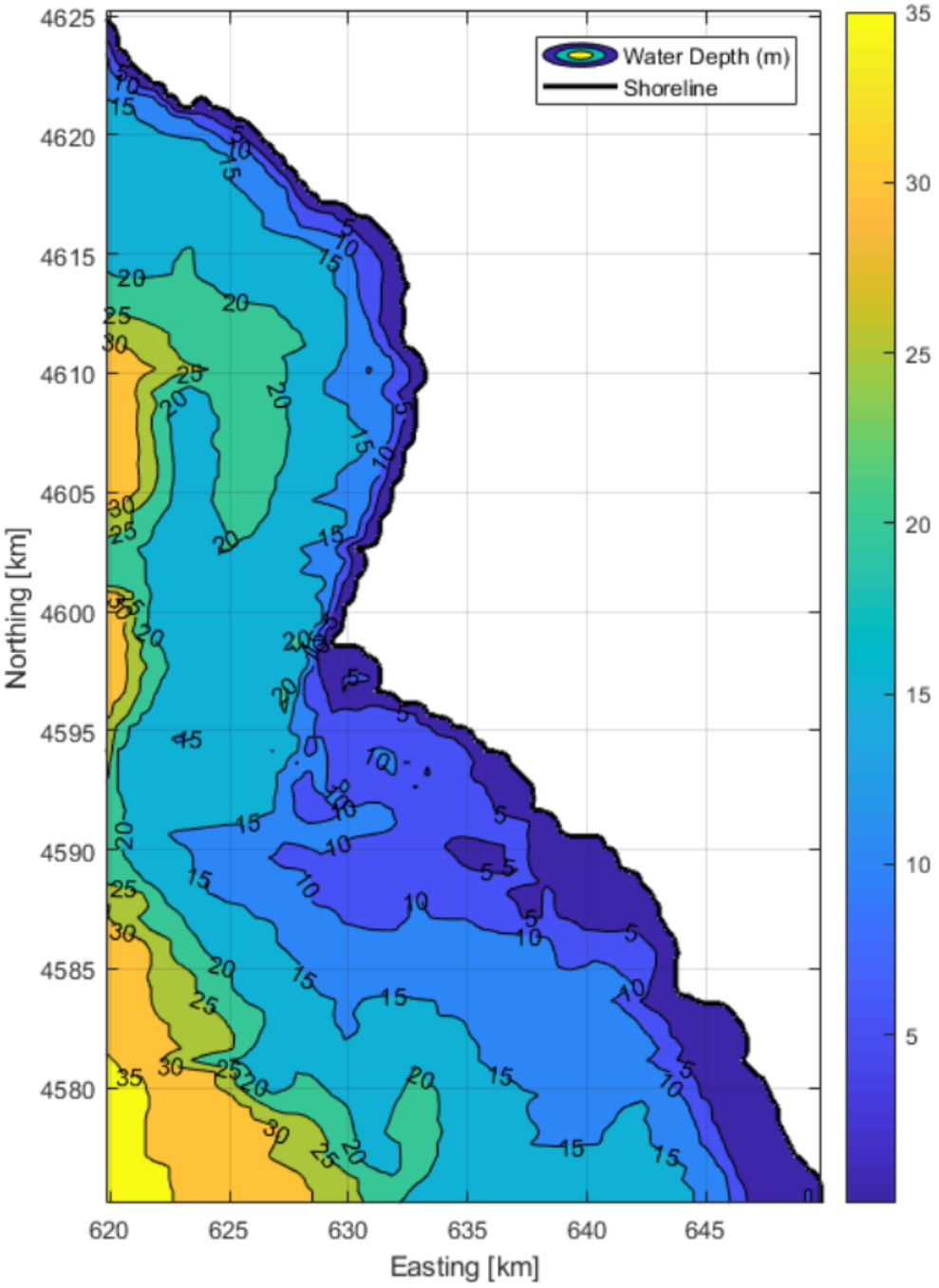

Figure B.1. Coarse mesh bathymetry data for 2020.

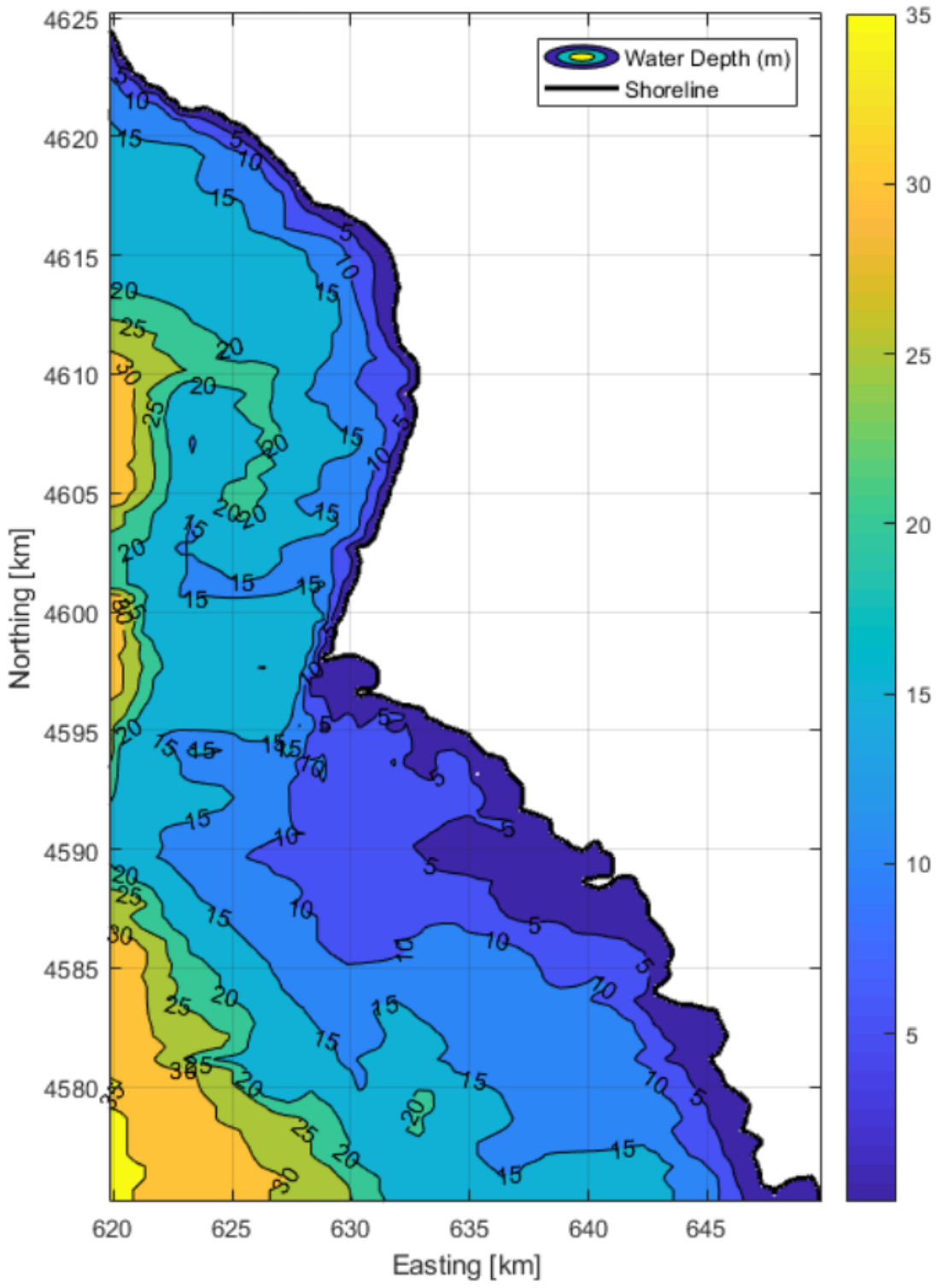

Figure B.2. Coarse mesh bathymetry data for 2030.

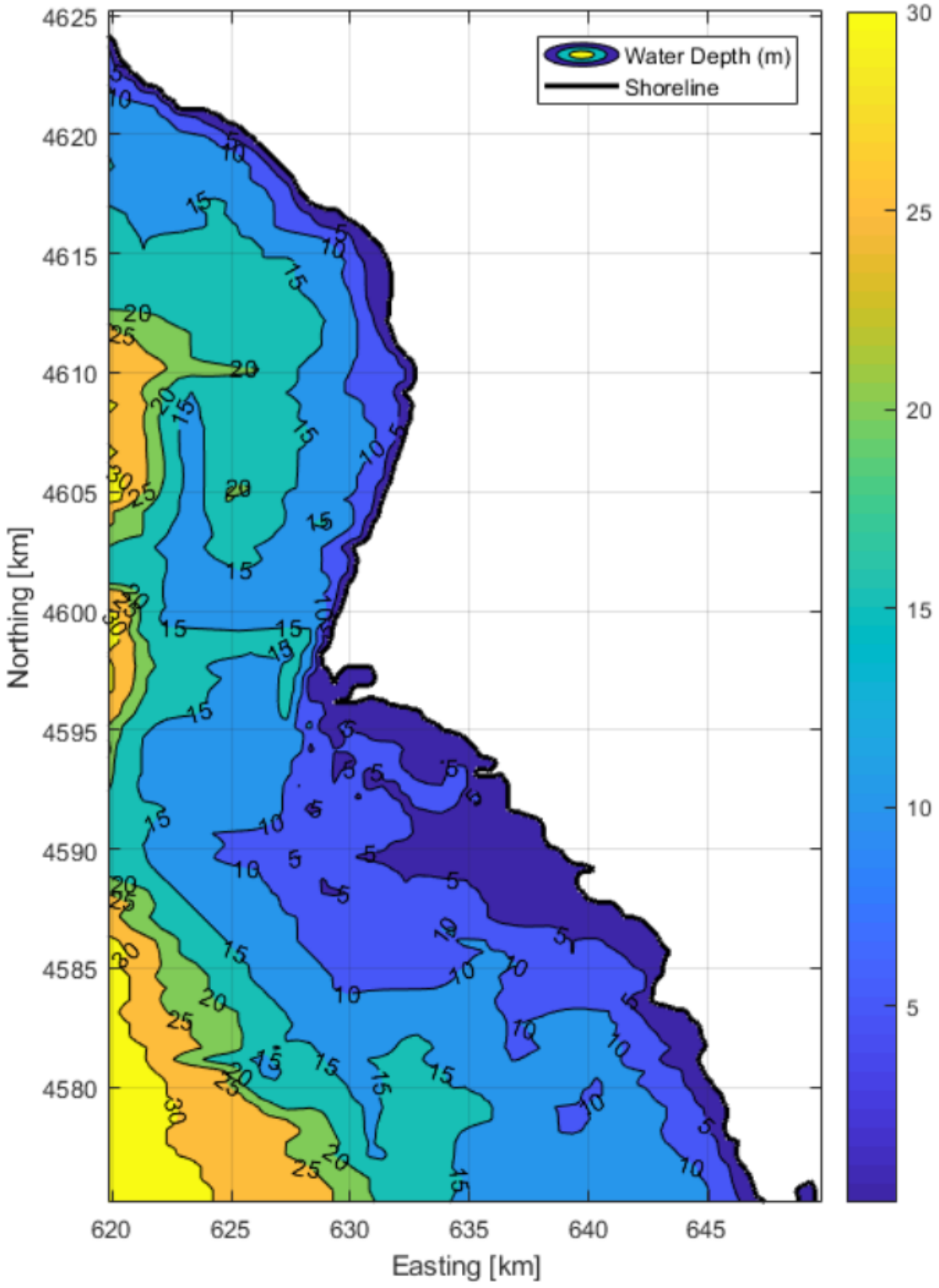

Figure B.3. Coarse mesh bathymetry data for 2040.

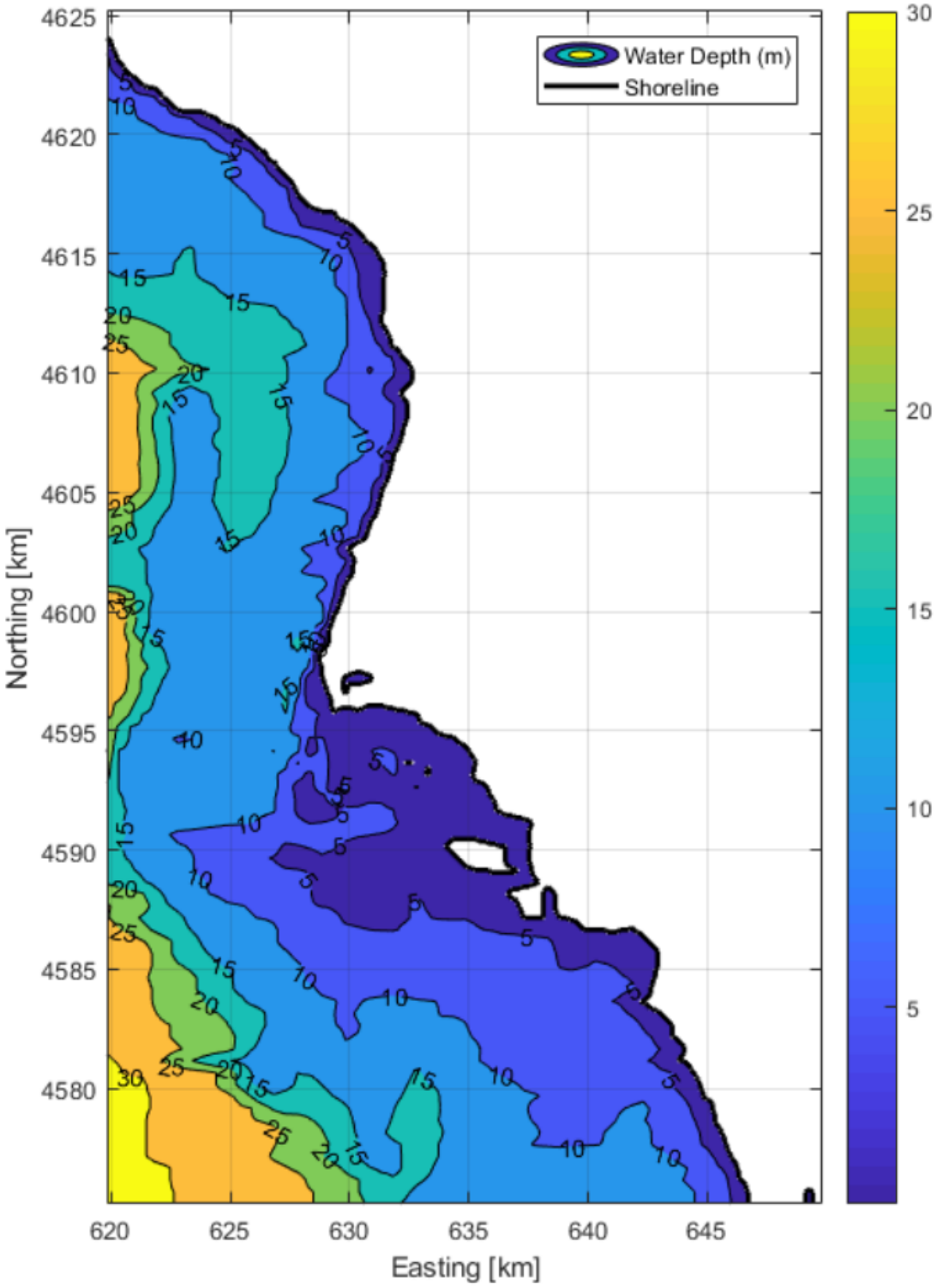

Figure B.4. Coarse mesh bathymetry data for 2050.

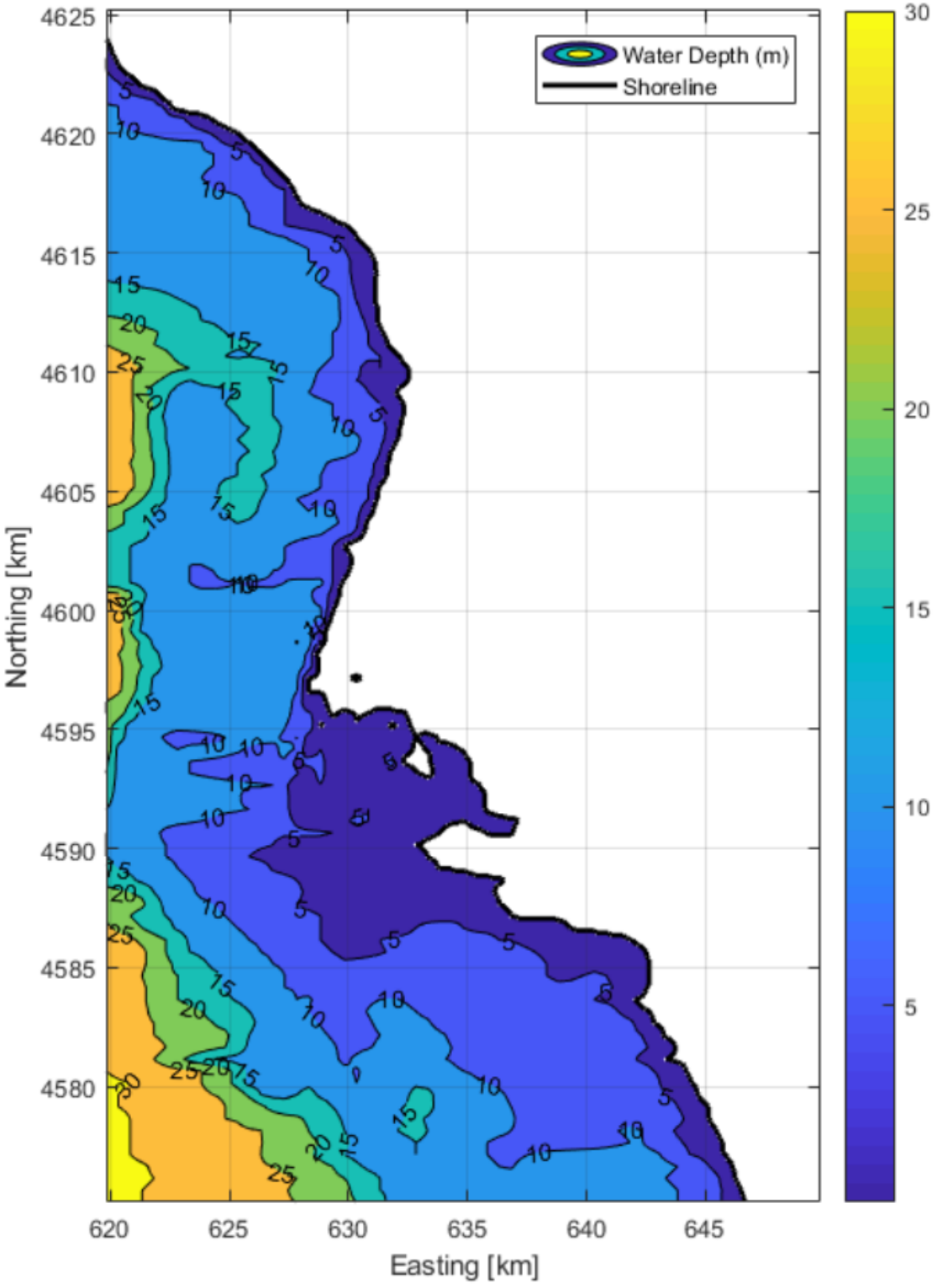

Figure B.5. Coarse mesh bathymetry data for 2060.

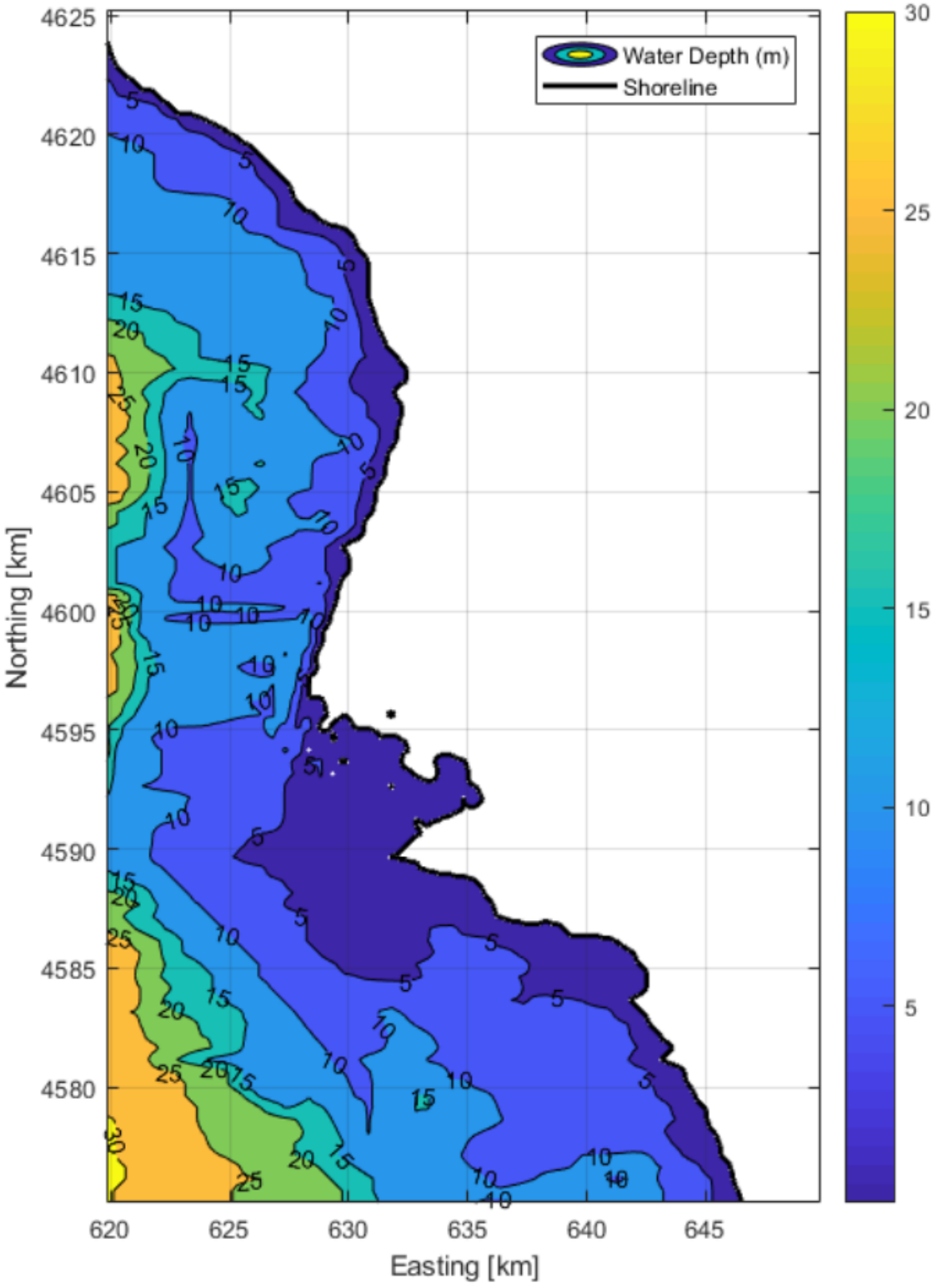

Figure B.6. Coarse mesh bathymetry data for 2070.

APPENDIX C: DIFFUSER ALIGNMENT AND PARAMETERS

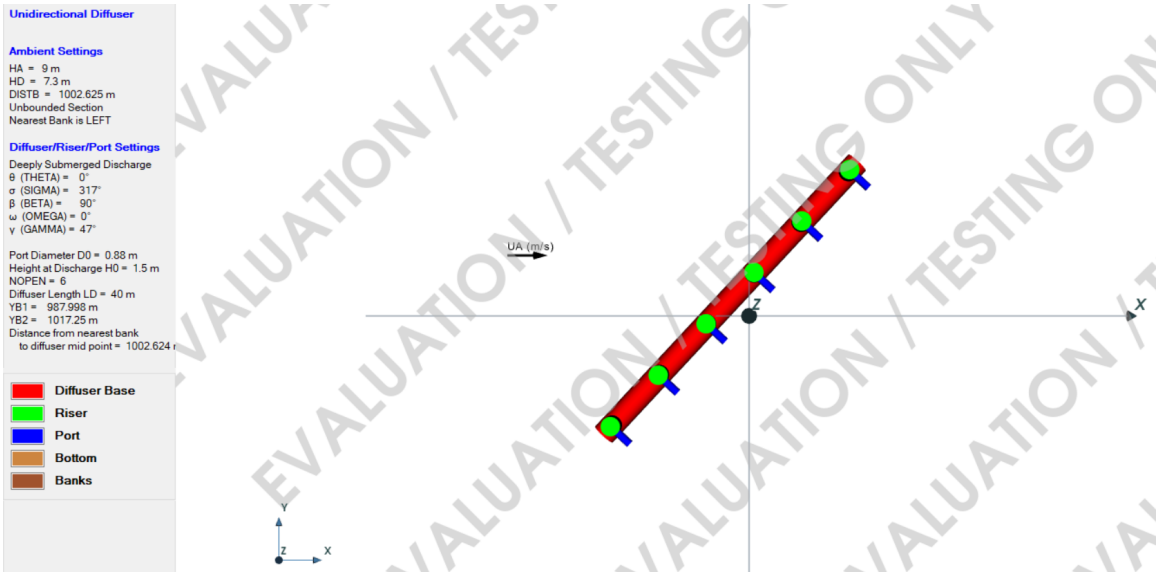

Figure C.1. Diffuser alignment and related parameters for 2020.

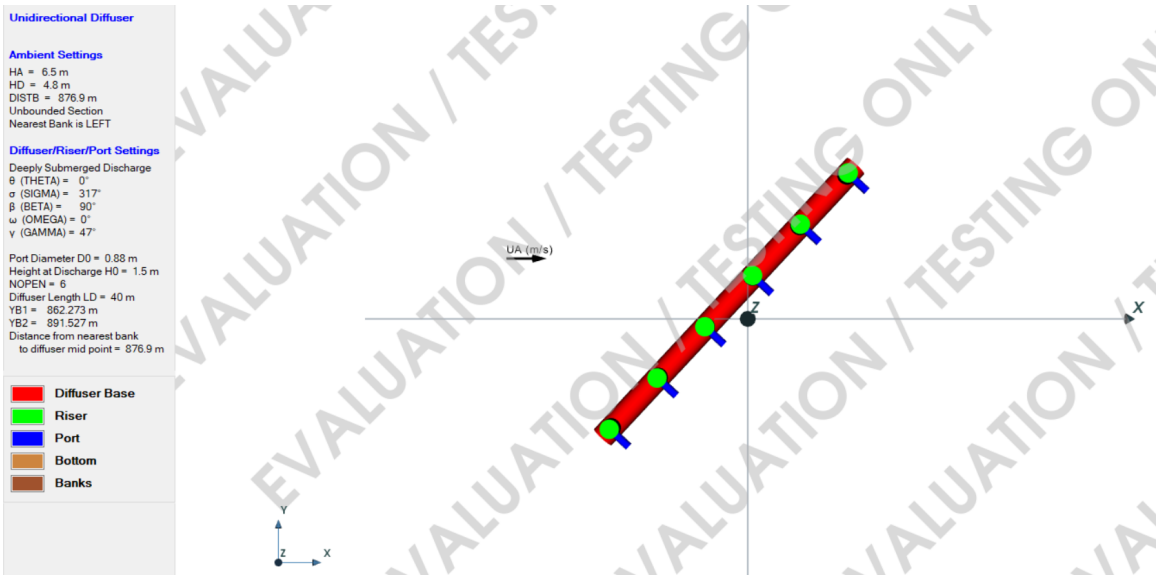

Figure C.2. Diffuser alignment and related parameters for 2030.

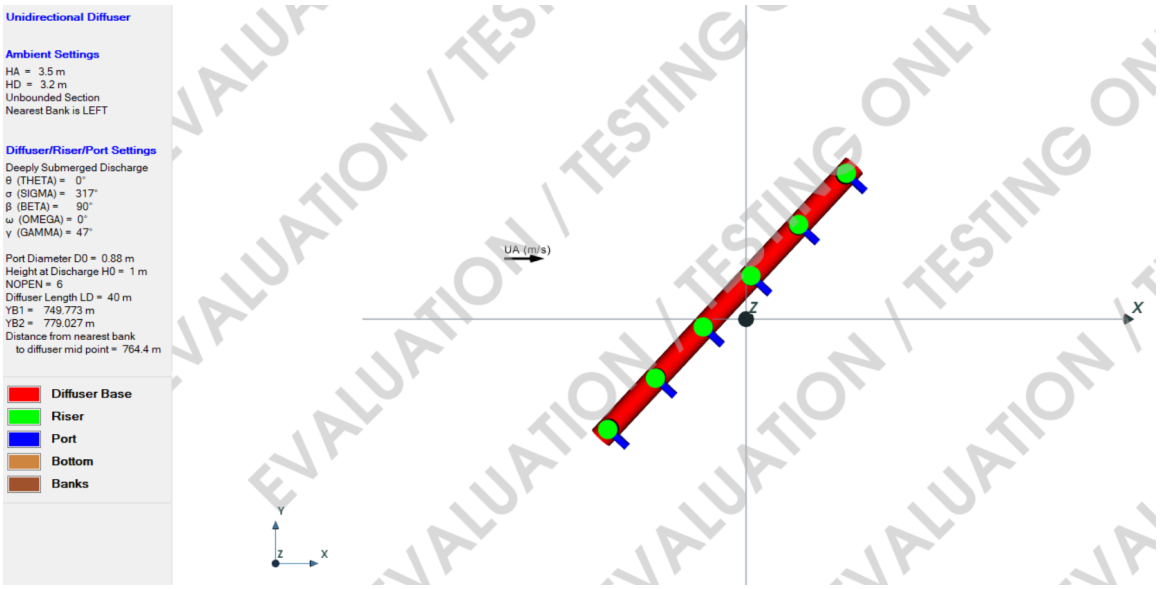

Figure C.3. Diffuser alignment and related parameters for 2040.

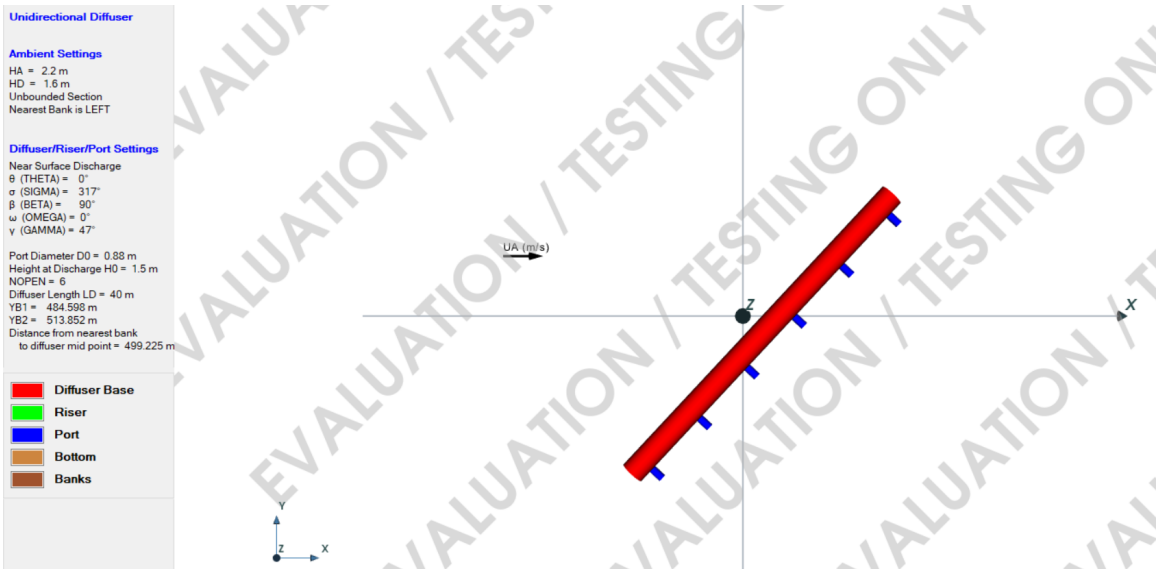

Figure C.4. Diffuser alignment and related parameters for 2050.

APPENDIX D: THE MONTHLY CIRCULATION MODEL

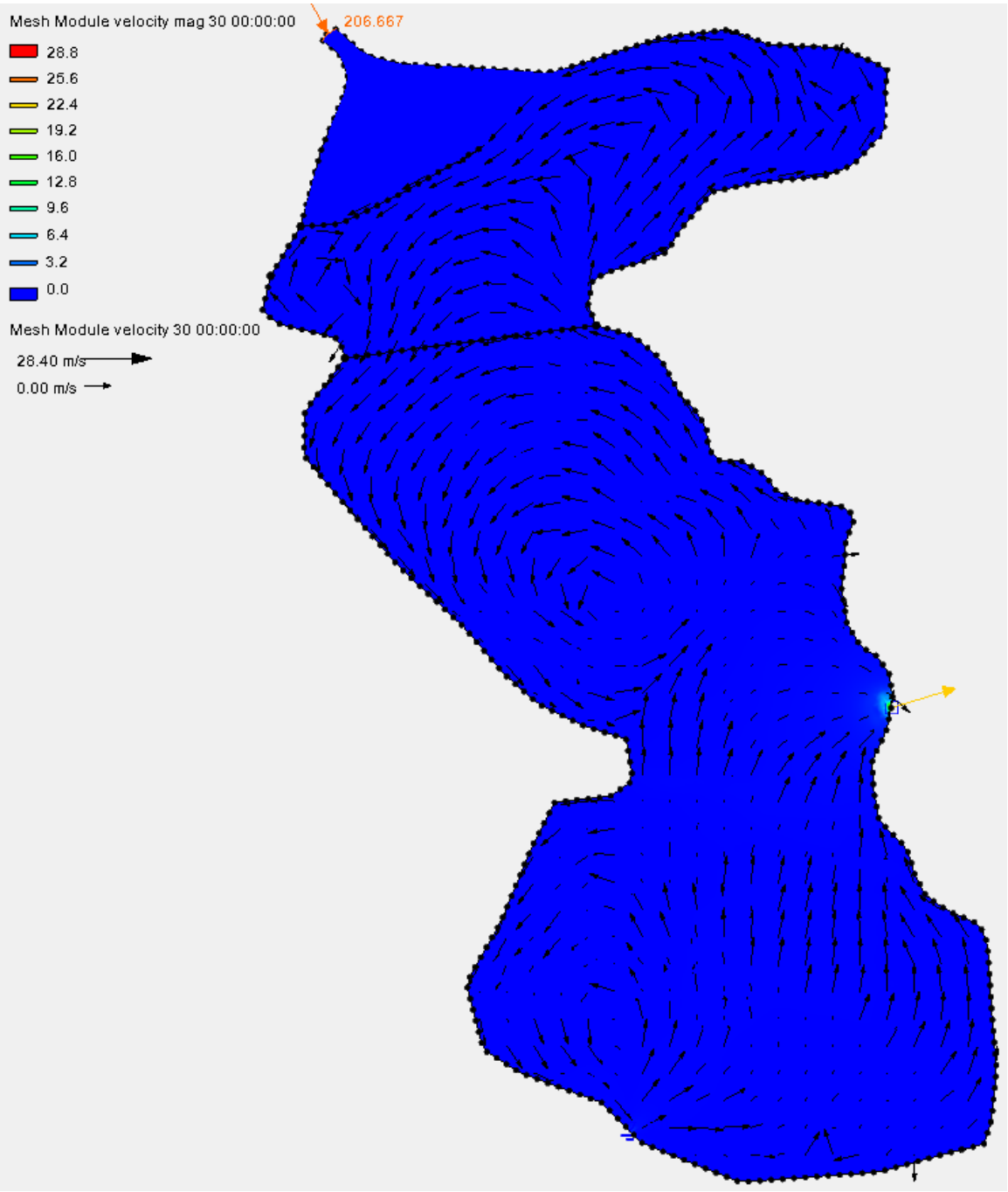

Figure D.1. Mean surface currents (m/s) for January.

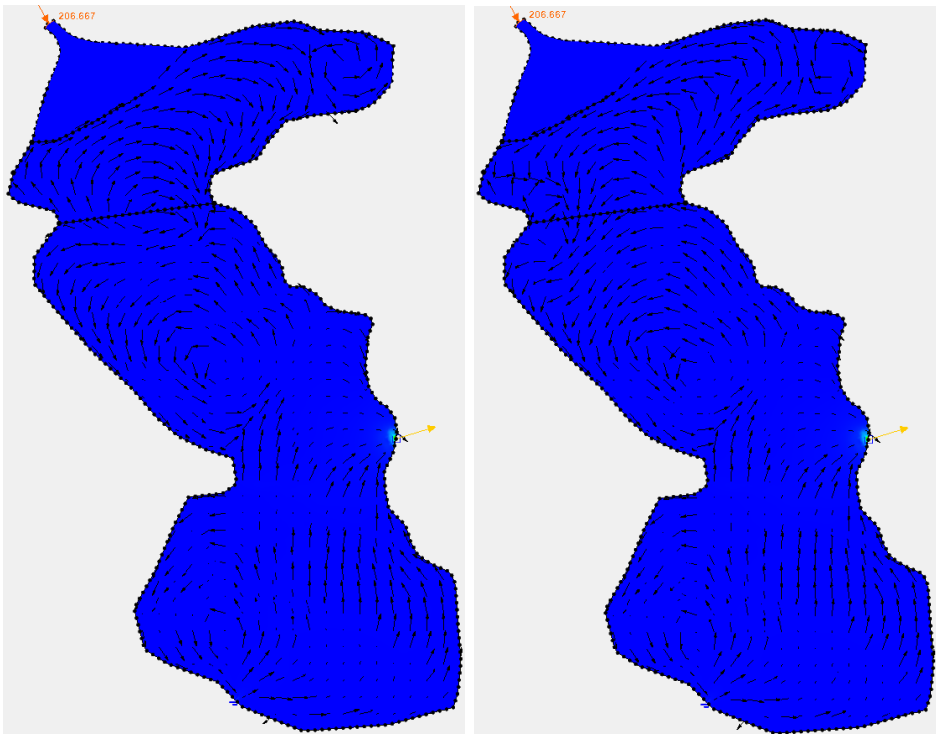

(a) (b)

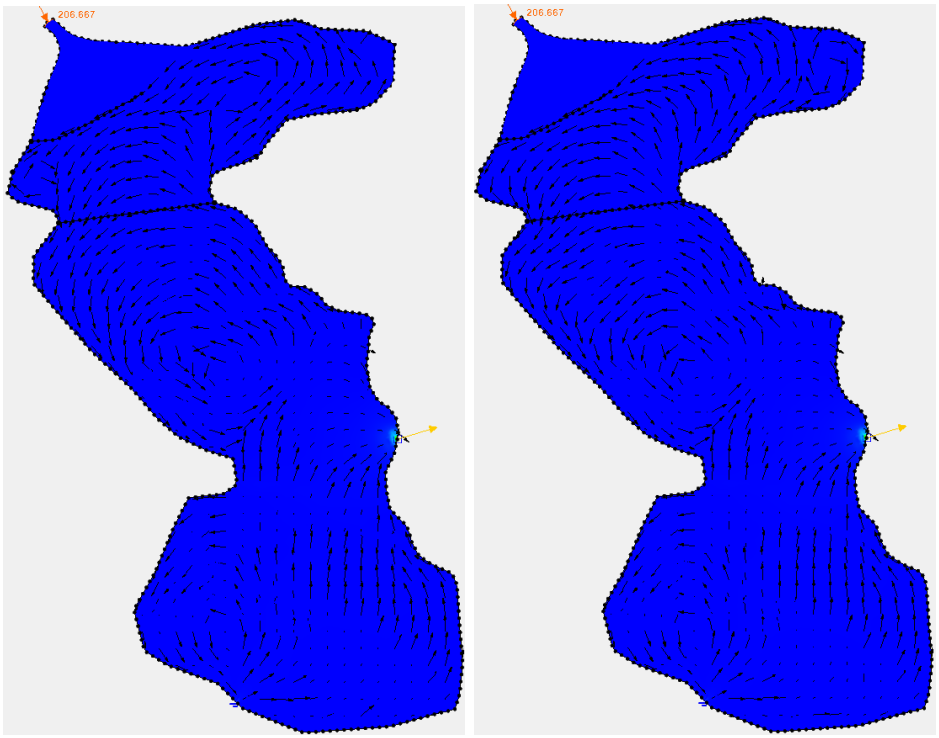

(c) (d)

Figure D.2. Mean surface currents (m/s) for (a) February, (b) March, (c) April and (d) June.

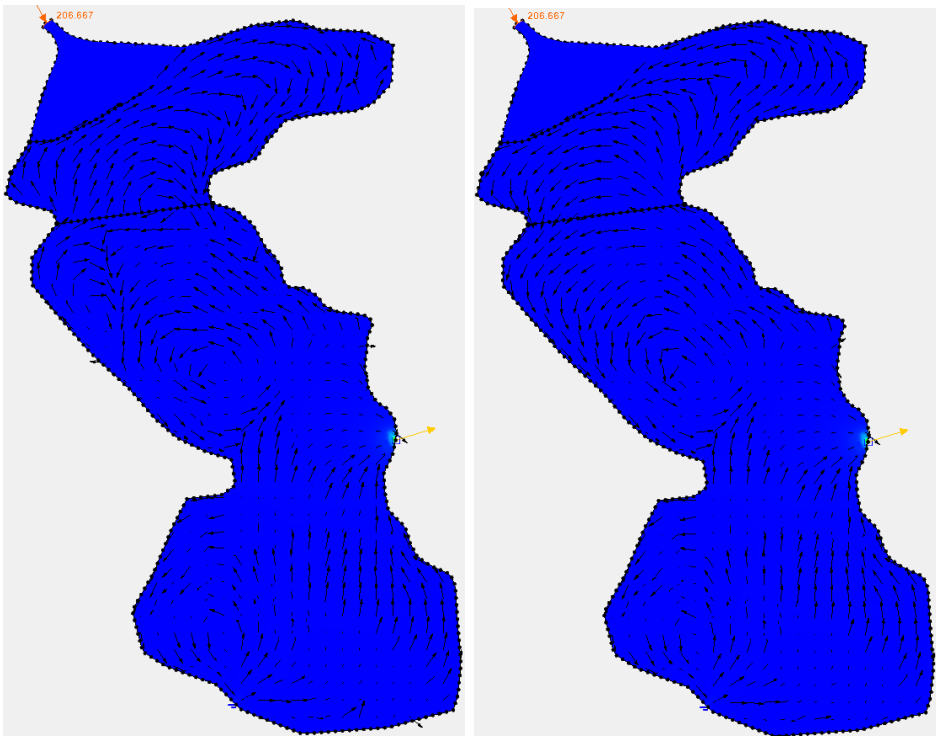

(a) (b)

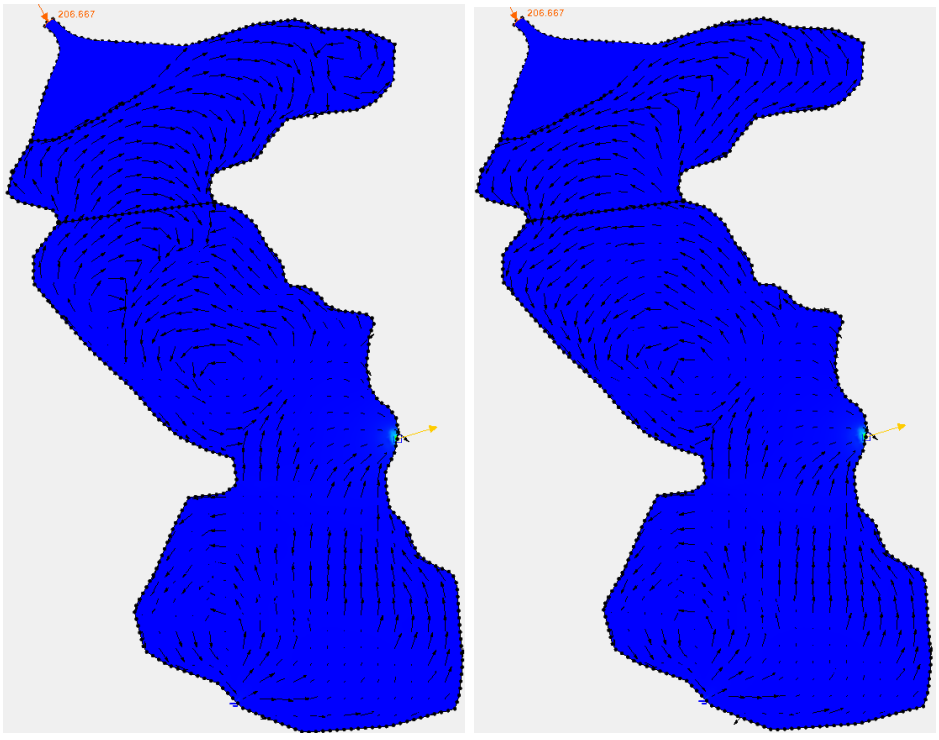

(c) (d)

Figure D.3. Mean surface currents (m/s) for (a) July, (b) September, (c) October and (d) November.

APPENDIX E: COARSE MESH SWAN RESULTS

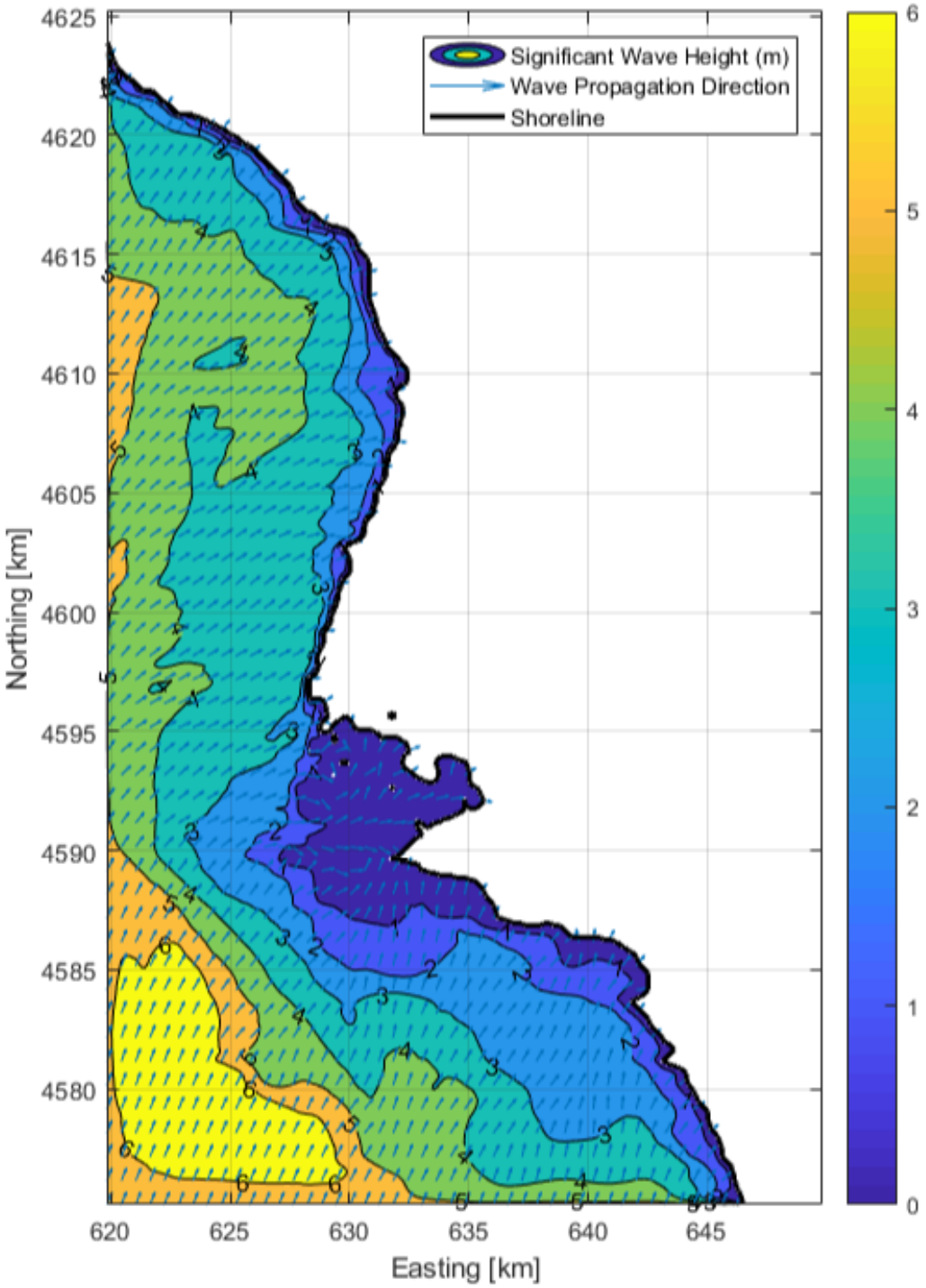

Figure E.1. Coarse mesh SWAN results for 2070.

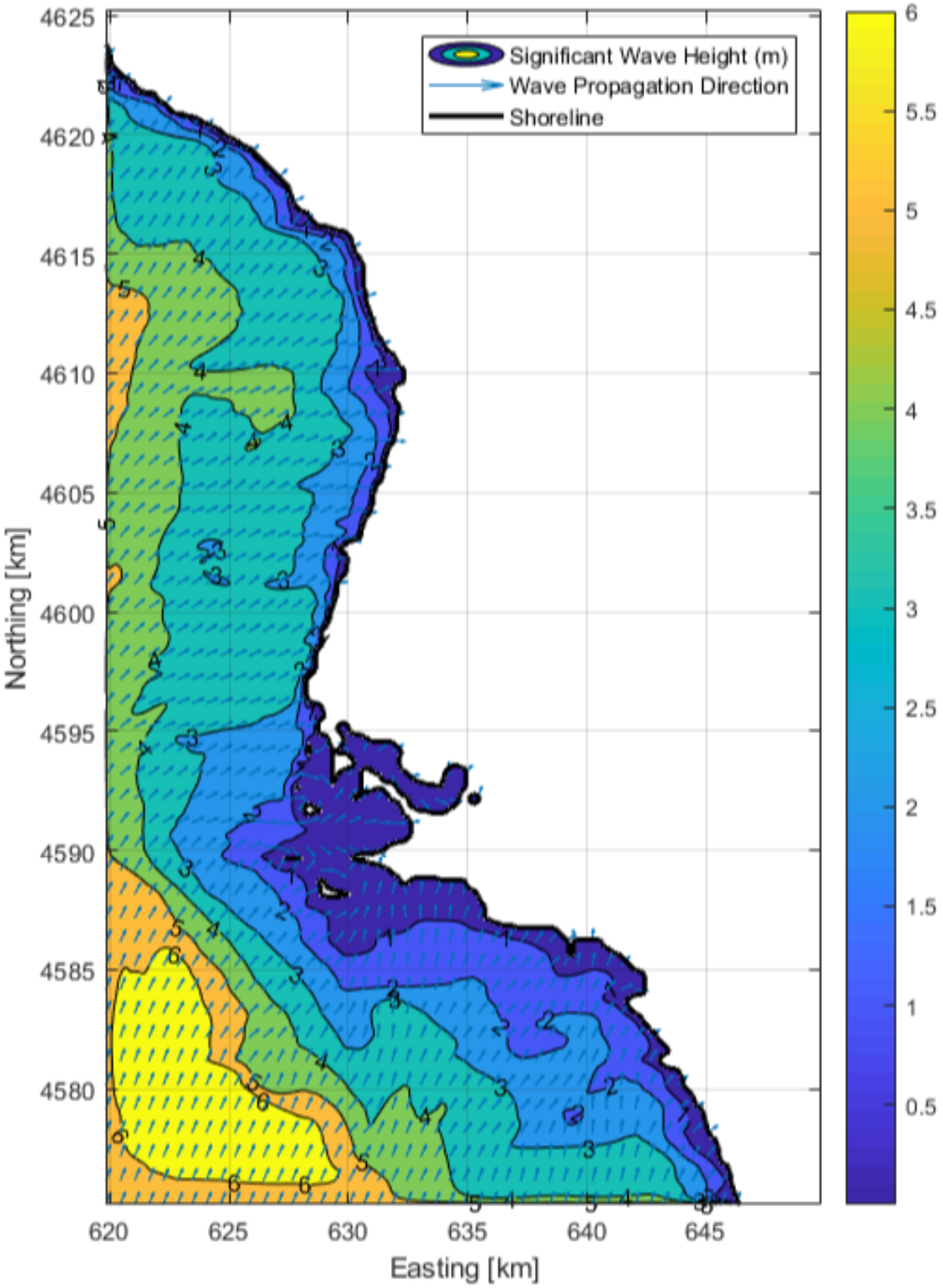

Figure E.2. Coarse mesh SWAN results for 2080.

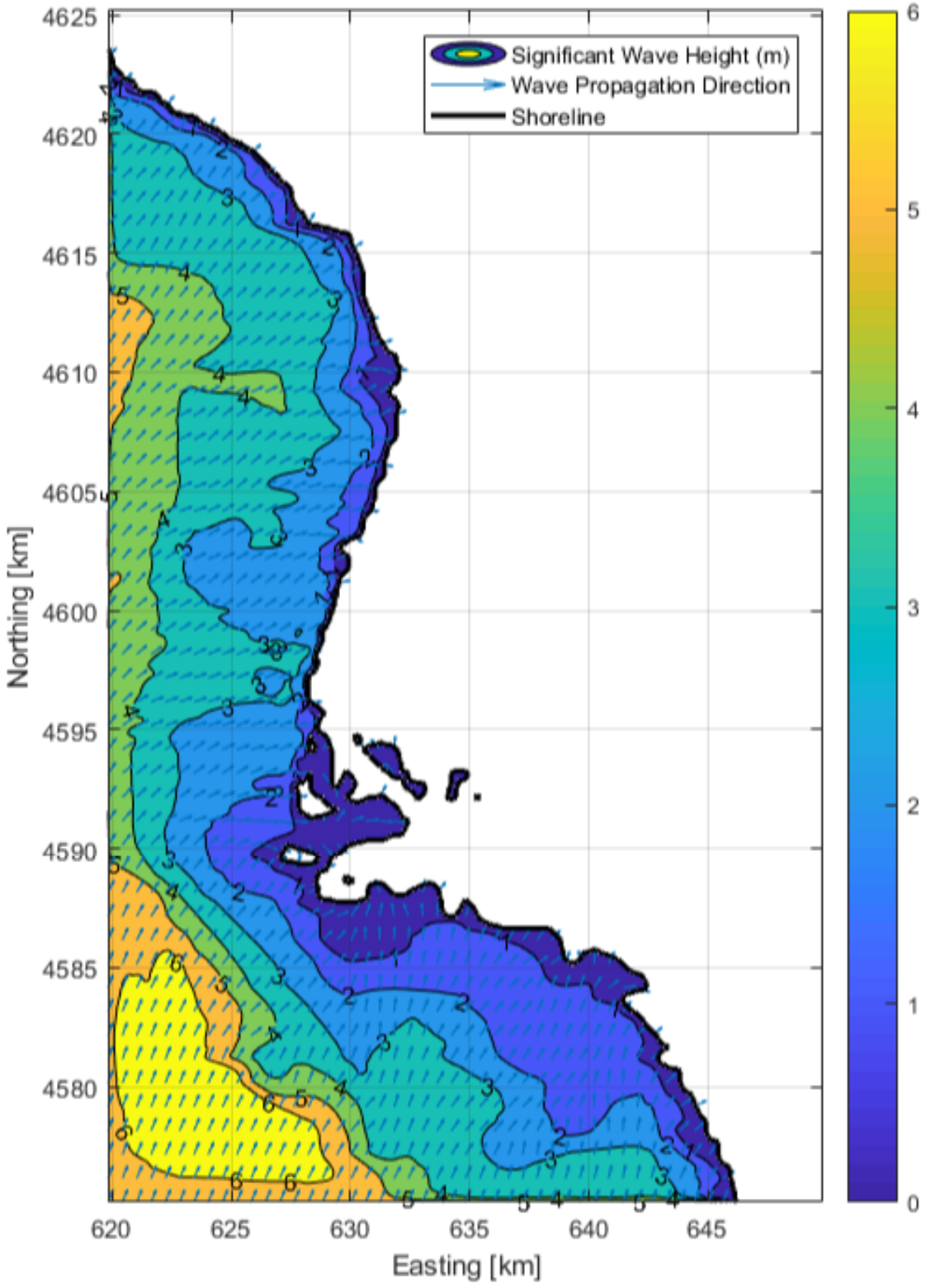

Figure E.3. Coarse mesh SWAN results for 2090.

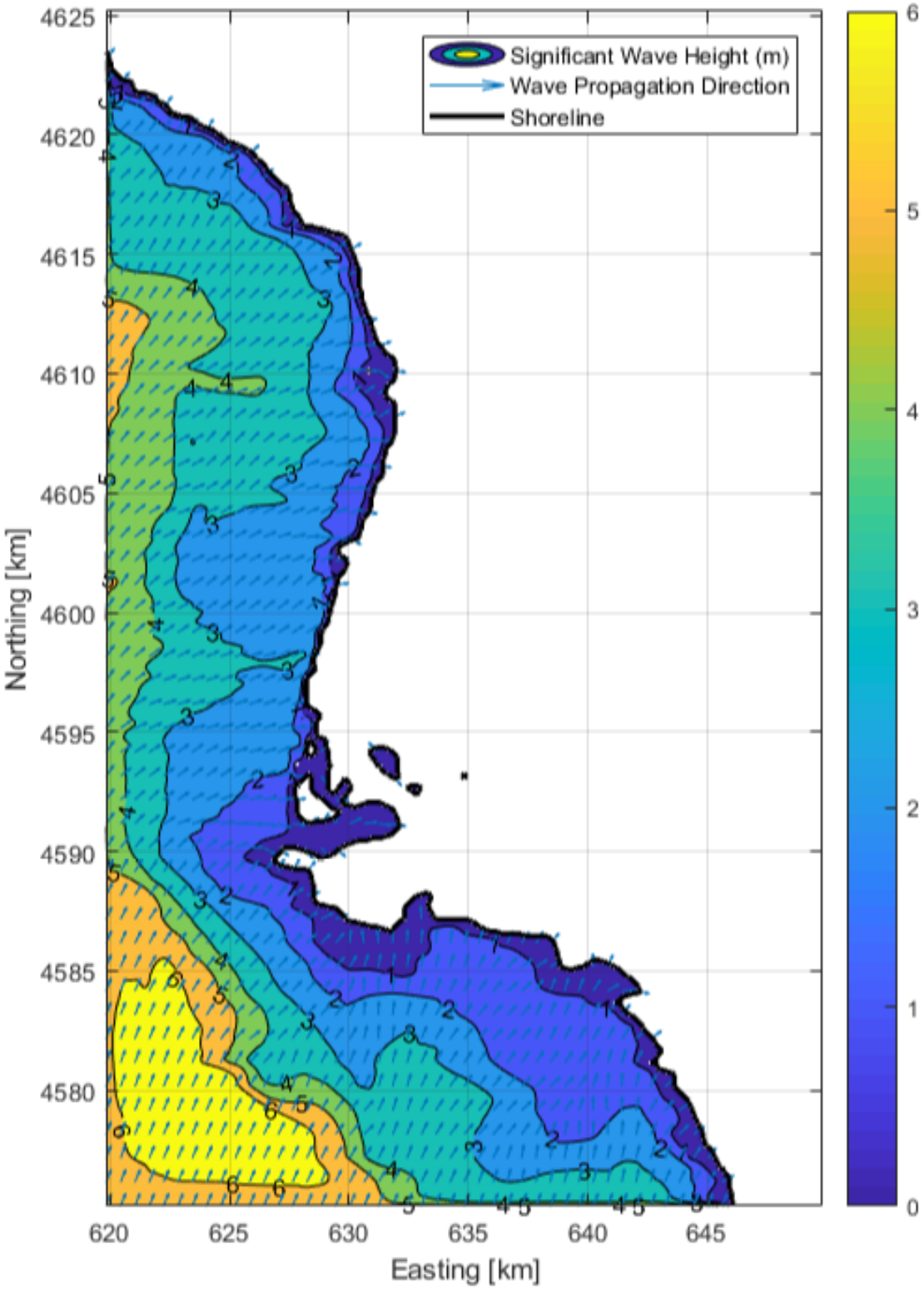

Figure E.4. Coarse mesh SWAN results for 2100.

APPENDIX F: FINE MESH SWAN RESULTS

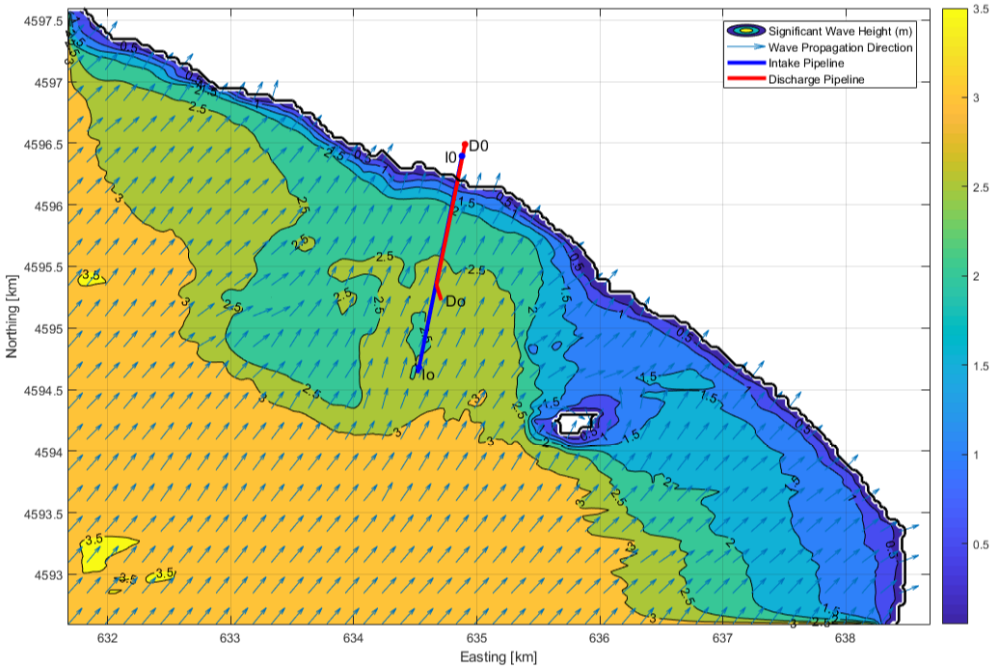

(a)

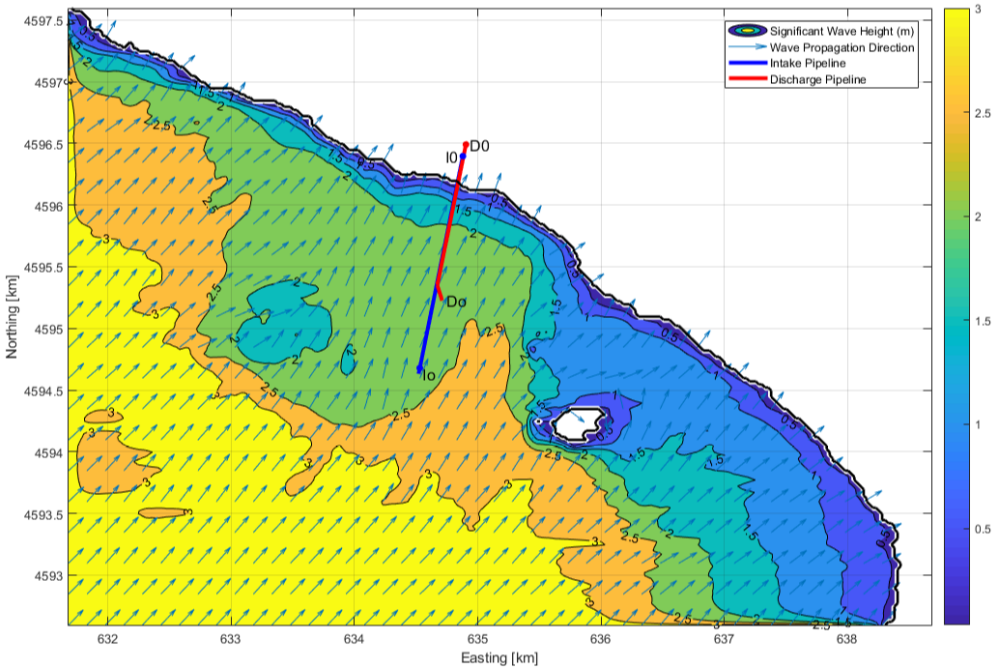

(b)

Figure F.1. Fine mesh SWAN results for (a) 2016 and (b) 2020.

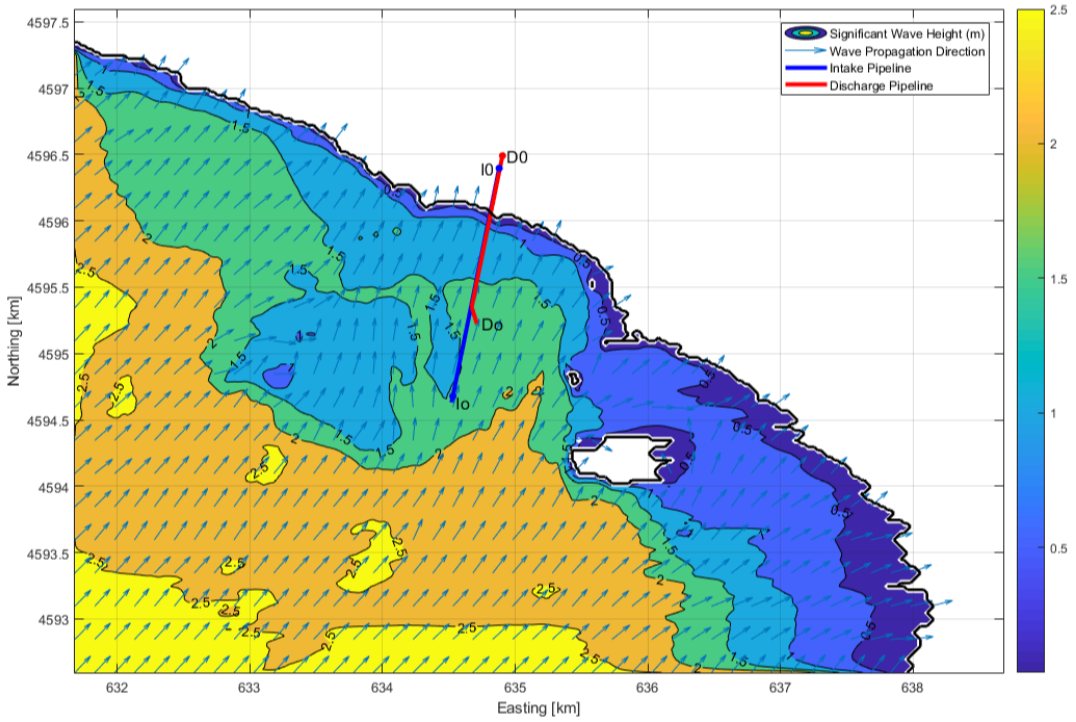

(a)

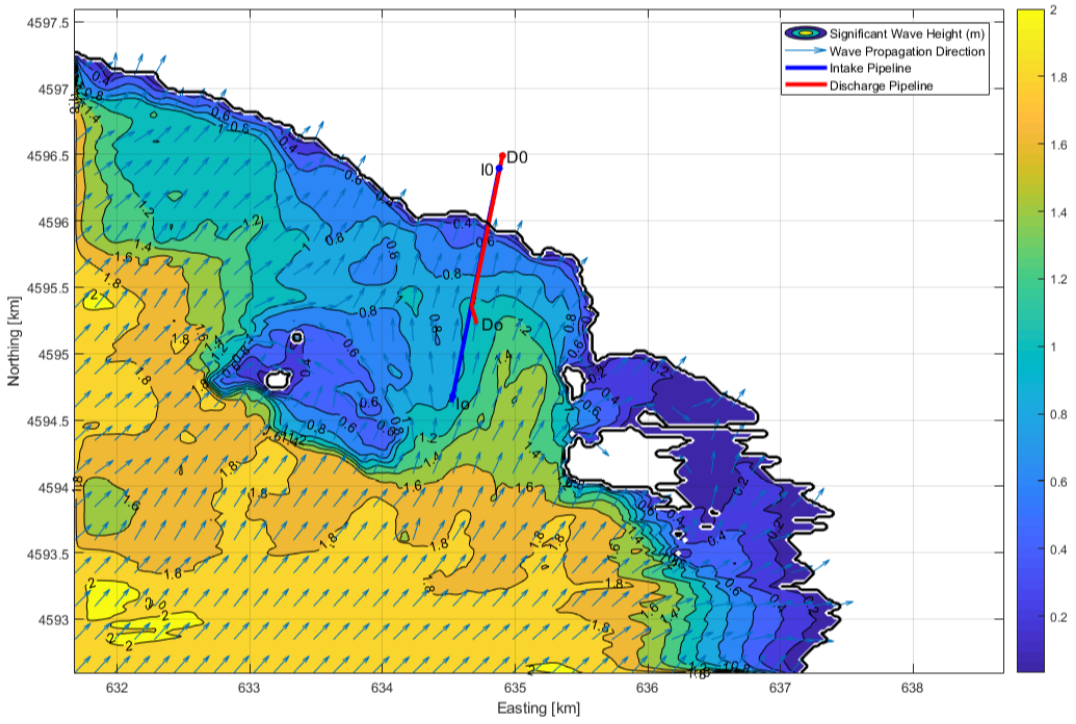

(b)

Figure F.2. Fine mesh SWAN results for (a) 2030 and (b) 2040.

APPENDIX G: WAVE BREAKING ANALYSIS

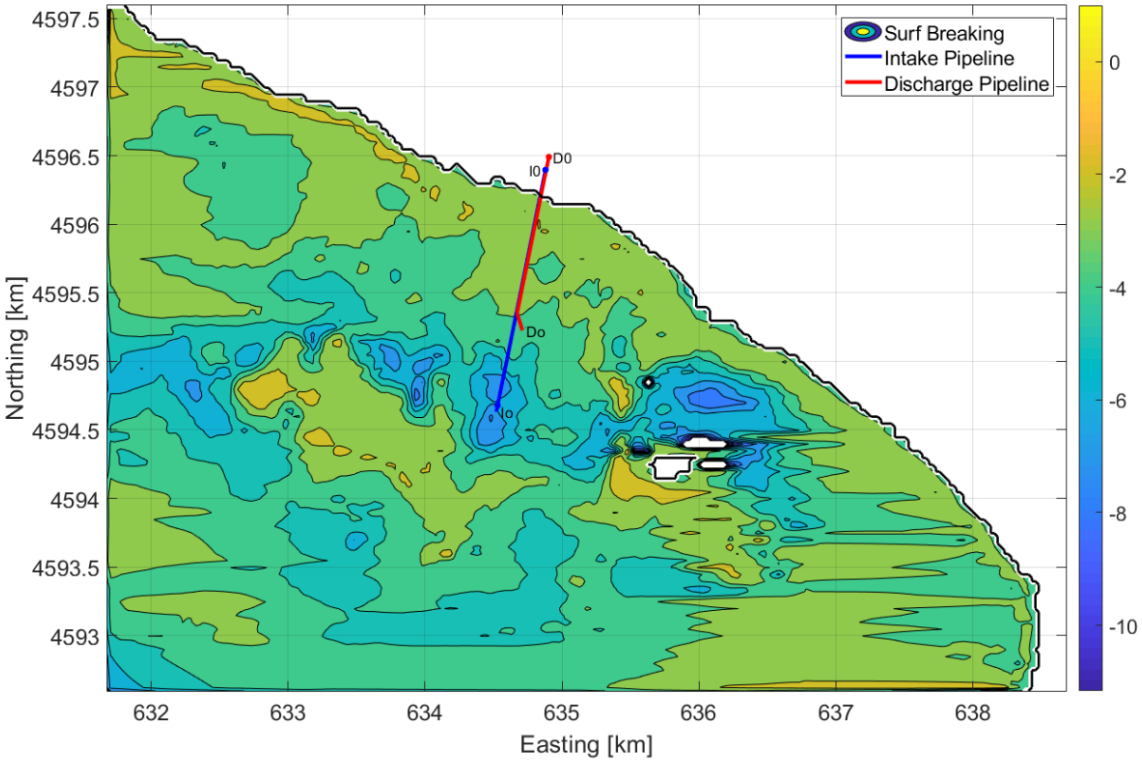

Figure G.1. The normalized source term magnitude for energy dissipation due to surf breaking in 2016.

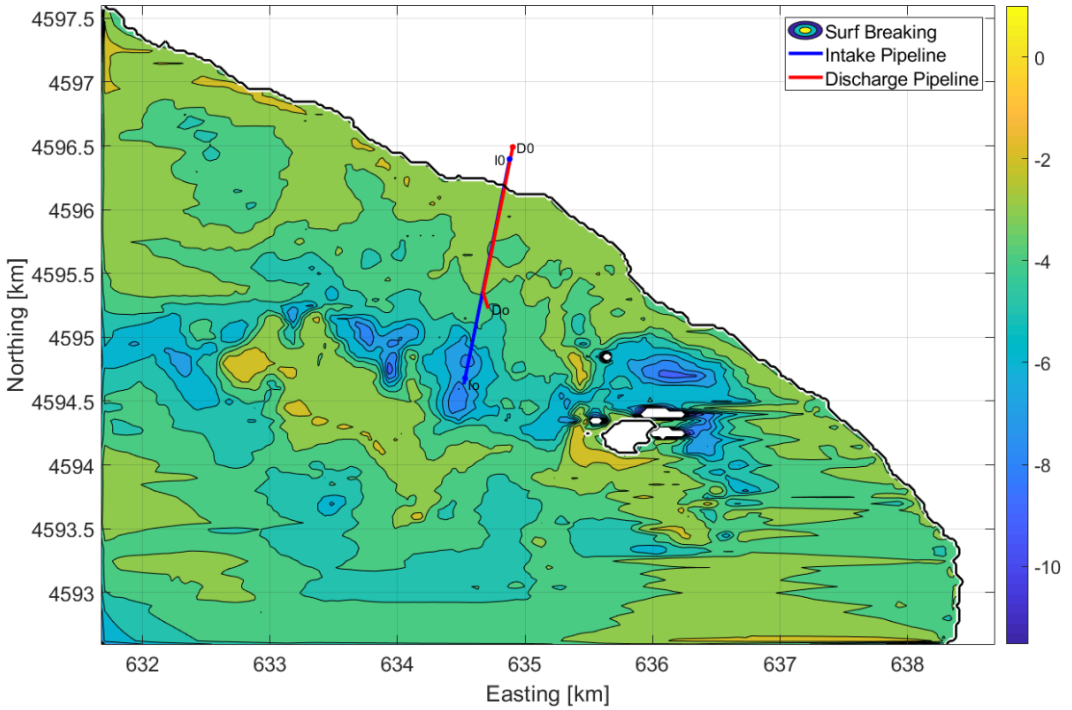

(a)

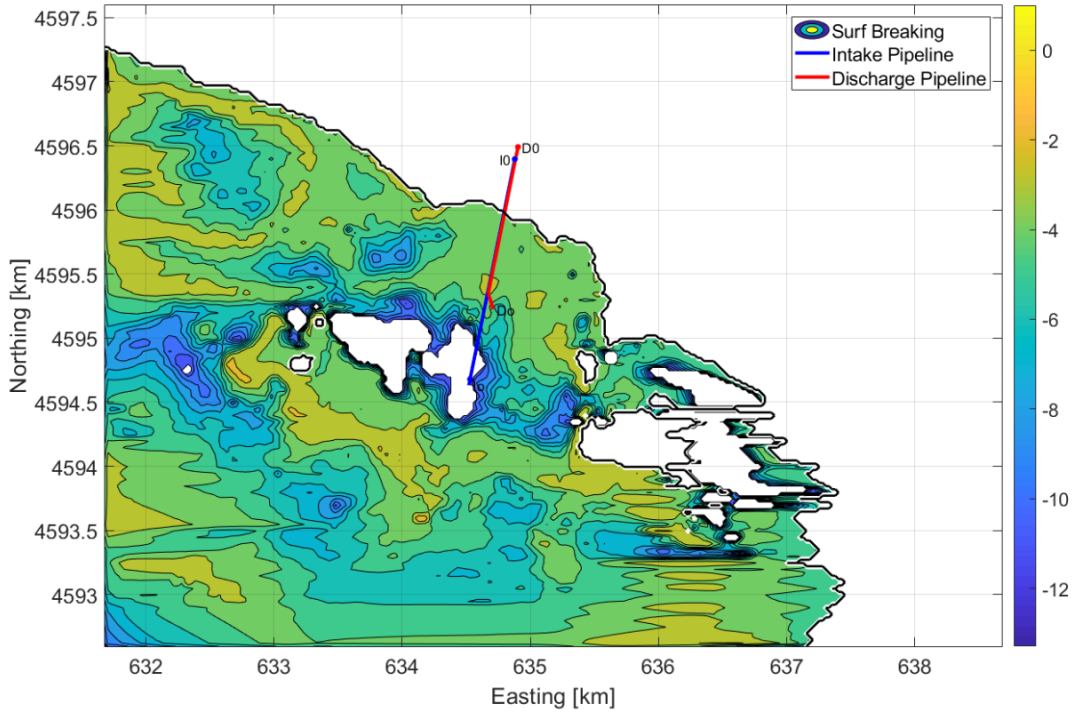

(b)

Figure G.2. The normalized source term magnitude for energy dissipation due to surf breaking in (a) 2020 and (b) 2040.

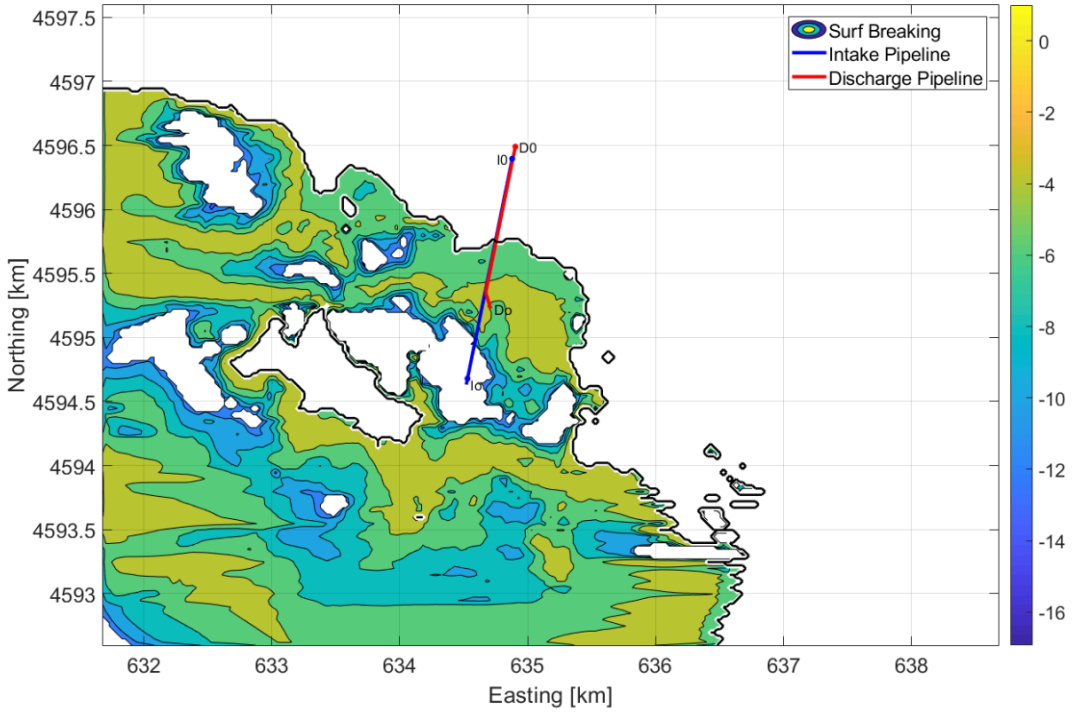

(a)

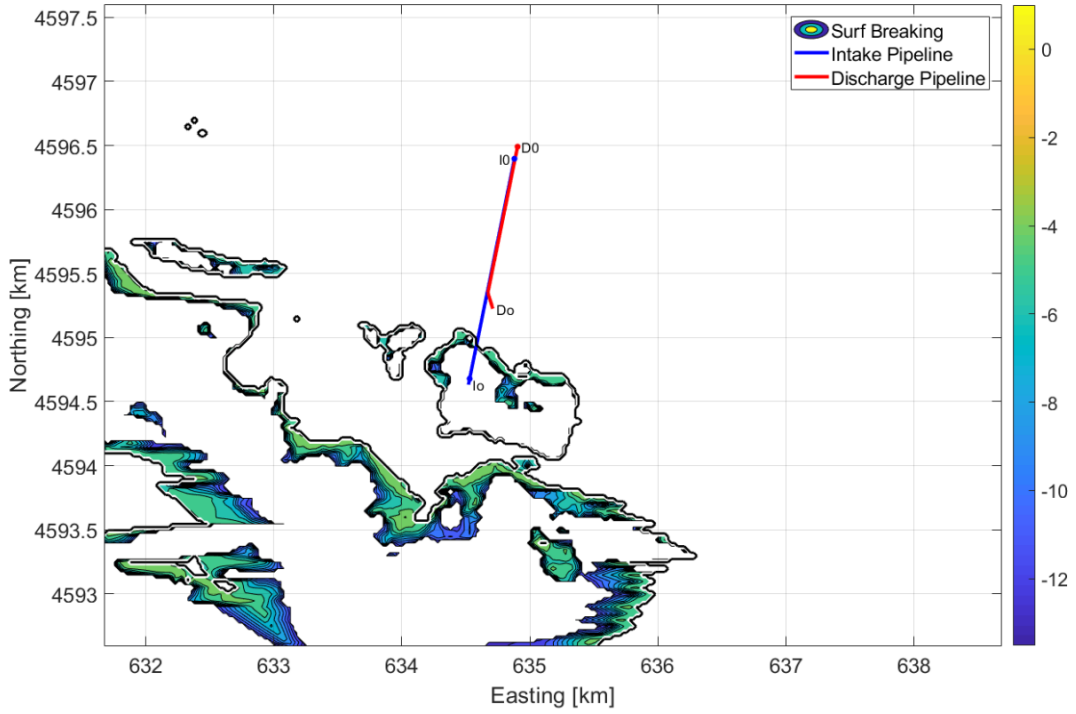

(b)

Figure G.3. The normalized source term magnitude for energy dissipation due to surf breaking in (a) 2050 and (b) 2070.

APPENDIX H: THERMAL DILUTION RESULTS

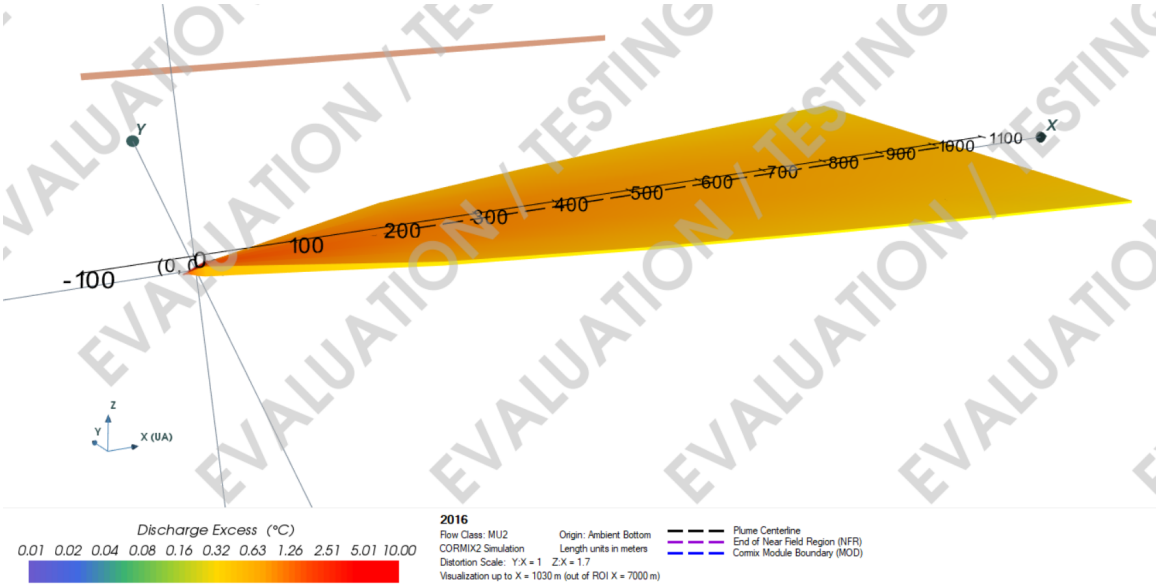

Figure H.1. Thermal dilution result for 2016.

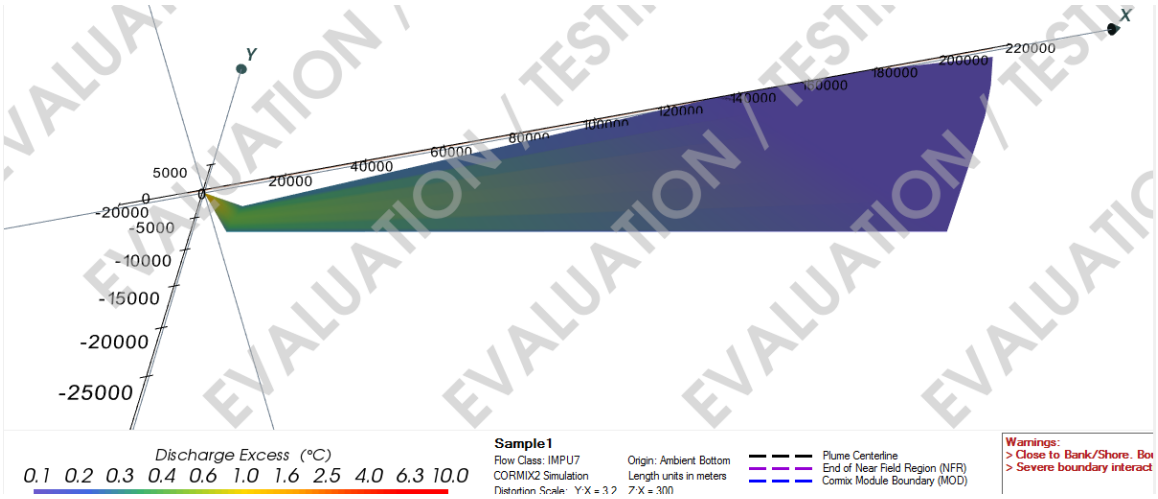

Figure H.2. Thermal dilution result for 2051.

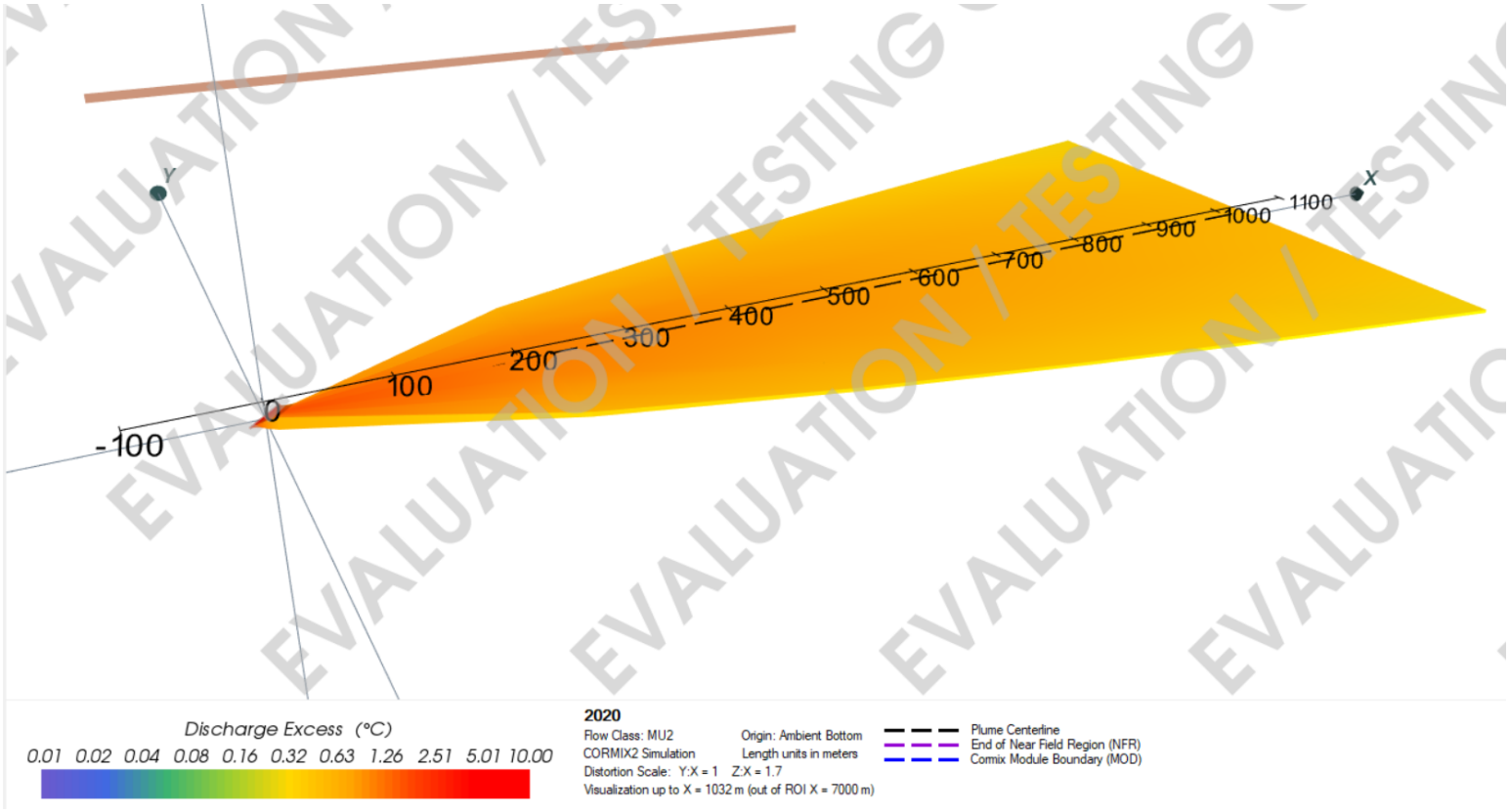

Figure H.3. Thermal dilution result for 2020.

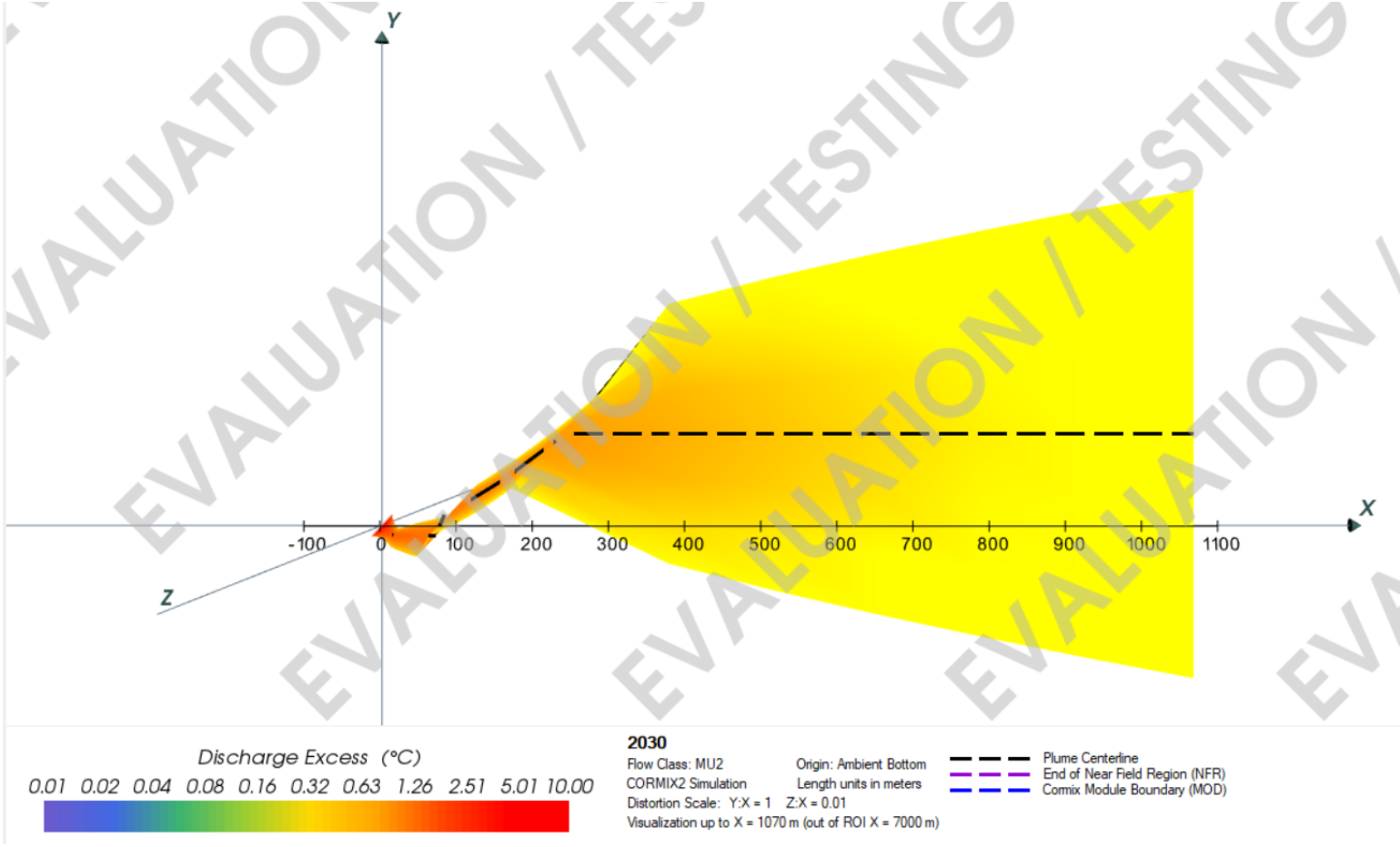

Figure H.4. Thermal dilution result for 2030.